Rocking Revisited 2

Measurement on Rocking of cubes in a Double Layer on a Breakwater

Master of Science Thesis

Author: Syed Shamsil Arefin

Erasmus +: Erasmus Mundus Mobility Programme

Master of Science in

COASTAL AND MARINE ENGINEERING AND MANAGEMENT

CoMEM

ROCKING REVISITED 2

MEASUREMENT ON ROCKING OF CUBES IN A DOUBLE LAYER ON A BREAKWATER

Delft University of Technology
JULY 2017

Syed Shamsil Arefin

The Erasmus+: Erasmus Mundus MSc in Coastal and Marine Engineering and Management is an integrated programme including mobility organized by five European partner institutions, coordinated by Norwegian University of Science and Technology (NTNU).

The joint study programme of 120 ECTS credits (two years full-time) has been obtained at two or three of the five CoMEM partner institutions:

- Norges Teknisk- Naturvitenskapelige Universitet (NTNU) Trondheim, Norway
- Technische Universiteit (TU) Delft, The Netherlands
- Universitat Politècnica de Catalunya (UPC). BarcelonaTech. Barcelona, Spain
- University of Southampton, Southampton, Great Britain
- City, University London, London, Great Britain

During the first three semesters of the programme, students study at two or three different universities depending on their track of study. In the fourth and final semester an MSc project and thesis has to be completed. The two-year CoMEM programme leads to a multiple set of officially recognized MSc diploma certificates. These will be issued by the universities that have been attended by the student. The transcripts issued with the MSc Diploma Certificate of each university include grades/marks and credits for each subject.

Information regarding the CoMEM programme can be obtained from the programme coordinator:

Øivind A. Arntsen, Dr.ing.
Associate professor in Marine Civil Engineering
Department of Civil and Transport Engineering
NTNU Norway

Telephone: +4773594625 Cell: +4792650455 Fax: + 4773597021

Email: oivind.arntsen@ntnu.no

CoMEM URL: https://www.ntnu.edu/studies/mscomem

CoMEM Master Thesis

This thesis was completed by:

Syed Shamsil Arefin
Student ID: 4536517

at Delft University of Technology

Under supervision of:

prof. dr. ir. W.S.J. Uijttewaal,	Delft University of Technology
dr. ir. B. Hofland,	Delft University of Technology / Deltares
ir. J.P. van den Bos,	Delft University of Technology
dr. ir. M.R.A. van Gent,	Deltares
ir. J.C. van der Lem,	Royal HaskoningDHV

In partial fulfillment of the requirements for the degree of

Erasmus+: Erasmus Mundus Master in Coastal and Marine Engineering and Management

(CoMEM)

Taught at the following educational institutions:

Norges Teknisk- Naturvitenskapelige Universitet (NTNU)

Trondheim, Norway

Technische Universiteit (TU) Delft

Delft, The Netherlands

University of Southampton,

Southampton, Great Britain

At which the student has studied from August 2015 to June/July 2017.

PREFACE

This thesis is the final Report for the partial fulfillment of the requirement for the degree in Masters of Science in Coastal and Marine Engineering & Management (CoMEM) at Delft University of Technology. This thesis describes the measurement of rocking for randomly placed double layer cubes on breakwater. The thesis has been conducted with cooperation with Deltares and Royal HaskoningDHV.

This thesis is supervised by prof. dr. ir. W.S.J. Uijttewaal (TU Delft), dr. ir. B. Hofland (TU Delft), ir. J.P. van den Bos (TU Delft), dr. ir. M.R.A. van Gent (Deltares) and ir. J.C. van der Lem (Royal HaskoningDHV) as my graduating committee. Firstly I would like to thank them for their kind input and guidance throughout the thesis work. Specially I would like to thank dr. ir. B. Hofland who has been really helpful and advising me all the way. Also like to thank Guido Wolters (Deltares) for his kind advice. Many thanks to Jelle Molenaar and Wim Taal (Deltares) for their kind help understanding the Tinyduino sensors. I would also like to thank Sander de Vree, Hans Tas and Jaap Van Duin (TU Delft) for their constant support during the experiments. Many thanks to Deltares for providing the Tinyduino sensors for the experiment.

Finally I would like to thank my wife Barsha, my parents and my friends and colleagues for their constant support and encouragement throughout my study.

Syed Shamsil Arefin

Delft, July 2017

ABSTRACT

Rocking behavior of breakwater research was conducted by Centre for Civil Engineering Research and Codes workgroup CUR C70 (1989) and after that no further validation of the research work has been done. In order to understand the rocking behavior and validate the previously conducted research CUR C70 (1989) wave flume test has been conducted in similar setup. One of the important parameter of rocking behavior is the magnitude of impact velocity and the distribution of this impact velocity stochastically and spatially. This research investigates the order of the magnitude of the impact velocity and distribution of the impact velocity comparing, validating and concluding new findings those were not incorporated in CUR C70 (1989) research.

During this research a new type of sensor Tinyduino has been used inside a cube to measure the acceleration and angular velocity of the cubes. Eight of these sensors were used in eight different cubes. All the sensors were tested properly in Deltares to check the sensors working properly and better understanding the sensors. Before this research two test programs were performed by Deltares in tetrapod in double layer using this Tinyduino sensor in stand alone mode but the data were not analyzed. This research analyzed the data for the tetrapods provided by Deltares and compared with CUR 70 (1989). During this analysis and the testing of the sensors it is found that angular velocity measurement can be much more reliable than acceleration hence the angular velocity measurement is used during data processing of instrumented cubes in double layer.

For experiments eight instrumented cubes were placed using very flexible wire in a randomly placed double layer cubes with same size and almost similar density over a permeable filter layer. The slope 1:1.5 is used for the experiment same as the CUR C70 (1989) research conducted. The cubes were placed in one constant level but the water level is varied in order to demonstrate different slope position. Three slope position $Y/D_n=0$, $Y/ D_n =-2$ and $Y/ D_n =-4$ is used during the research program. Three different wave heights and two wave steepness were used during this test program. Due to time limitation 18 test setups within two days were performed. The data were collected real-time using wire and saved in text file simultaneously with eight instrumented cubes stored in a laptop provided by Deltares.

After the test program all the data is processed with matlab script and analyzed. The result of the analysis showed that the order of the magnitude of impact velocities is same as the CUR C70 (1989) research. It has also been found that the impact velocities are also dependent on the wave steepness which was not included in the CUR C70 (1989) research. So it is recommended for future work to update the equation incorporating wave steepness. Another important parameter is number of collision which was assumed to be 3 times is CUR C70 (1989) but found incorrect during this thesis. It is concluded that number of collision is dependent wave height, wave steepness, position over slope and also exposure to wave

attack. It is also found that the number of collision is continuous during wave attack after a certain impact velocity.

One of the finding of CUR 70 (1989) was the location of maximum impact velocity over slope. It was concluded in CUR 70 (1989) that the maximum impact velocity lies on Y/Dn=0 meaning on the water level but during this research all the sample those worked observed that the maximum impact velocity is located on Y/D_n =-2 over the slope under the water level.

For future research work it is recommended to use different types of armor unit in single layer to understand the rocking behavior and also it is recommended using the Tinyduino sensors which provides accurate data on movement of the armor units.

Table of Contents

List of Symbols

Y/ D_n	Position of the cube relative to the water level	[-]
ω	Angular Velocity	[rad/s]
Δ	Relative Density	[-]
υ	Kinematic Viscosity	[m^2/s]
θ	Angle of Rotation	[º]
ρ	Density of Material	[kg/m^3]
a	Acceleration during impact	[m/s^2]
ax	Acceleration in X direction from Sensor	[g]
ay	Acceleration in Y direction from Sensor	[g]
az	Acceleration in Z direction from Sensor	[g]
$a(res)$	Resultant Acceleration from Sensor	[g]
B	Compressive Strength	[N/mm^2]
C	Dimensionless Coefficients	[-]
d	Diameter of Leg	[m]
Dn	Nominal Diameter	[m]
Fr	Froude Number	[-]
G	Gravitational acceleration	[m/s^2]
gx	Angular Velocity around X axis from Sensor	[rad/s]
gy	Angular Velocity around Y axis from Sensor	[rad/s]
gz	Angular Velocity around Z axis from Sensor	[rad/s]
$g(res)$	Resultant Angular Velocity from Sensor	[rad/s]
H_{m0}	Significant wave height from wave energy spectrum	[m]
H_s	Significant wave height from wave record	[m]
I_0	Moment of Inertia	[kgm^2]
K_p	Elastic Parameter	[N]
L	Distance of Impact velocity from Center of Rotation of Armor unit	[m]

M	Mass	[kg]
N_l	Factor for length	[-]
N_{od}	Total number of displaced units	[-]
N_{otot}	Total number of moved units	[-]
Ns	Stability number	[-]
N_T	Factor for Time	[-]
N_u	Factor for velocity	[-]
Re	Reynolds Number	[-]
S	Actual Collision duration	[N/mm^{2}s]
S_0	Reference duration of 0.1	[N/mm^{2}s]
$s_{m-1.0}$	Fictitious wave steepness based on H_{m0} and $T_{m-1.0}$	[-]
s_m	Fictitious wave steepness based on H_s and T_m	[-]
St	Strouhal Number	[-]
T	Time	[s]
$T_{m-1.0}$	Wave period based on the ratio of the wave energy spectral moments $_{m-1}$ and $_{m0}$	[s]
u	Flow Velocity	[m/s]
V	Impact velocity	[m/s]
Vi	Impact Velocity from Sensors	[m/s]
We	Weber Number	[-]

List of Figures

List of Tables

1. Introduction

Breakwaters are offshore structures to provide protection from wave action and currents. They can be used to protect port facilities, beaches from erosion, valuable habitat or reducing siltation in channels by withstanding the design condition loads. There are different types of breakwater e.g. rubble mound breakwater, composite breakwater, floating breakwater and monolithic breakwater and each consist their own structural feature. A typical rubble mound breakwater consists of core from fine material, underlayer(s) to act as filter layer to protect the core material being washed out and armor layer. The armor layer provides the stability for the breakwater by dissipating and reflecting wave energy and limiting the wave run-up. A typical cross section is shown in figure 1.1.

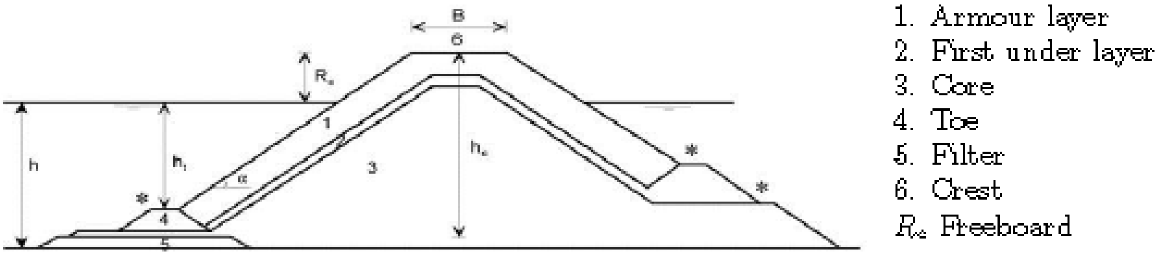

Figure 1.1 Cross section of a typical rubble mound breakwater [Verhagen et al.(2009)Verhagen, d'Angremond, and van Roode]

1.1 Background

Throughout the centuries the rubble mound breakwater has been used to protect the ports and coasts from severe wave attack from the sea. The design of these breakwaters consists of a core layer of fine materials covered by different layers of armor stones and heavy concrete blocks or quarried rocks over the top. Most of the cases these armor units and concrete blocks obtained their stability by self weight from the severe wave attack. Now a day’s the slender armor units is replacing the existing armor stones and concrete block which are based on interlocking with each other increasing the stability of the armor layer from the wave attack and decreasing the weight of the armor units. There has been significant development in the armor units in last half century. The first generation armor units such as Dolosse, Tetrapods, cubes and etc were used in double layers until recently the armor units such as Xbloc, Accropode, Coreloc and single layer cubes have been developed to use in a single layer. The major advantage of these single layer armor units is that it reduces the amount of concrete thus reducing cost without compromising the stability of the breakwater. Typical cross sections of breakwater with single layer and double layer armor units are shown in Fig 1.2.

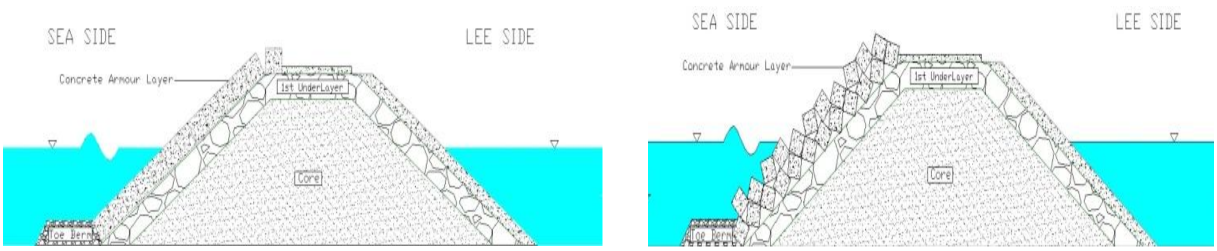

Figure 1.2 Cross Section of a Typical Breakwater with i) Single layer Armor unit & ii) Double Armor unit

1.2 Problem Description:

During Late 70's and Early 80's several breakwaters were severely damaged which were large slender armor units (20- 60 Tons) and in double layer. These units were collapsed due to the mechanical failure in most cases. After these failures a joint industry research program was commenced under the coordination of the Center for Centre for Civil Engineering Research and Codes (CUR) in the 1980's in order to incorporate the strength of the armor unit in the breakwater design procedure covering the analysis of the damage cases, applying physical model test on rocking behavior, force-time behavior during collision of concrete units and to develop design procedure for practical application of double layer armor units such as Tetrapods and cubes.

Now a day's most of the rubble mound breakwaters are designed with single layer armor units nevertheless in recent years it has also been observed that breakage also occurs in these units as well. In order to understand the behavior of single layer armor units a theoretical assessment is conducted for an exposed cube, which rotates around a hinge (Tuan Le, 2016). The analysis of the assessment shows that the analytical model overestimates the impact velocities and therefore, is too conservative. The assumptions made for the analytical model should be further investigated to derive a more accurate calculation method (Tuan Le, 2016).

1.3 Objective:

The objective for this research program is followed by the problem discussed in Section 1.1.

- Determination of spatial and stochastic distribution of rocking behavior of armor units.

Sub-aims

- Further develop dedicated measurement technique for rocking analysis
- Formulate new parameters indicating rocking based on this technique
- Validate some crucial assumptions in the existing rocking calculation (CUR 1980)

1.4 Methodology:

In order to achieve the goal of this thesis methodology is as follows,

a. A literature review of previously conducted research.
b. Design of a representative model breakwater allowing all possible movement randomly-placed double cube layer with a simplified breakwater slope.
c. Measure the rocking behavior of cubes subjected to varying wave height, wave steepness, position relative to the water level and degree of exposure regarding wave attack. The measurements are conducted with an accelerometer and gyroscope placed in the center of the cubes that measures the movements and angular velocity of the cubes.
d. Analyzing impact/collision of armor units.
e. A comparison of the results from the current research project with the results from previously conducted research.

2. Literature Review

After several damages in breakwater armor units different breakwaters an intensive research were conducted by Center for Centre for Civil Engineering Research and Codes (CUR) in the 1980's in order to incorporate the strength of the armor unit in the breakwater design procedure. The tested armor units were double layer cubes and tetrapods. But now a day's most of the rubble mound breakwaters are designed with single layer armor units. In recent years it has been observed that breakage also occurs in these single layer armor units. In order to understand the behavior of single layer armor units a theoretical assessment is conducted for an exposed cube, which rotates around a hinge (Tuan Le, 2016). This chapter gives the thorough analysis of the research performed by CUR C70 1980, Van der Meer 1991 and Tuan Le, 2016 for his master's thesis.

2.1 CUR C70 1989

In order to incorporate the strength of the armor unit in the breakwater design procedure after failure of several breakwaters in late 70's and early 80's, a joint industry research program was initiated under the coordination of the Centre for Civil Engineering Research and Codes workgroup C70 (CUR C70). This research program concluded with a numerical application known as "Rocking" (CUR, 1990b). "Rocking" computes whether double layer armor units break for given hydraulic and geometric conditions in a statistical manner.

2.1.1 Overview

The research program incorporated the analysis of damage cases, physical model tests on rocking behavior, force time relation of colliding concrete units and developing a design procedure for practical application. The tests were conducted on double layer cubes and tetrapods in in order to investigate the strength of the units. These tests result gave an estimation of the probability of breakage of an armor unit which was related to wave height and position of the armor unit in the slope. The number of failed units was calculated using the estimation of the number of moved units and the probability of breakage. The numerical application 'Rocking' was used to conduct Monte Carlo simulation on the calculation procedure. In the application the hydraulic condition and breakwater geometry gives the number of displaced unit using the stability formula. An adjustment was done to represent the range of armor layer movement to incorporate the collision of the units. The total number of moved units was calculated instead of the number of displaced unit for small movements and displaced units. The relationship between impact velocity and momentum during collision was incorporated using the measurement from accelerometer placed inside the armor units during model tests. Maximum stresses inside the armor unit were calculated using the load-time relationship during impact and the momentum of the collision. When the maximum stresses exceed the strength in the critical part of the armor unit it considered to be broken. The average number of collisions, number of moved units and the probability of breakage gave the total number of broken unit on the slope.

2.1.2 Hydraulic Condition and Test Plan

The following hydraulic condition and test plans were used during the research program for double layer cubes.

Table 2.1 Hydraulic Condition for Model Test (Golfbrekers, sterkte betonnen afdekelementen, impulsbelastingen voor kubussen en tetrapodes als gevolg van rocking bij golfaanval) G. Heijdra; M. Sokolewicz; T.M.P.M. Rol-Hoenderop 1988

No	H_{si} (m)	$H_{si'}$ (m)	Tp (sec)
1	0.095	0.080	1.28
2	0.135	0.120	1.46
3	0.170	0.150	1.58
4	0.215	0.185	1.86

H_{si} = Wave height in 40m distance, $H_{si'}$ = Wave height in 8m distance Tp = Peak Period

Position of the armor unit tested were as follows,

- 2Dn over the water line
- At the water line
- 2Dn under the water line
- 4Dn under the water line

2.1.3 Calculation of Collisions and Number of Moved Units

In order to calculate the total number of moved units (N_{otot}) total number of displaced units (N_{od}) using the armor unit stability formula by Van der Meer (1988) for double layer cubes were used as shown in equation 2.1.

$$\frac{H_s}{\Delta Dn} = (6.7\frac{{N_{od}}^{0.4}}{N_{0.3}} + 1){s_m}^{-0.1} \qquad (2.1)$$

The total number of moved units was calculated taking into account the number of displaced units (N_{od}), number of units moved more than 0.5 times the diameter ($N_{o>0.5D}$) and the number of units moved less than 0.5 times the diameter ($N_{o>0.5D}$). After analyzing the data it was found that the reduction in $\frac{H_s}{\Delta Dn} = 0.5$ in equation 2.1 gives the representation of the total number of moved units.The relationship for the cubes in double layer became

$$\frac{H_s}{\Delta Dn} = (6.7\frac{{N_{od}}^{0.4}}{N_{0.3}} + 1){s_m}^{-0.1}\text{-}0.5 \qquad (2.2)$$

In order to calculate the number of broken units the average number of collision was taken into account. For this video image analysis was performed where units were marked moved one time and moved more than one time and it was concluded that the 40% of the moved units collided once but the other 60% could not obtained from the analysis and roughly assumed that the collision of the moving units were more or less on average is 3.

According to the Van der Meer (1988) Stability formula, the initiation of damage for double layer cubes occur when,

$$\frac{\mathrm{Hs}}{\Delta \mathrm{Dn}} = 2.4 \tag{2.3}$$

The CUR 70 (1989) (CUR 1989) shows that the number of moved unit or Rocking occurs with reduction in the stability number by 0.5 which gives the start of rocking can be expected from,

$$\frac{\mathrm{Hs}}{\Delta \mathrm{Dn}} = 1.9 \tag{2.4}$$

2.1.4 Impacts

In order to determine the breakage of a armor unit loads during the collision was estimated using the integration of the acceleration, the impact velocity which then used with incorporating the type of movement for estimation of the momentum during collision. These were used to determine the stresses inside the armor units.

In order to calculate the impact velocity only the acceleration peaks larger than one third of the maximum peak values were used. A relation between hydraulic conditions and acceleration peaks were used instead of using the integrating the acceleration signal over time to determine the impact velocity. This relationship was not explained properly so it’s needed to validate the assumption. The relationships are shown in 2.5, 2.6, 2.7 and 2.8.

For Cubes,

$$p(V/\sqrt{gD_n}) = exp[-((V/\sqrt{gD_n}) - c)/B))] \tag{2.5}$$

$$c = 0.049\, exp(-0.4|y/Dn|) \tag{2.6}$$

$$B = 0.025 exp(-0.4|y/Dn|)Hs/\Delta Dn \tag{2.7}$$

$$(V/\sqrt{gD_n}) = 0.0049\ (a/g) \tag{2.8}$$

For Tetrapods,

$$p(V/\sqrt{gD_n}) = exp[-((V/\sqrt{gD_n})^{1.43} - c)/B))] \tag{2.9}$$

$$c = 0.0103\, exp(-0.4|y/Dn|) \tag{2.10}$$

$$B = 0.0051 exp(-0.4|y/Dn|)Hs/\Delta Dn \tag{2.11}$$

$$(V/\sqrt{gD_n}) = 0.0081\ (a/g)^{0.7} \tag{2.12}$$

Here,

V is the impact velocity [m/s]

a is the acceleration during impact [m/s^2]

B and C dimensionless Coefficients

g is the gravitational acceleration [m/s^2]

H_s is Wave height [m]

D_n Nominal Diameter [m]

Momentum was calculated using the impact velocity and the rocking mode either translation or rotation. For the double layer cubes it was assumed that only translation occurs and no rotation. For translation velocity before impact (Vcollision) was equal to velocity at the center of the unit. The relationships for the velocity of collision and momentum (Vcollision) of the translating unit were applied as follows (CUR, 1990b),

$$\text{Momentum} = MV \tag{2.13}$$

$$V_{collision} = V \tag{2.14}$$

For rotation the relationship are as follow,

$$\text{Momentum} = I_0\omega/Arm_r \tag{2.15}$$

$$\omega = V/0.65h \tag{2.16}$$

$$V_{collision} = \text{Momentum}/M \tag{2.17}$$

Here,

M is mass [Kg]

I_0 is the moment of inertia [kgm^2]

ω is the   angular Velocity [rad/s]

Arm_r is the Distance from Center to the point of Collision [m]

2.1.5 Stresses

In order to determine the stresses in armor units relationship between momentum and forces were applied. “Therefore, as a function of the velocity of collision, momentum and the material contact stiffness, the force-time relationship during collision was obtained. The applied force- time model is shown in Figure 2.1. This diagram is established based on the theory of Hertz (Mier & Lenos , 1991). The maximum force P_m in the armor unit was obtained from this diagram by deriving the maximum value.” (Tuan Le, 2016)

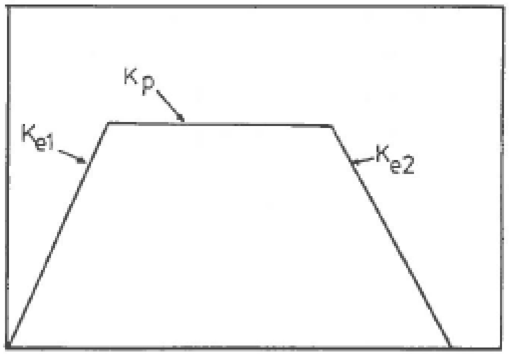

Figure 2.1 Force-Time relationship (CUR , 1990a)

“The parameters Ke1 [N/mm1.5], Ke2 [N/mm1.5] and Kp [N] shown in Figure 2.1 are concrete contact stiffness parameters and were applied for a specific part of the force-time diagram in Figure 2.1. The upward trend took into account the elastic deformation in concrete. The horizontal trend was the plastic deformation and the downward trend represented the restitution of force. Theoretically, the area underneath the diagram represented the momentum of the colliding unit”. (Tuan Le, 2016)

To determine whether a collision was plastic or elastic parameter Kp [N] was applied (CUR , 1990b),

$$K_p = \left(\frac{d}{420}\right)^2 90^2 \frac{\pi}{4} \frac{B}{45} 150 \quad (2.18)$$

Here,

d = Diameter of the leg [m]

B = Compressive Strength [N/mm^2]

This Kp [N] was compared with the theoretical maximum force $P_{max,2}$ [N] over time $T_{max,2}$ [sec] in the descending brunch (CUR, 1990b),

$$Pmax,2 = (1.25\alpha V^2 {K_{e2}}^{0.65})^{0.6} \quad (2.19)$$

$$Tmax,2 = 1.47(1.25\alpha/\ (V^{0.5} K_{e2}))^{0.4} \quad (2.20)$$

For Pmax,2 <Kp the collision was considered elastic and during the model test the cubes were observed to have elastic collision. For elastic collision following relationship was applied,

$$Te2 = Tmax,2/л/2\ arccos((Pmax,2\ Tmax,2 - (0.5MV)0.5л)/(Pmax,2\ Tmax,2) \quad (2.21)$$

$$Pe2 = Pmax,2\ sin(Te2\ л/2\ /Tmax,2) \quad (2.22)$$

The rising brunch was characterized (CUR, 1990b) by,

$$Pmax,1 = (1.25\alpha V^2 {K_{e1}}^{0.65})^{0.6} \quad (2.23)$$

$$Tmax,1 = 1.47(1.25\alpha/\ (V^{0.5} K_{e1}))^{0.4} \quad (2.24)$$

$$Te2 = Tmax,1/л/2\ arcsin(Pe2/Pmax,1) \quad (2.25)$$

The surface area A1 [kgm/s] underneath the rising brunch was calculated using (CUR, 1990b),

$$A1 = Pmax,1\ Tmax,1/л/2\ (1 - cos(Te1/Tmax,1\ л/2)) \quad (2.26)$$

For elastic deformation the surface area A2 [kgm/s] underneath the descending brunch was (CUR, 1990b),

$$A2 = 0.5MV \tag{2.27}$$

After construction of the force-time relationship, the maximum force (Pm) was determined. Parameter Pm [N] was considered to be equal to Pe2 [N]. In addition, the time span in which the maximum force was built up Tm [s] was equal to Te1 [s]. For a plastic collision the following relations were applied for the time span (CUR , 1990b)

$$Tp = MV - (A1 + A2)/Pe2 \tag{2.28}$$

$$Tm = Te1 + Tp \tag{2.29}$$

The stresses of failure mode for cubes were considered as the tensile stresses perpendicular to the plane and determined using the following relation,

$$\sigma = 0.64\, Pm/Dn\hat{}2 \tag{2.30}$$

2.1.6 Strength

“The actual concrete strength was needed to conclude whether an armor unit fails. The strength was compared with the stresses calculated in Subsection 2.1.5. A calculation was done by multiplying the characteristic axial tensile strength of a cylinder with diameter of 150 mm and height of 600 mm with the following correction factors for (CUR , 1989)” (Tuan Le 2016),

1. Volume
2. Temperature
3. Duration of collision

“Correction factors for fatigue were not taken into account, since these effects only play an important role after 10 collisions. It was assumed that not many elements collide more than 10 times. A reduction of the tensile strength was considered for a larger volume than the considered cylinder parameter Kv.” (Tuan Le 2016)

For cubes in double layer the volume taken into account is as follows,

$$Kv = 0.80 D_n{}^{-0.12} \tag{2.31}$$

The reduction in tensile strength Kt for cubes in double layers were calculated using,

$$Kt = 0.74\, D_n{}^{-0.20} \tag{2.32}$$

The correction factor for effect of duration of collision Ks was calculated using ,

$$Ks = (S/S0)^{0.42} \tag{2.33}$$

Here,

S = Actual Collision duration [N/mm^{2}s]

S_0 = Reference duration of 0.1 [N/mm^{2}s]

The total strength of concrete was calculated using the following equation,

$$fc = 0.80Dn^{-0.12}\ 0.74\ D_n{}^{-0.20}(S/S0)^{0.42}fco \qquad (2.34)$$

2.1.7 Summary

Although the discussed research programs give very detailed results on the rocking behavior there are several aspects that can be discussed.

Rocking can occur due to the collision of the unit with the neighboring unit as well as with units in the underlayer. The latter were not taken into account during calculation of N_{0tot}, so it may be possible that the number of colliding units may be underestimated. And also there is a possibility for a rocking armor unit to move back to its original position. The proposed analysis of the changing position of units before and after the test may not give satisfactory result for such units.

The number of collision calculated using the average number of collision was a rough assumption and did not provide any proof and Tuan Le 2016 has shown in is research that the number of collision is continuous after the initiation of movement (Section 2.2.4).

The tests were conducted using non directional wired accelerometer and these measurements were accurate when the acceleration was in the direction of the installed accelerometer. As they were wired it can be assumed the wire would have influenced the degrees of freedom of the armor units which cannot be excluded from the result.

The mode of movement is restricted to either rotation or translation for simplistic calculation but there is no analysis if the rotation or translation both causes movement.

The force from plastic deformation was always assumed to be constant. In practice this does not have to be the case, since hardening or softening of the material can occur during the loading (Mier & Lenos, 1991).

The relationship in equation 2.5 and 2.9 needed to be validated as these relationship were not explained briefly in the research program.

The impact in the model will be prone to scale and model effects (the elements have a different material, and the scaled elasticity is different (Cauchy-scaling), while the impact velocity is expected to follow Froude scaling. Therefore the focus on measuring the acceleration during the impact itself seems suboptimal.

2.2 Tuan Le's work:

For better understanding of the rocking behavior the research project done by Tuan Le, 2016 was to obtain knowledge on and measurements of the rocking behavior and failure mode of single layer armor units by wave flume experiments are conducted on a single cube.

2.2.1 Hydraulic Condition and Test Plan

The following hydraulic condition and test plans were used during the research program for cubes.

H_{m0} = 0.06 – 0.16m

$T_{m-1.0}$ = 1.1 – 2.5s

$s_{m-1.0}$ = 0.02 – 0.04

Here,

H_{m0} is the model wave height,

$T_{m-1.0}$ is the Wave Period

$s_{m-1.0}$ is the wave steepness

Position of the armor unit tested were as follows,

- $2D_n$ above the waterline
- At the water line
- $2D_n$ under the water line
- $4D_n$ under the water line

2.2.2 Experimental Set-up

An experimental set-up was done in the wave flume using a cube attached with a hinge allowing it to rotate only in one direction was placed on a smooth, continuous slope of 1/1.5. The experiment was performed in instrumented unit placed on at $2D_n$ above mean water level, at mean water level, $2D_n$ below mean water level. The hydraulic conditions were varied in terms of wave height, wave steepness and wave type. Another cube was used which was fixed at its location without any rotation to measure the water pressure. Additionally measurements of the wave run-up velocity were conducted. Another set of experiment was done using the embedded cube as representation of a prototype breakwater.

2.2.3 Measurement Equipment

The measurement was done using an accelerometer (ADXL335) to calculate the angular acceleration of the center of the armor unit. The device was placed in the center of the armor unit. As the accelerations were linked to the wave conditions, wave gauges (Deltares Wave Height Meters) were used to measure the wave conditions. Furthermore, velocities on the slope and pressures exerted on a fixed cube were measured using pressure sensors. In order to measure the wave front velocity an industrial camera is used from “The Imaging Source” with sensor of type Aptina MT9P031.

2.2.4 Analysis of Experiments Results

Most realistic observation for the test program ran by Tuan Le was with the embedded Cubes. This section will focus on the comparison of Le’s observation for embedded cube with the CUR 70 (1989) research program.

The test program showed that the probability of exceedance for larger wave height tends to have larger angular velocity. This dependency is also observed in CUR 70 (1989) measurements.

The test program also identifies the dependency on wave steepness which was not included in CUR 70 (1989) and research by Sokolewicz (1986) also pointed out that in CUR 70 (1989) the wave steepness were similar. So equation 2.5 and 2.9 needed to be modified with wave steepness parameter.

The test program gives different result regarding the dependency on the slope position. According to Tuan Le’s work the Y/D_n= -2 gives the highest probability of exceedance which is different from the CUR 70 (1989) indicating the highest probability of exceedance occur at the water line Y/D_n =0. This result is also needed to be validated.

The test program observed that the embedded cube shows that the embedded cubes are showing 25% higher values regarding the relation developed in CUR 70 (1989) test program. But two test program has completely different setup therefore no quantitative conclusions can’t be made. This should also need to be validated.

2.2.5 Summery

Several simplifications were made in order to determine the acceleration and velocity analytically which leaded to deviation from the experimental wave flume result. Firstly it was assumed that the drag force was working over the entire front area of the cube. Second assumption was using the relation for the impact velocities by Goda et al (as cited in Chella, Torum & Myrhaug (2012)) on the armor unit. Third assumption was using the formulae by Van Gent (2002) and Schuttrumpf & Oumeraci (2005) but these formulae neglect the variations of velocities over the flow depth and neglect fluctuations in form of vortices. The forth assumption was a constant acceleration of water in time. Final assumption was taking into account only the accelerations at the start of the movement.

The experiment showed that the number of collisions increased with the increasing wave height which was valid for all the positions used in the experiment. The result of the tests also showed that the numbers of collisions were increased with the increased steepness (0.02 to 0.04). The result of the test also indicated that the numbers of collisions were dependent of the wave height, wave steepness and the position of the cube in the slope. It was observed that all hydraulic conditions for a position of -2Dn, both exposed and embedded cube, result in the same range for the start of collisions.

3. Model Setup

In order to determine the spatial and stochastic distribution of the rocking behavior and strength of the breakwater armor unit this research program is going to perform some physical model test of cubes in double layer and single layer. If one can understand the behavior for cubes it will be possible to go further checking the different armor unit. This section of the report will discuss the different parameter to be used in this model setup.

3.1 Overview

Determination of rocking behavior is a complicated process and it depends on many parameters such as wave height, wave period, the position of the armor unit, the acceleration and the impact velocity of the armor unit. In this report the main focus would be on the distribution of the impact velocity for different position on the slope. Firstly the test would be running in double layer cube and compare with the previous research data discussed in Chapter 2 and then the test would be running in cube in single layer.

3.2 Scaling

The model has to represent the physical behavior of the prototype breakwater. There are several criteria for the model to be met (Frostick, McLelland & Mercer, 2011) as follows,

Firstly, the model must be geometrically undistorted in length scale. Meaning the model must represent the geometry of the prototype.

Secondly, the kinematic similarity of the model representing the fluid particle motion similarity between model and prototype. So the time must be representative of the fluid particle motion of the prototype.

Thirdly, the dynamic similarity must be representative meaning the similarity of the masses and the forces of model and prototype. This third similarity may be impossible to maintain completely as surface tension, dynamic viscosity and density cannot be scaled.

For these reason the breakwater modeling is performed using dimensionless relationship discussed in this section.

3.2.1 Dimensionless Scaling

Froude Number

The first dimensionless criteria is the Froude number (equation 3.1) which represent the ration of inertia and gravitation. In order to represent similarity of the behavior of the model with prototype the Froude number should be same. The scaling factor for length is a function of time and velocity using the relationship $N_u = N_T = N_l^{0.5}$ (N_l = Factor for length, N_T = Factor for Time & N_u = Factor for velocity).

Froude Number, $Fr = \frac{u}{\sqrt{gh}}$ (3.1)

Reynolds Number

The Reynolds number as presented by Dai & Kamel (1969) shown in equation 3.2 represents the relationship between inertia and viscosity and depends on the significant wave height (Hs) and Nominal Diameter (D_n). According to Dai & Kamel (1969) in order to maintain turbulent flow for the model Re should be greater than $3*10^4$.

Reynolds Number, $Re = \frac{\sqrt{gh}Dn}{v}$ (3.2)

Weber Number

The relation between the inertia and surface tension is represented by the dimensionless relationship of Weber Number as in equation 3.3.The effect of the surface tension should be kept minimum and this implies that the minimum wave height should be 5cm, the minimum wave period should be 0.35s and the wave runup should be at least 0.022 m (Pullen et al, 2007).

Weber Number, $We = \frac{\rho u^2 L}{\sigma}$ (3.3)

Strouhal Number

Relation between the local inertia and convective inertia is represented by the dimensionless Strouhal number as in equation 3.4. The vortex shading effects (Von Karman) having the same frequency and the relationship as Froude number can be stated, $N_u = N_T = N_l^{0.5}$ (N_l = Factor for length, N_T = Factor for Time & N_u = Factor for velocity).

Strouhal Number, $St = \frac{L}{uT}$ (3.4)

Stability Number

This dimensionless relationship represents the wave height over the multiplication of relative density (△) and the dimension of the unit (D_n) as shown in equation 3.5 have to be same for the prototype and model.

Stability number, $Ns = \frac{Hs}{\Delta Dn}$ (3.5)

3.3 Dimension of Model Armor Unit

The model of the armor unit has to be a size so that the measuring instrument can be placed inside it with the cable. The cube with 4cm height seems to satisfy the criteria. If a fictional prototype of 1m is represented with the model cube then the scaling factor for the cube is 1/25 according to the Froude and Strouhal number.

The nominal diameter of the cube is 4.03cm and the average density of the cube is 2464 Kg/m^3. Figure 3.1 shows the instrumented cubes,

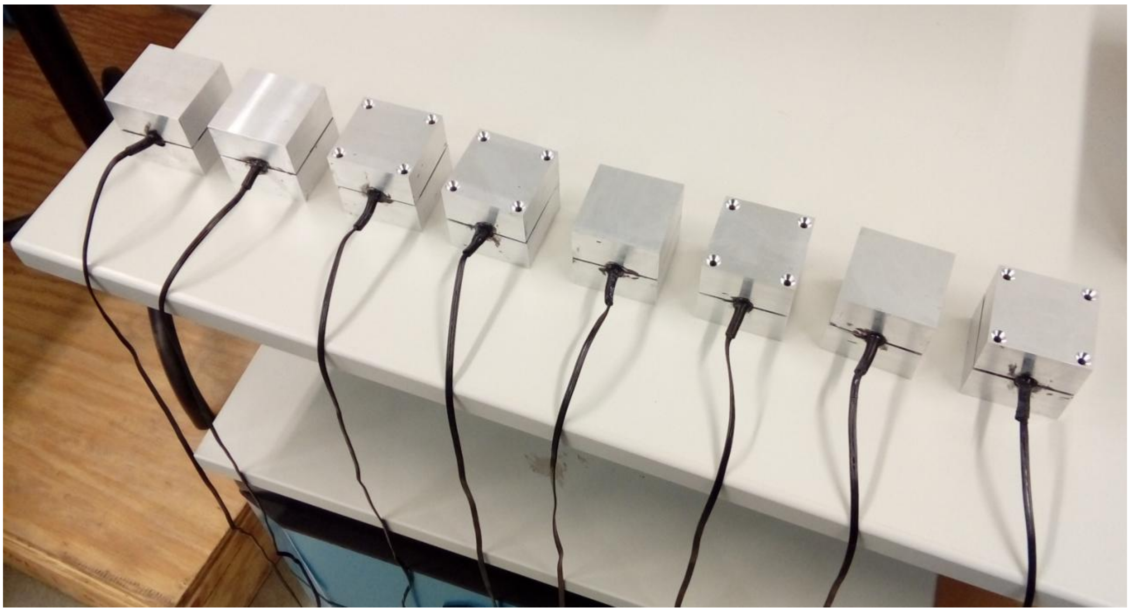

Figure 3.1 Instrumented Cubes

3.4 Hydraulic Condition

To get sufficient data hence sufficient movement of the model armor unit the range for the stability number is chosen to compare the result with the CUR 70 (1989) (CUR 1989) as follows,

$$\frac{Hs}{\Delta Dn} = 1.4 - 2.4 \tag{3.8}$$

To represent the wind wave characteristics the wave steepness is chosen $s_{m-1.0}$ = 0.02-0.04 which gives the representing the both plunging and surging breaker types. With the following relation the hydraulic condition for the model setup is chosen as follows,

Table 3.1 Hydraulic Condition for the Model Test

Hs (m)	$s_{m-1.0}$	$T_{m-1,0}$ (s)
0.08	0.02	1.60
0.11	0.02	1.85
0.14	0.02	2.12
0.08	0.04	1.13
0.11	0.04	1.31
0.14	0.04	1.50

These hydraulic conditions are within the scaling restrictions following from the surface tension/Weber number (H >0.05m and T >0.35s) discussed in Section 3.2.1, and from the Reynolds number/viscosity. The latter for the above hydraulic conditions starts at $3.53*10^5$ which satisfy the Reynolds Number criteria ($Re_{(H)}>3*10^4$) discussed in Section 3.2.1.

3.5 Experimental Setup

The wave flume setup is done using double layer cube of 4cm height and the underlayer acting as a permeable layer with D_n = 2cm to represent the breakwater situation. As the underlayer is permeable there will be no water level difference inside and outside of the breakwater. The slope of the flume is taken as 1:1.5 as it was in the CUR 70 (1989) (CUR 1989). The setup is shown in figure 3.1.

In this test program the instrumented cubes (8 Cubes) will be placed in a stable position and the water level will be varied to change the position of the cube related to water level. Here Y is the distance of the cube center to the mean water level (MWL) and D_n is the nominal Diameter of the instrumented cube. So the level Y= $2D_n$ represent the position above the water MWL to the twice the distance of the cubes nominal diameter. The position Y=$0D_n$ Represent the cubes at the MWL and Y=-$2D_n$ & Y=-$4D_n$ represent the cube position below the water level. The front view of the setup is shown in Figure 3.2 below,

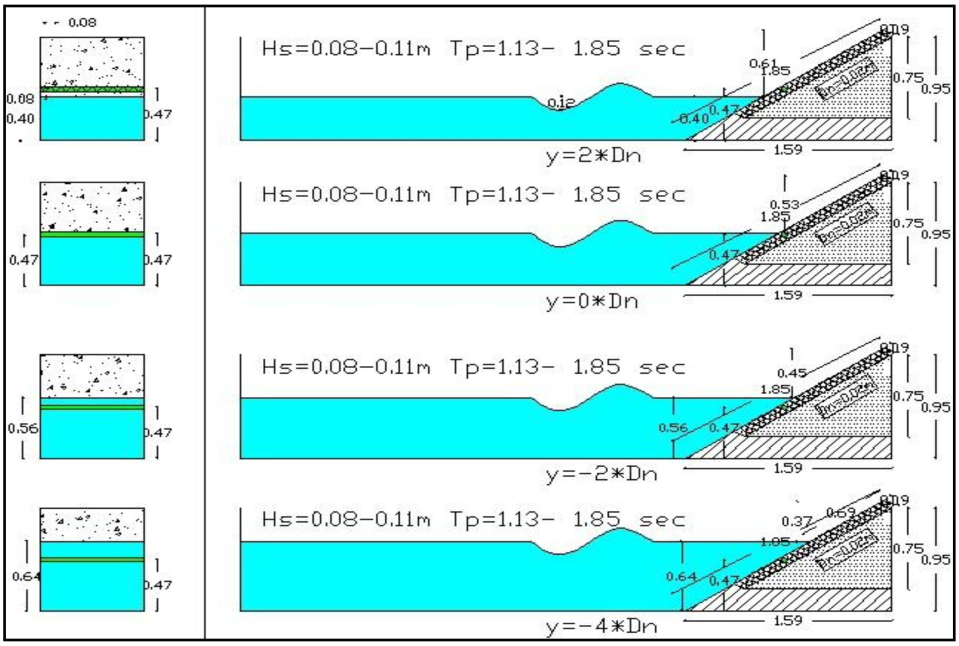

Figure 3.2 Flume Setup (Side View)

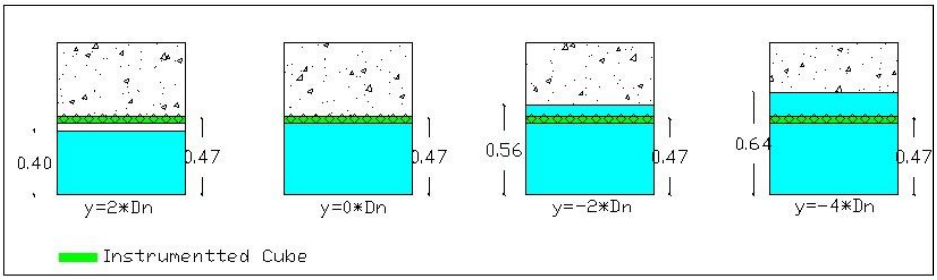

Figure 3.3 Position of the instrumented cube (Front View)

During each water level and cube position the wave height and the wave period will be changed in order compare the data with the CUR 70 (1989) (CUR 1989). The change of wave period will represent the change in the wave steepness.

3.6 Measuring Equipment

For this test program eight cubes of 4 cm is used and the measuring device Tinyduino will be placed in center of the cube. These cubes will be placed for measurement as discussed in section 3.5.

For the measurement of the acceleration and the angular velocity the measuring sensor from Deltares Tinyduino (Figure 3.2) is used. The following sensor can measure the acceleration from ±2g to ±16g and gyroscope can measure the angular velocity ranging from ±250°/s to ±2000°/s. The following datasheet from the manufacture show the full specification as follows in Table 3.2.

Figure 3.4Tinyduino Sensors

Table 3.2 Specification of the Tinyduino Sensor

Sensor	Feature
Accelerometer	Digital-output 3-Axis accelerometer with a programmable full scale range of ±2g, ±4g, ±8g and ±16g Integrated 16-bit ADCs enable simultaneous sampling of accelerometers while requiring no external multiplexer Orientation detection and signaling Tap detection User-programmable interrupts High-G interrupt
Gyroscope	Digital-output X-, Y-, and Z-Axis angular rate sensors (gyroscopes) with a user-programmable full-scale range of ±250, ±500, ±1000, and ±2000°/sec External sync signal connected to the FSYNC pin supports image, video and GPS synchronization Integrated 16-bit ADCs enable simultaneous sampling of gyros Enhanced bias and sensitivity temperature stability reduces the need for user calibration Improved low-frequency noise performance Digitally-programmable low-pass filter Factory calibrated sensitivity scale factor

3.6.1 Calibration and Validation

As the accelerometer sensor gives the data in ‘g’ each of the sensor when placed in a plane the vertical value should give the 1g value and if it’s placed in a slope the acceleration vectors will give a resultant acceleration of 1g irrespective of the orientation. To validate the accelerometer simply placing the sensor in a horizontal plane would exert acceleration in vertical direction with 1g and other direction will show zero.

The gyroscope measure the angular velocity which can be validated using the sensor placed in a plane in a vertical axis and let it fall. As the height of the arm is known and the time is known it would be possible to calculate the average angular velocity. It should be kept in mind this average angular velocity will give higher value than the mean angular velocity and the lower than the peak velocity measured by the gyroscope.

3.6.1.1 Static Condition Measurement

In this test the sensor is placed in static condition for continuous three hours without movement figure 3.4. This way the axis in the direction of the earth gravity should give the value 1g and other values should be zero. As the sensor is not moving the angular velocity along all axis should also give zero value.

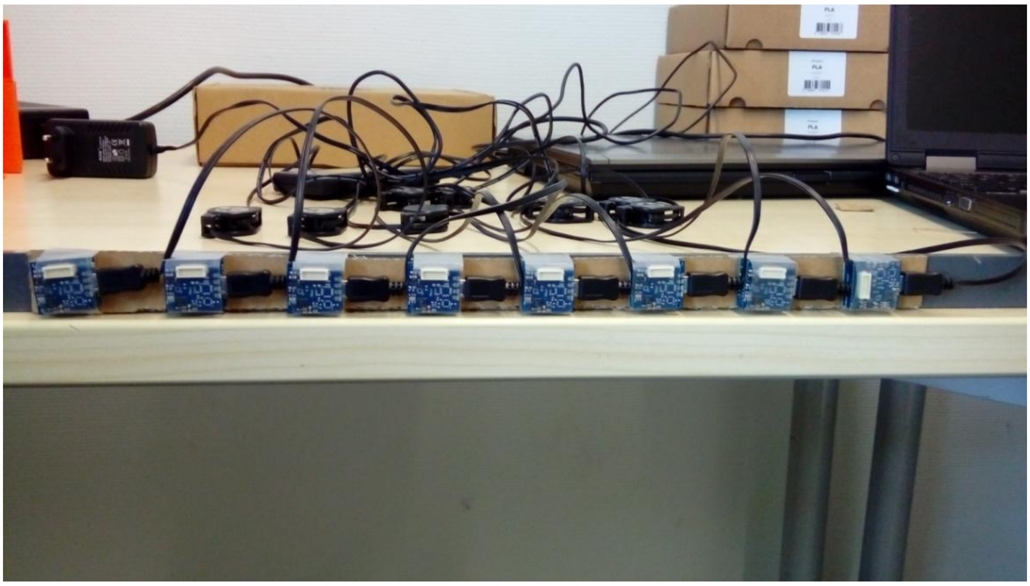

Figure 3.5 Static Condition Measurement of the Sensors

All of the sensors give zero value for angular velocity during static condition in all direction but all the accelerometers gives slightly different value than 1g in the direction of gravity. The value of acceleration varies from 0.97g to 1.04g and also the value show a lot of noise during even in static condition.

So Bias in acceleration measurement is about +/- 0.03g. The noise was 0.07g.

The noise in the rotation measurement was 0 rad/s.

3.6.1.2 *Falling test*

This test is done to check the accuracy of the angular velocity measurement figure 3.5. In this test all the sensors are placed on a plate that falls with one hinged end. As the sensor falls freely no other force was applied apart from the self weight of the plate with sensor. The calculation is done using the gravitational force only other forces (centrifugal force, centripetal force, winds induced resistance and tangential force) were not taken into account.

Initially the sensor's X axis was perpendicular (90º) and Z axis was in parallel (0º) with respect to the surface direction and the change in angle was 90º. All sensors should measure the angular velocity which should give the final angle of 90º. As the angular velocity is the time derivative of the change in angle. This angle can be calculated using the following integration formula,

$$\theta = \int_0^t \omega dt \qquad (3.9)$$

θ is the angle

ω is the angular velocity in respective direction

t is the time

The signal from acceleration is also used to calculate the angle using the following formula,

$$\theta = \sin^{-1}(ax) \qquad (3.10)$$

ax is acceleration in X axis.

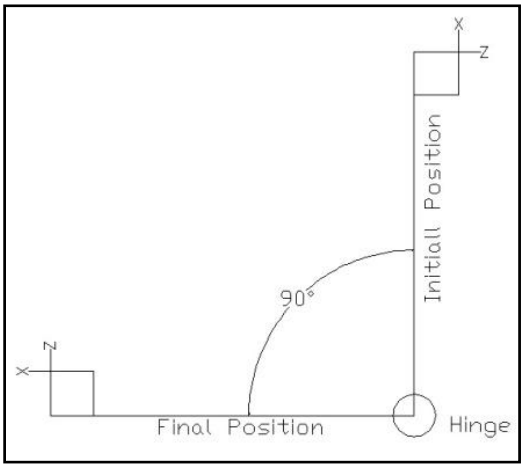

Figure 3.6 Falling Test

After the falling test all the sensor gives the angle value of 89.34º on average. The result of the integration is shown in figure 3.7 for all eight sensors. The X axis shows the time as the data acquired in different time there is a time lag between all the sensors. Y axis shows that the initial change in angle is 0 and final change in angle is 90º.

The legend c7, c8, c9, c10, c11, c13 and c14 represent the angle from angular velocity and c7_accel, c8_accel, c9_accel, c10_accel, c11_accel, c12_accel, c13_accel and c14_accel are representing data calculated from acceleration from. It can be seen from the figure that the angle calculated from the acceleration is giving noisy signal as discussed in 3.6.1.1.

The signal from the gyroscope has an error of 0.43°/s (0.007 rad/sec).

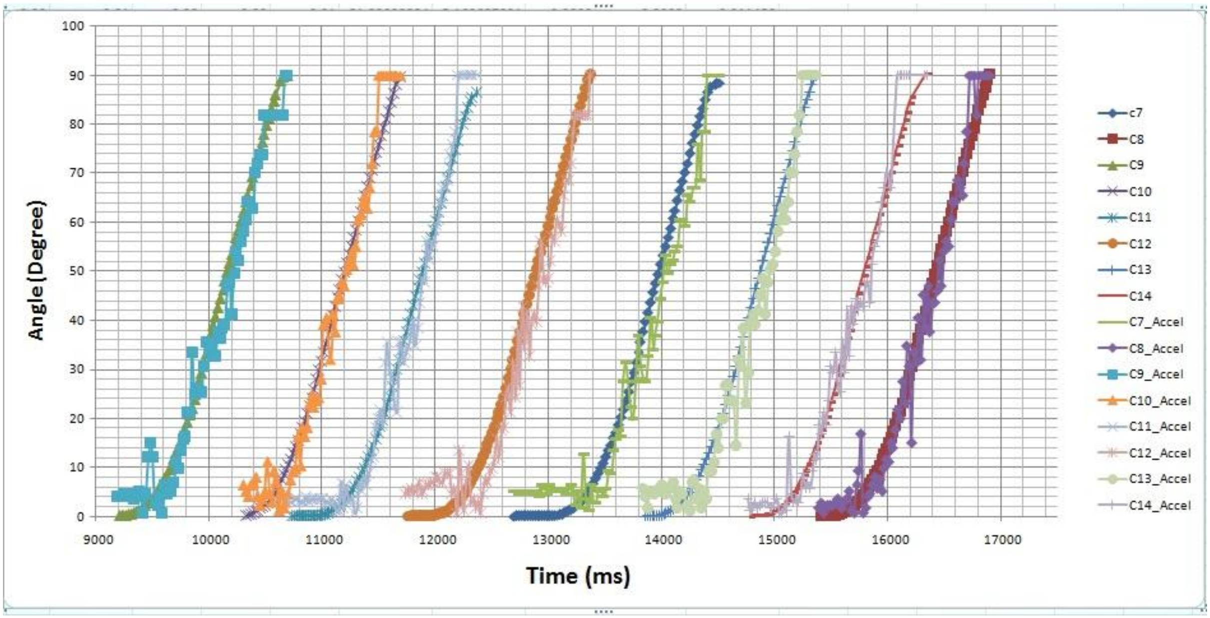

Figure 3.7 Change in angle over time due to falling test of eight sensors

3.7 Test Program

The test program is chosen to be executed with irregular wave conditions as previous research in CUR 70 (1989) (CUR 1989) showed that most movements occur for irregular waves, thus giving large variation in the acceleration and angular velocities. For this purpose the standard Jonswap spectrum is chosen to simulate the model to represent the common breakwater in a coastal region with young sea state. The hydraulic condition for the model test is shown in Table 3.1. Test program for the irregular waves are given below in Table 3.3.

Table 3.3 Test Program for Irregular Wave

File Name	Wave Height, H_{m0} (m)	Wave Period, $T_{m-1,0}$ (s)	Wave Steepness, $S_{m-1,0}$ ( )	Stability Number, $\frac{Hs}{\Delta Dn}$ ( )	Position, Y/Dn ( )	Water Depth, d (m)
0811347	0.08	1.13	0.04	1.4	0	0.47
0816047	0.08	1.60	0.02	1.4	0	0.47
1113147	0.11	1.31	0.04	1.8	0	0.47
1118547	0.11	1.85	0.02	1.8	0	0.47
1415047	0.14	1.50	0.04	2.4	0	0.47
1421247	0.14	2.12	0.02	2.4	0	0.47
0811356	0.08	1.13	0.04	1.4	-2	0.56

File Name	Wave Height, H_{m0} (m)	Wave Period, $T_{m-1,0}$ (s)	Wave Steepness, $S_{m-1,0}$ ( )	Stability Number, $\frac{Hs}{\Delta Dn}$ ( )	Position, Y/Dn ( )	Water Depth, d (m)
0816056	0.08	1.60	0.02	1.4	-2	0.56
1113156	0.11	1.31	0.04	1.8	-2	0.56
1118556	0.11	1.85	0.02	1.8	-2	0.56
1415056	0.14	1.50	0.04	2.4	-2	0.56
1421256	0.14	2.12	0.02	2.4	-2	0.56
0811364	0.08	1.13	0.04	1.4	-4	0.64
0818564	0.08	1.85	0.02	1.4	-4	0.64
1113164	0.11	1.31	0.04	1.8	-4	0.64
1118564	0.11	1.85	0.02	1.8	-4	0.64
1415064	0.14	1.50	0.04	2.4	-4	0.64
1421264	0.14	2.12	0.02	2.4	-4	0.64

4. Analysis of Tetrapod Data

This chapter is focused on the analysis of rocking measurements with an instrumented tetrapod in a double layer. Existing measurements obtained at Deltares will be used. The results of these tests will be analyzed and the results will be compared with the CUR 70 (1989) test program. These tests were done using the Tinyduino device inside the tetrapod as a stand alone device in Deltares, as described in Section 3.6. The data are not publicly available.

4.1 Test Setup

The tests on the tetrapods were done in a 3D model and the measuring tetrapod was placed at the water line $Y/D_n=0$ as it was found in CUR 70 (1989) that armor unit at water level shows maximum probability of exceedance. The senor is placed in the center of the tetrapod unit. The sensor acts as a standalone condition which was powered by a small battery. And the data were stored in the flash memory.

The Nominal Diameter of the tetrapod is 0.068 cm (Figure 4.1) and the density of the unit is 2450 kg/m^3 which is almost similar (2400 Kg/m^3) to the other concrete tetrapod units in the test program.

Figure 4.1 Instrumented Tetrapod for Test Program

The test setup was performed in 1:1.5 slope and the instrumented tetrapod was placed on the waterline. The sampling frequency of the instrument was set to 32.5 Hz to acquire the data. The test setup before the test program is demonstrated by Figure 4.2 and Figure 4.3 demonstrate the position of the instrumented tetrapod. In the Figure 4.3 it can be clearly seen that the instrumented tetrapod is placed just on the water line.

Figure 4.2 Tetrapod Position in Test Setup

Figure 4.3 Tetrapod Position During the test with respect to water level

4.2 Hydraulic Condition

Test program with the instrumented device was ran using two different wave height with same wave steepness 0f 0.02 and same position at Y/D_n=0 (Water line). The wave heights used during the measurements were 0.09m and 0.11m with wave period of 1.84s and 1.81s. Below table demonstrate the hydraulic condition of the test setup.

Table 4.1Hydraulic condition of the test setup for instrumented tetrapod

Test program t203		Test program t203b	
Hs (m)	Tp (s)	Hs (m)	Tp (s)
0.09	1.81	0.11	1.84

4.3 Processing of the Data

4.3.1 Raw data Processing

There are two sets of data collected using the Tinyduino processor. These data is processed using Matlab script (APPENDIX 1). The raw data is very scattered and in order to process the raw data different threshold values are used for accelerometer and gyroscope (Figure 4.1 & 4.2).

Threshold values for the sample ‘t203’ processed used with 1.05 m/s^2 & 1.025 m/s^2 for the accelerometer data and for gyroscope the threshold value applied are 0.30 rad/s and 0.205 rad/s. The second sample ‘t203b is applied with value of 1 m/s^2 and 0.95 m/s^2 for accelerometer and for gyroscope the threshold values is 0.15 rad/s.

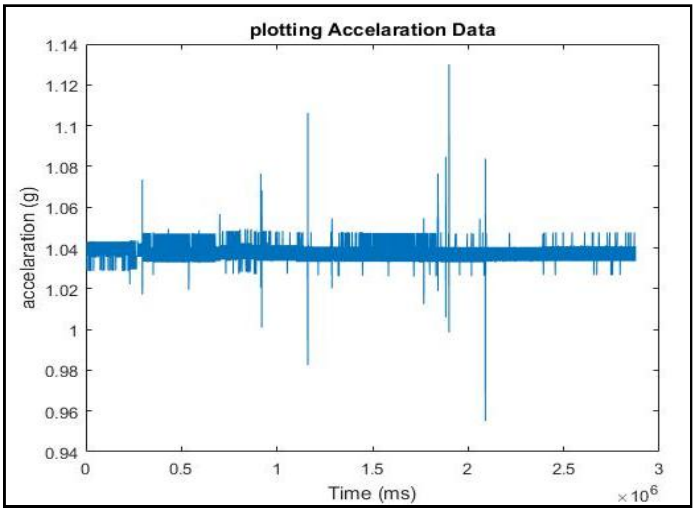

Figure 4.4 Raw accelerometer data of t203

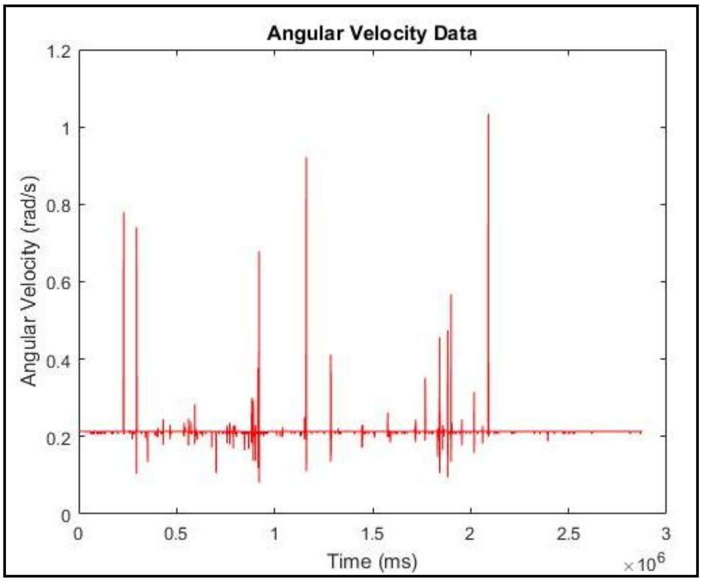

Figure 4.5 Raw angular velocity Data t203

After application of the threshold value the raw data are smoothed and it is possible to process them properly. The impact velocity was calculated using by finding the peak values for both acceleration and the gyroscope. To compute the impact velocity both acceleration and gyroscope data is used.

4.3.2 Impact Velocity Calculation

Impact velocity is calculated using both the accelerometer and gyroscope data. This segment briefly explains the calculation procedure.

4.3.2.1 Assumptions for Data Processing

There are few assumptions taken into account during data processing to reduce complexity of the calculation of impact velocity. The assumptions are described below,

- Number of collision is equal to the number of peaks in angular velocity signal.
- Impact velocity is caused by the resultant angular velocity from three axis (section 4.3.2.3).
- Impact velocity is the tangential velocity of the armor unit rotating (section 4.3.2.3).

4.3.2.2 Accelerometer Data

The accelerometer gives three values of acceleration ax, ay and az in X, Y and Z direction respectively and this three acceleration causes a resultant acceleration which cause this element to move on the direction of the resultant acceleration as crudely demonstrated in figure 4.6. So during data processing using the accelerometer it is assumed that the movement of the instrumented tetrapod is caused by this resultant acceleration a(res). In the figure subscript (a) represent the initial condition just before movement and subscript (b) is demonstrating the position after the movement. It is also needed to be reminded that the figure 4.6 is a qualitative representation of the movement.

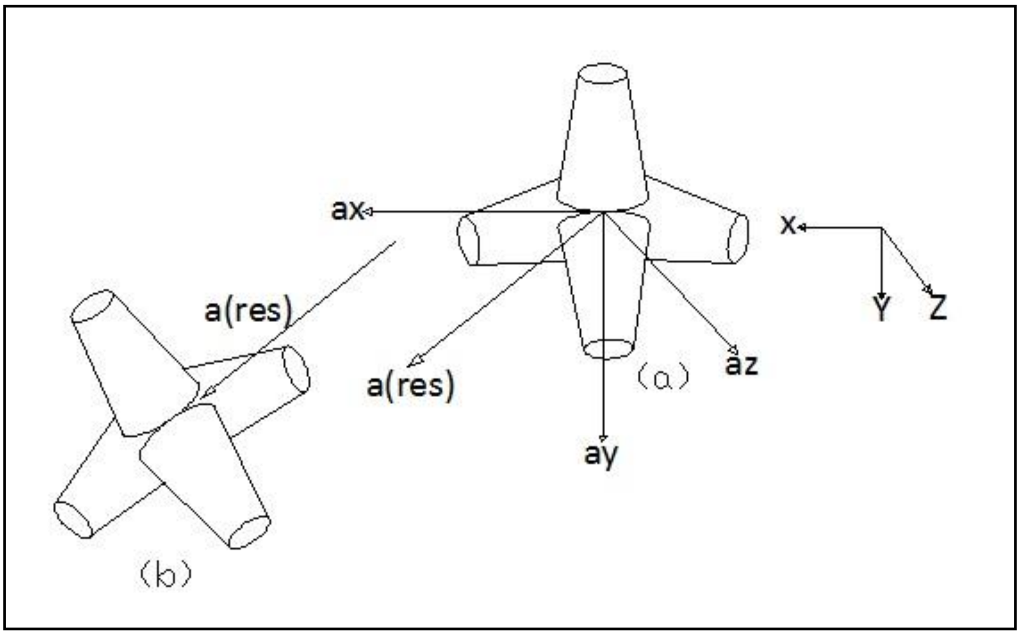

Figure 4.6 Tetrapod movement due to acceleration

This resultant acceleration has a magnitude and a direction. During this report the direction is neglected and only the magnitude of this resultant acceleration is taken into account. The magnitude of the resultant acceleration is calculated using the formula below,

$$a(res) = \sqrt{ax^2 + ay^2 + az^2} \tag{4.1}$$

The impact velocity is then calculated using the resultant acceleration magnitude by integrating the area under the curve of the peak of the resultant acceleration just before collision. The figure 4.7 demonstrates the procedure.

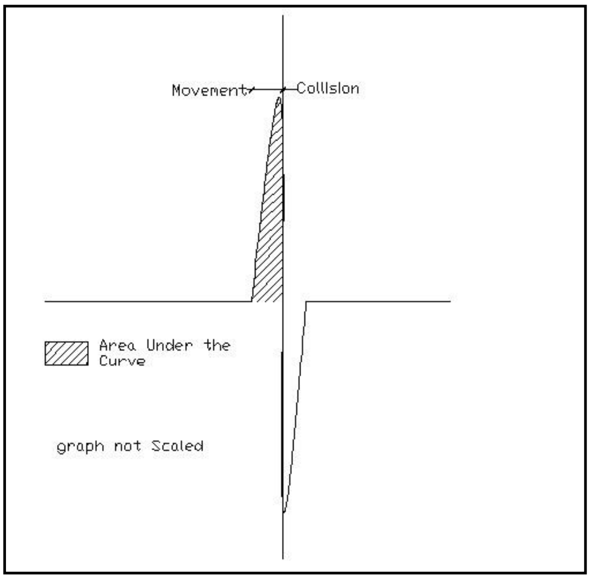

Figure 4.7 Representation of impact velocity calculation using area under the curve

4.3.2.3 Gyroscope Data

Like the acceleration, the angular velocity from gyroscope is also working as gx, gy and gz around X, Y and Z axis respectively. But as the element only moves in one direction due to these three angular velocities so here also it is assumed that the movement is caused by the resultant g(res) of these three angular velocities. Figure 4.8 tries to demonstrate crudely the movement due to the resultant angular velocity.

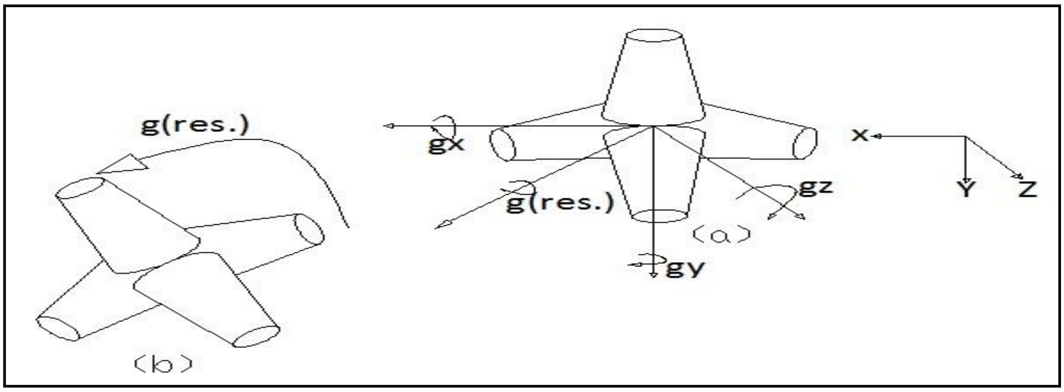

Figure 4.8 Tetrapod movement due to angular velocity

The magnitude of the resultant angular velocity is calculated using the following formula,

$$g(res) = \sqrt{gx^2 + gy^2 + gz^2} \tag{4.2}$$

The impact velocity is calculated by calculating the tangential velocity from the magnitude of the resultant angular velocity as it is assumed that the impact velocity is the tangential velocity of the armor unit moving. The tangential velocity is then calculated using the following formula,

$$Vi = g(res) * L \tag{4.3}$$

$g(res)$ is the instantaneous magnitude of the resultant angular velocity

L is the distance from the center to the impact point

Due to reduce complexity it is assumed for tetrapod L is the equal to the nominal diameter of the Tetrapod unit. For the cube this parameter L is equal to the nominal diameter of the cube which has been applied during the data process for cubes. Figure 4.9 demonstrating the impact velocity from the angular velocity.

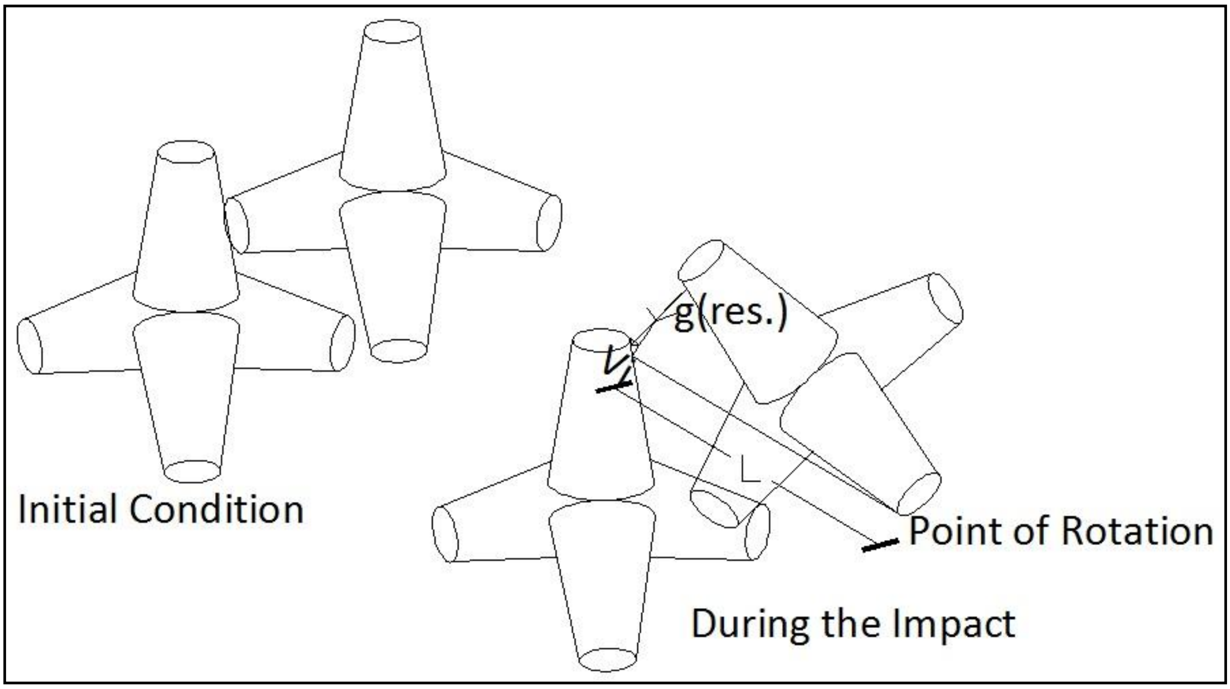

Figure 4.9 Impact velocity from the angular velocity

For the calculation of impact velocity each peak angular velocity is counted as an impact and this peak g(res) from the resultant angular velocity signal is used to calculate the impact velocity in the matlab script. Figure 4.10 demonstrate the peak angular velocity from signal.

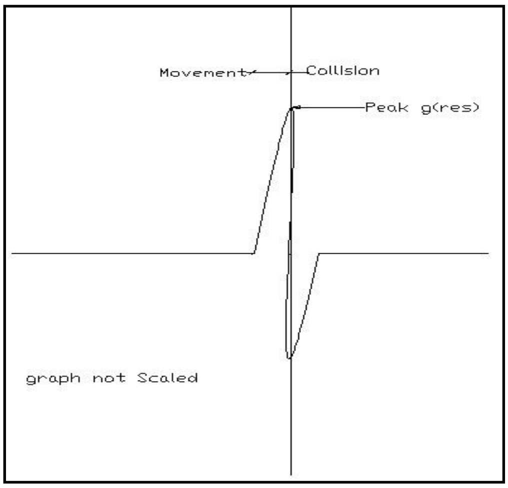

Figure 4.10 Peak angular velocity from the signal

4.3.3 Comparison of Angular Velocity Calculation

As there is no integration required for calculating the angular velocity this method will be used to calculate the impact velocity for the test program of this thesis project. Figure 4.3 shows the result of impact velocity from both acceleration data and the angular velocity data.

From figure 4.3 it can be seen that the magnitude of the impact velocity is larger for calculation using the angular velocity data than the acceleration data but the trend of the data is similar. By analyzing this trend it can be said that as the impact velocity from the acceleration data is calculated by integrating the area under the curve before collision which may be underestimating the impact velocity and therefore for this thesis project the impact velocity will be calculated using the angular velocity data using the procedure described in section 4.3.2.

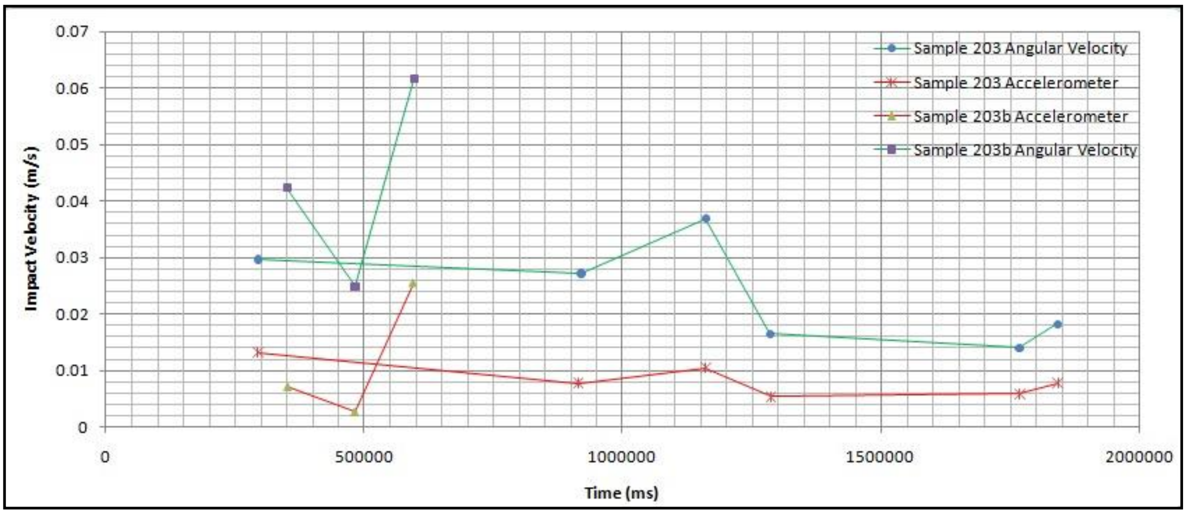

Figure 4.11 Impact Velocity from both acceleration and angular velocity

4.4 Result analysis

The result from the analysis is discussed in this section comparing the previously conducted research CUR 70 (1989).

4.4.1 Distribution of Impact Velocity

Distributions of exceedance of impact velocities are drawn for both the datasets to compare the data with the CUR 70 (1989) impact velocity relation in order to validate the relationship in equation 2.9. In order to compare the data the equation 2.9 is applied with same dimensionless ration of $\frac{\text{Hs}}{\Delta\text{Dn}}$ for both dataset conditions for $Y/D_n=0$ (water line) respectively. The distribution is showed in the figure 4.4.

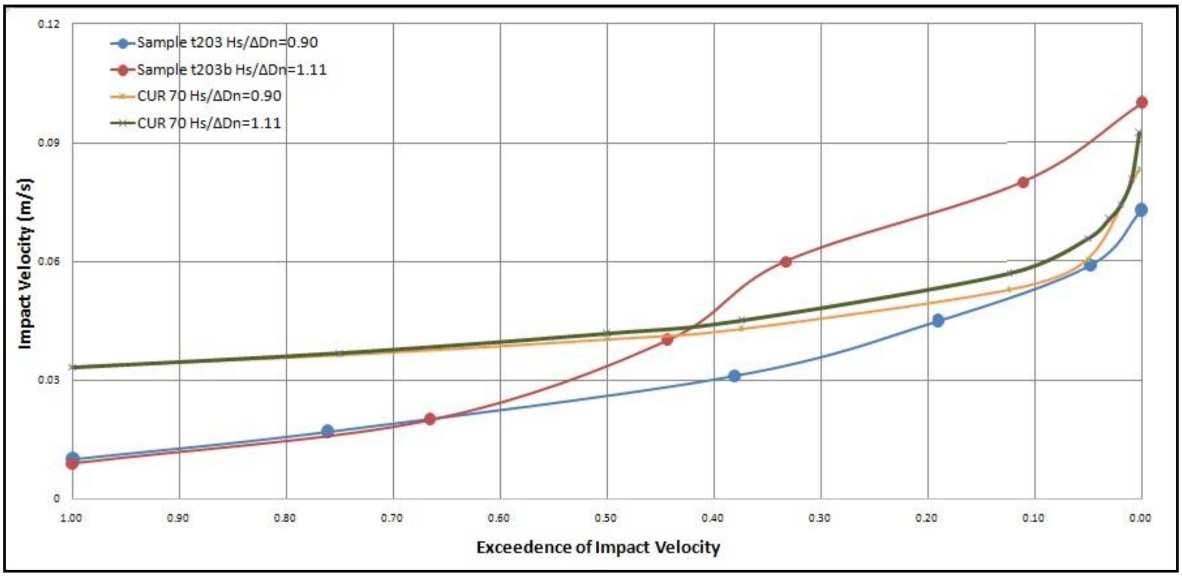

Figure 4.12 Exceedance probability per rocking event of tetrapod

In figure 4.4 it can be seen that the order of magnitude of the presently measured velocity distribution and the one predicted by CUR 70 (1989) is similar. It can be seen that with increasing wave height the impact velocity increases which is also similar with CUR 70 (1989).

In CUR 70 (1989) shows that the rocking start from the stability number $\frac{\text{Hs}}{\Delta\text{Dn}} = 1.8$ as described in section 2.1.3 but the test result shows that there was movement with stability number $\frac{\text{Hs}}{\Delta\text{Dn}} = 0.9$ and 1.1 which differs from the result CUR 70 (1989) given in equation 2.2. This indicates that rocking can occur even before the derived stability number in CUR 70 (1989).

4.4.2 Number of Collisions

The number of collisions is presented in figure 4.13 in dimensionless manner. In X axis the stability number $\frac{Hs}{\Delta Dn}$ is presented and in Y axis the number of collision over number of waves are presented.

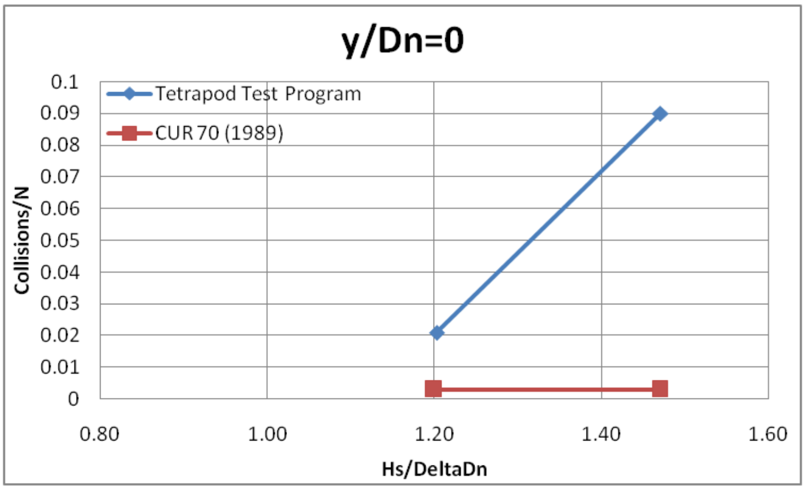

Figure 4.13 Number of Collisions for Y/Dn=0

As described in CUR 70(1989) the number of collision is divided by the number of waves are presented in Y axis and in X axis the dimensionless stability number represented. For CUR 70 (1989) the number of collisions remains the same for all stability numbers hence giving straight lines parallel to the X axis while the original test shows that number of collisions is not limited to three times but continuous and increases with increasing wave height and more than three times.

5. Model Tests

This chapter describes the execution of the model test of instrumented cubes randomly placed in double layer. The model test is performed in the WaterLab of TU Delft.

5.1 Slope Preparation

The slope of 1:1.5 is prepared using stones with a nominal diameter of 2.0cm and glued together, such that the core shape remains unaltered during the whole test series. For this stone of required size were sieved, washed, dried, glued and placed in a mould to maintain the slope properly. Due to time shortage the slope was not finished with perfection which leads to a small berm near the bottom of the slope which lies 5.5Dn below the bottom of the instrumented cubes and also the slope is really straight as it should be and some visible bump is present in the middle of the slope as well. Figure 5.1 shows the different phases of the slope,

Figure 5.1 Empty mould for slope preparation

Figure 5.2 Prepared slope for testing

5.2 Placement of Double Layer Cubes

The cubes are placed randomly in double layer and the instrumented cubes are placed 47cm above the bottom of the slope and the spacing of each of the instrumented cubes were 10cm center to center from each other and one normal concrete cube were placed in between one cube. The packing density of the cubes was approximately 60%. Due to the small berm near the bottom the cubes on the respective layer is 3cm higher than normal slope position (marked red in Figure 5.3). Instrumented cubes were causing some difficulties due to wire presence and all the wires were passed under the cubes to higher position then moved over the slope. Due to the short length of the cable of the instrumented cubes extension cables were used to connect the cubes with the computer. Figure 5.2 and 5.3 shows the instrumented cube position on slope before the tests.

Figure 5.3 Cubes placed randomly in double layer

Figure 5.4 Position of the cubes just before start of the tests

5.3 Wave gauge calibration

Three wave gauges were placed 3m front from the breakwater. Wave gauge were placed and calibrated after the first four tests as due to time limitation the first four tests were done without the wave measurements. For these first four measurements the incoming wave height $H_{m0(i)}$ and $T_{m-1.0(i)}$ is used for described in Table 3.3 is used. After placing the gauge in the water the voltage is calibrated to zero and then the wave gauges were placed 10 cm below the zero value and from the change in voltage the calibration factor was calculated. The calibration parameter is added in Appendix 2. The wave data was processed using the method of Matrix decomposition (Henk Jan Bakkenes, June 2002). The wave data from the wave gauge after the processing are also presented in Appendix 2.

5.4 Data Collection

The cube-motion data were collected using wires from the instrumented cubes connected to ausb hub and then connected to the Laptop provided by Deltares. The Arduino software coding is used by modifying the base code to collect the data using wire. The sampling frequency of 50Hz is used as it is the optimum sampling frequency for the Tinyduino sensors. To save the data and collecting data from all the cubes simultaneously another software package Coolterm is used which uses the Arduino coding and act as bridge for Arduino coding and the processors. All the data files are saved as text file as designated there name in the test program described in Table 3.3.

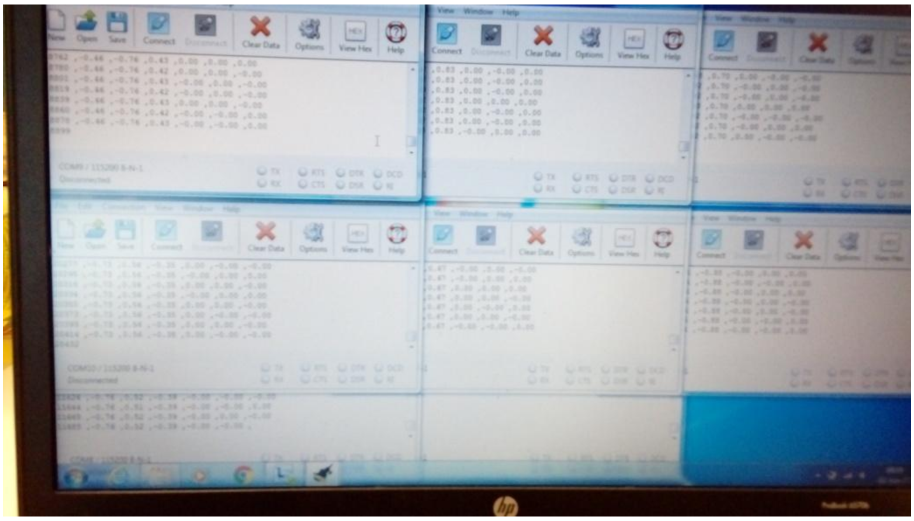

Figure 5.5 Screenshot of data collection during test program using the laptop

5.5 Observation during Test

The whole test program is observed visually to note any significant event during the tests. Some of tests were video recorded which is also added in the data folder of this thesis project. No visible movement were noted during the smaller wave condition of 0.08m and 0.11m but during the 0.14m wave cause several concrete blocks to displaced from there position and also one of the instrumented cube (c11) is displaced from its original position. Other cubes moved but not displaced from there original position. Unfortunately the displaced instrumented cube malfunctioned long before these so the data of this observation cannot be presented in the data sheets. Figure 5.6 shows the closeup of the displaced instrumented cube.

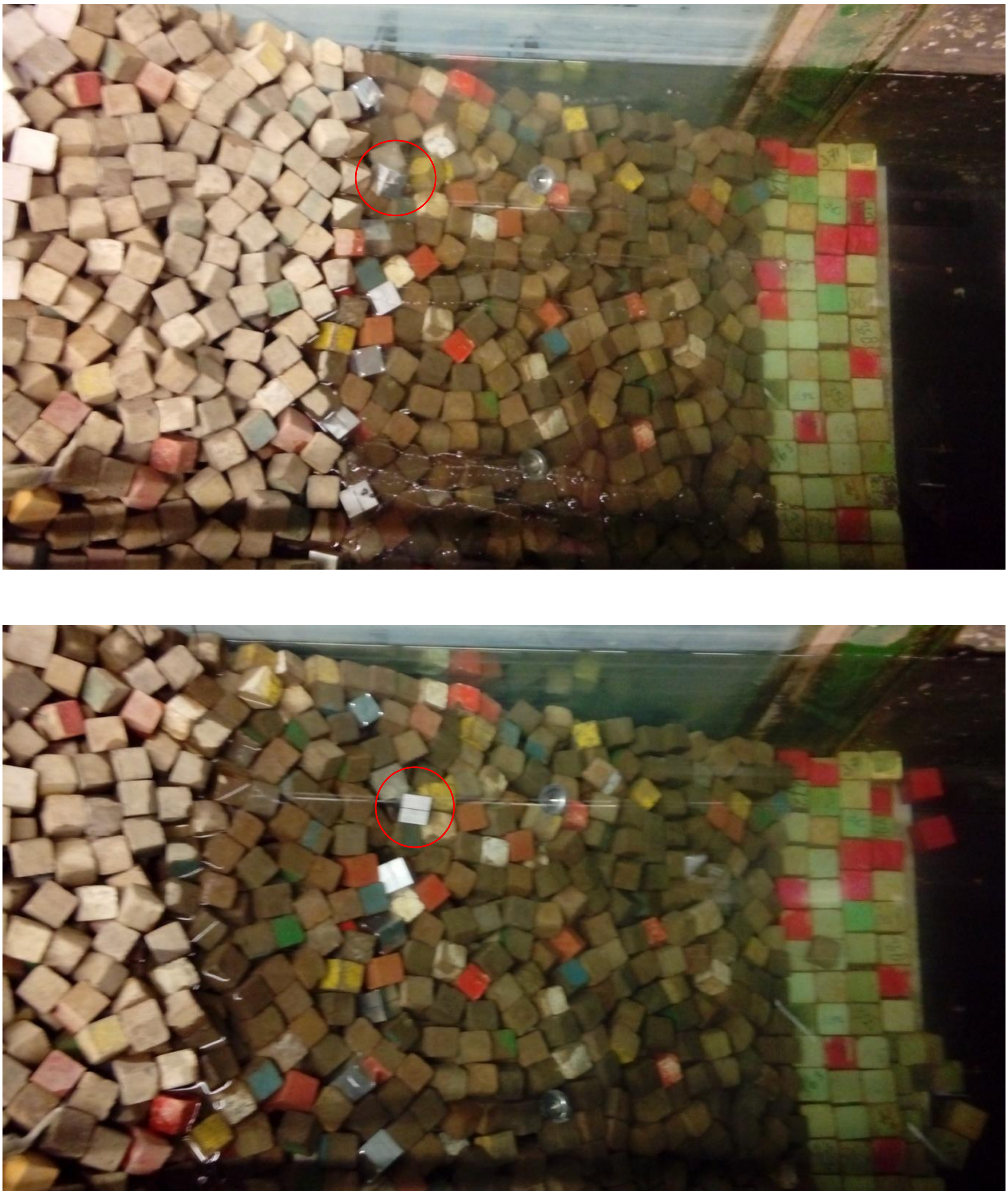

Figure 5.6 Displaced instrumented cube before and after test (marked in red circle)

5.6 Difficulties faced during Test

The presence of wire is one of the problems during the test program as the shortage of length cause connecting of extension cables which lead to several malfunctions of instrumented cubes due to water penetration of the cable although wire also ensures real-time data collection.

Due to time limitation the slope was not prepared up to the mark as there is a small berm present in the slope (section 5.1).

As all measurements of the sensors in the cubes and the wave gauge measurements are started manually one after another by clicking data so the data is not exactly synchronized. As the main aim is to obtain statistics, this is not a problem for the present study.

A noise of 0.01 rad/s is present in the gyroscope readings from the tests which is exactly equal to the error described in falling test 3.6.1.2

6. Data Processing and Analyzing

This chapter is focused on the analysis of rocking measurements with instrumented cubes placed in double layer. The results of these tests will be analyzed and the results will be compared with the CUR 70 (1989) test program.

6.1 Data processing

The raw data collected from the instrumented cubes are processed using the matlab script in Appendix 1 and the procedure is same as described in section 4.3.1. As there are eight different cubes and placed in different position the threshold values can be found in the data file containing the name 'ProcessedDataInputs' in the raw file folder of each of the test program files. The sample of the processed data is given below in figure 6.1 and the close-up view of the data is shown in second caption.

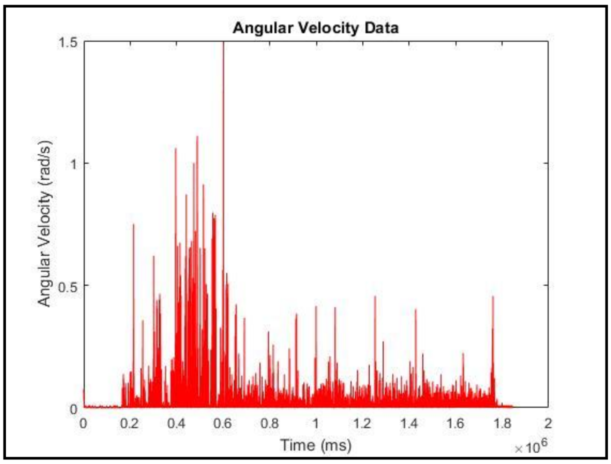

Figure 6.1 Angular velocity from test 1415056 (cube c4 Y/Dn=-2, Hs/DeltaDn=2.4)

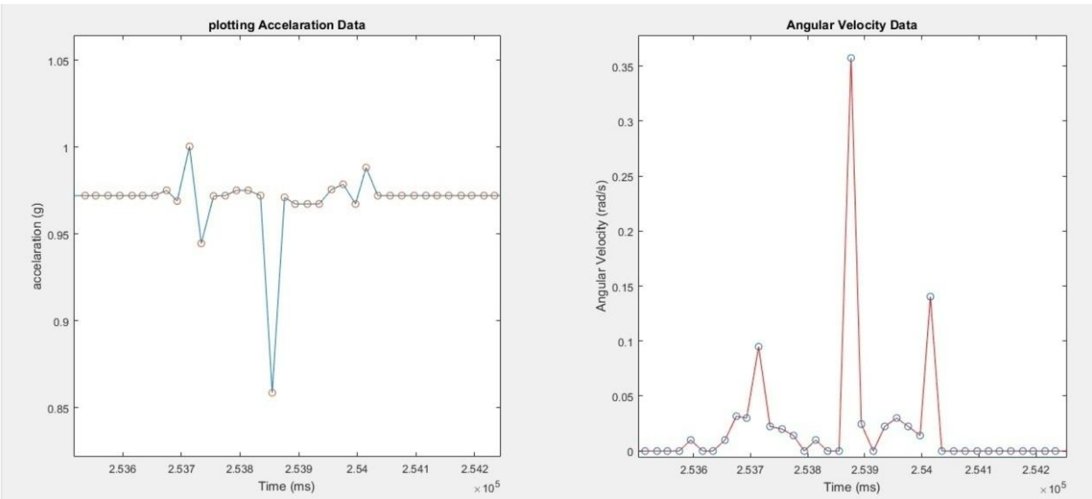

Figure 6.2 Comparison of angular velocity and Acceleration data from test 1415056 (cube c4 Y/Dn=-2, Hs/DeltaDn=2.4)

From figure 6.2 it can be seen that the angular velocity and acceleration are showing peak values at the same time indicating the impact before collision but from the acceleration data the first and last peak is within the range of the threshold level (1 and 0.95) applied for acceleration which will automatically be removed due to this threshold. But the angular velocity with applying 0.01 rad/sec will provide the impact velocity for all the peaks. Due to this fact acceleration data from the sensor will always give less number of impacts as some of the peaks are removed during data processing. On the other hand the angular velocity will take into account all the peaks for impact velocity. Due to this fact during data processing angular velocity is used for the calculation of impact velocity for having much precise result than the acceleration data from the accelerometer.

6.2 Impact Velocity Calculation

Impact velocities for the instrumented cubes are calculated using the method described in section 4.3.2.2 using the angular velocity. For cubes the parameter L in equation 4.3 is used as the nominal diameter of the cube 0.0403m. This input value can be found in the file mentioned in the section 6.1.

After calculating the Impact velocities the exceedence curve for each of the instrumented cubes in each position is plotted in graph in Appendix 3.

6.3 Result Analysis

This section is focused on analysis comparing the previously conducted research CUR 70 (1989). The analysis will include the comparison of number of collision, Order of magnitude of exceedance of impact velocity comparison and spatial distribution with the CUR 70 (1989) research.

6.3.1 Number of collision

The first assumption made for the data processing is that the number of collision is equal to the number of peaks in the angular velocity signal. The number of peaks is calculated applying a threshold level of 0.01 rad/s in the matlab script (Appendix 1) for all the instrumented cubes. Then a dimensionless number of collisions over number of waves is established. Each test program is ran for thousand waves.

Number of collision for irregular wave tests are presented in figure 6.2 and other figures are presented in Appendix 3. Both axes of the figures are kept dimensionless. As X axis the dimensionless stability number is used and in Y axis the number of collisions are divided by number of waves. The figures are representing both the wave steepness 0.02 and 0.04. It can be seen easily that all the graphs are showing upward trend due to increasing wave height and this trend is followed in all the position on the slope. Due to the fact that not all the cubes were showing movement during test so the graphs has been created for the cubes were displaying movement in all the tests in order to compare the result better. In the figure 6.5, 6.6 and 6.7 as there were no movement found at Y/Dn= -4 for $\frac{Hs}{\Delta Dn} = 1.4$

there were only two data points for all the sample cubes. An overview of the number of collisions over the number of waves is presented in table 6.1for all the test results.

Table 6.1 Number of collision over number of waves

Date Performed	Test Number	Number of Collisions/Number of Waves							
		C4	C5	C6	C7	C8	C9	C10	C11
02.06.2017	0811347	0.286	0.045	0.000	0.313	0.650	0.027	0.021	0.000
	0816047	0.250	0.024	0.036	0.000	0.027	0.027	0.015	0.000
	1113547	0.539	0.044	0.000	0.000	0.000	0.150	0.096	x
	1118547	0.422	0.893	0.000	0.000	0.127	0.057	0.083	x
	0811356	0.127	0.000	0.000	0.245	0.000	0.000	0.000	x
	0816056	0.050	0.000	0.000	0.000	0.000	0.000	0.000	x
	0811364	0.000	0.00	0.000	0.000	0.000	0.000	0.000	x
	0816064	0.000	0.00	0.000	0.000	0.000	0.000	0.000	x
	1113556	0.868	0.000	0.000	0.278	0.027	0.000	0.000	x
	1118556	0.780	0.471	0.000	0.000	0.000	0.013	0.008	x
06.06.2017	1415047	0.725	x	0.915	0.716	0.000	0.472	x	x
	1421247	0.624	x	0.808	0.053	0.054	0.155	x	x
	1415056	0.966	x	0.062	0.127	x	0.052	x	x
	1421256	0.920	x	0.032	0.082	x	0.008	x	x
	1113564	0.370	x	0.190	0.000	x	0.030	x	x
	1118564	0.050	x	0.060	0.000	x	0.020	x	x
	1415064	0.830	x	0.480	0.170	x	0.060	x	x
	1421264	0.690	x	0.180	0.140	x	0.030	x	x

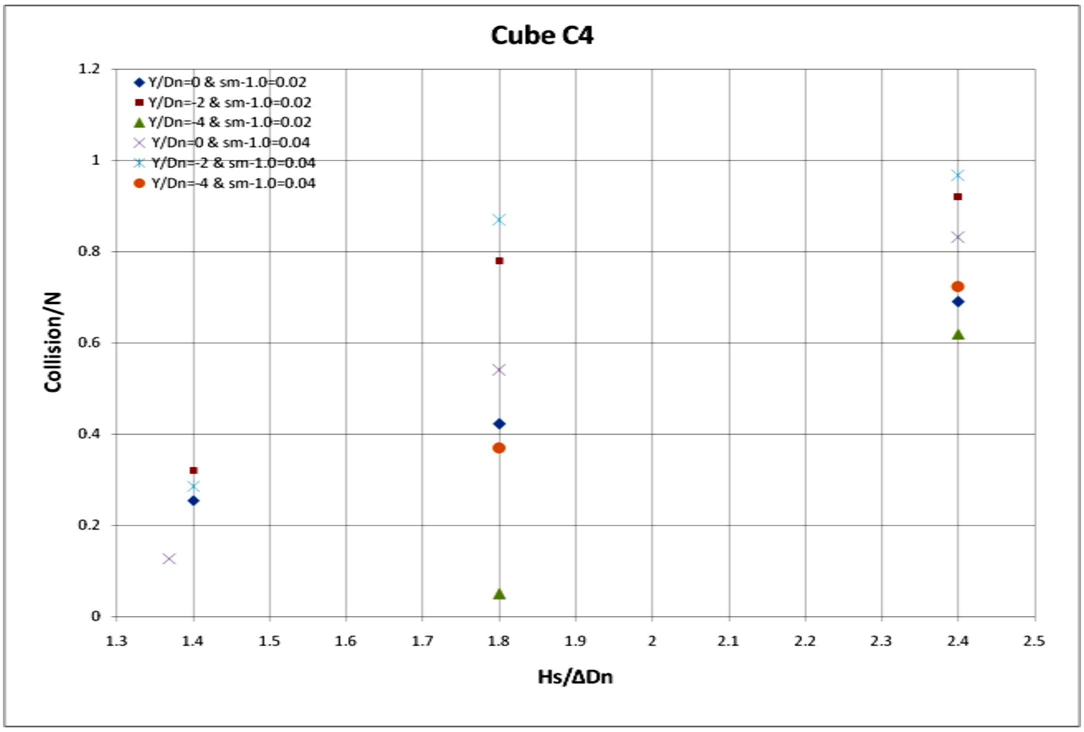

Figure 6.3 Number of collision for sample C4 at different location varying wave steepness

Figure 6.3 and 6.4 representing the positional distribution for constant wave steepness. The axes are representing dimensionless stability number in X axis and collisions over number of waves are represented in Y axis. From the figure it can be seen that the maximum number of collision is found in Y/D_n=-2 for both the wave steepness 0.02 and 0.04. It can also be seen that the number of collision is minimum in the Y/D_n=-4 for both the wave steepness. The figure also shows that the trend is upward with the increasing wave height and true for both the wave steepness. From the graph it can also be seen that with higher stability number $\frac{Hs}{\Delta Dn} = 2.4$ the number of collision is 0.9 indicating constant rocking of cubes due to the wave attack.

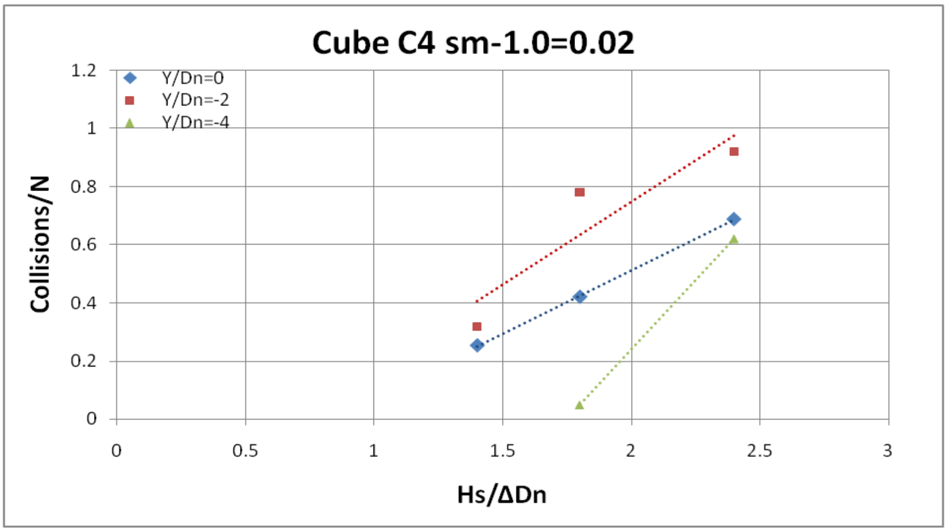

Figure 6.4 Number of collisions for wave steepness sm-1.0=0.02 for cube C4

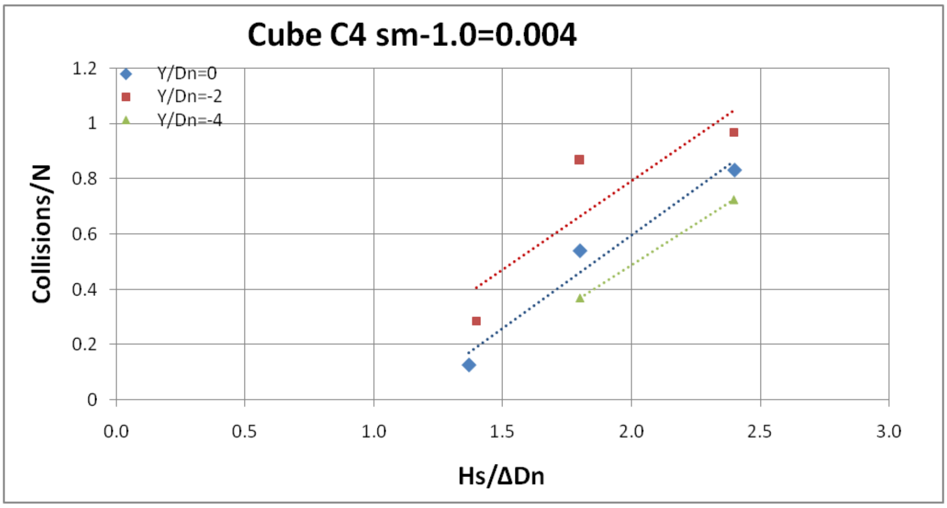

Figure 6.5 Number of collisions for wave steepness sm-1.0=0.04 for cube C4

The CUR 70 (1989) as discussed in 2.1.3 that the number of collision was considered to be 3 regardless the hydraulic and spatial condition. But from the current test program shows that number of collisions depends on wave height, wave steepness and the position of cube on the slope.

6.3.2 Distribution of Impact Velocity

This section is focused for discussion of the order of magnitude of impact velocity, wave height dependencies, wave steepness dependencies, maximum impact velocity dependencies and slope position dependencies comparison with CUR 70 (1989) research.

6.3.2.1 Order of Magnitude of Impact Velocities

In table 6.1 the overview of the $V_{i2\%}$ and the number of collision over number of waves are presented. Figure 6.5 shows the order of magnitude of impact velocities with compare to the CUR 70 (1989) research program. The magnitude of impact velocities for the CUR 70 (1889) is calculated using equation 2.5 for exceedance. The equation was subjected to similar hydraulic condition of the sample instrumented cubes. For the instrumented cubes the exceedance curve is established for the total number of rocking events.

In figure 6.5 X axis representing the probability of exceedance of impact velocity and Y axis representing the impact velocity. All exceedance curves for different test programs are presented in Appendix 4. It can be easily seen in the figures that the impact velocities are in same order of magnitude with the CUR 70 (1989).

Table 6.2 Vi2% for instrumented cubes

Date Performed	Test Number	$V_{i2\%}$ (m/s)							
		C4	C5	C6	C7	C8	C9	C10	C11
02.06.2017	0811347	0.002	0.011	0.000	0.010	0.012	0.002	0.005	0.000
	0816047	0.007	0.006	0.009	0.000	0.005	0.002	0.007	0.000
	1113547	0.021	0.001	0.000	0.000	0.000	0.004	0.015	x
	1118547	0.021	0.016	0.000	0.000	0.008	0.006	0.010	x
	0811356	0.034	0.000	0.000	0.004	0.000	0.000	0.000	x
	0816056	0.009	0.000	0.000	0.000	0.000	0.000	0.000	x
	0811364	0.000	0.000	0.000	0.000	0.000	0.000	0.000	x
	0816064	0.000	0.000	0.000	0.000	0.000	0.000	0.000	x
	1113556	0.150	0.000	0.000	0.088	0.011	0.000	0.000	x
	1118556	0.036	0.000	0.000	0.006	0.000	0.007	0.003	x
06.06.2017	1415047	0.062	x	0.032	0.017	0.000	0.005	x	x
	1421247	0.057	x	0.011	0.010	0.005	0.009	x	x
	1415056	0.096	x	0.041	0.063	x	0.058	x	x
	1421256	0.070	x	0.015	0.011	x	0.012	x	x
	1113564	0.029	x	0.010	0.000	x	0.017	x	x
	1118564	0.023	x	0.012	0.000	x	0.003	x	x
	1415064	0.071	x	0.008	0.003	x	0.023	x	x
	1421264	0.070	x	0.005	0.005	x	0.005	x	x

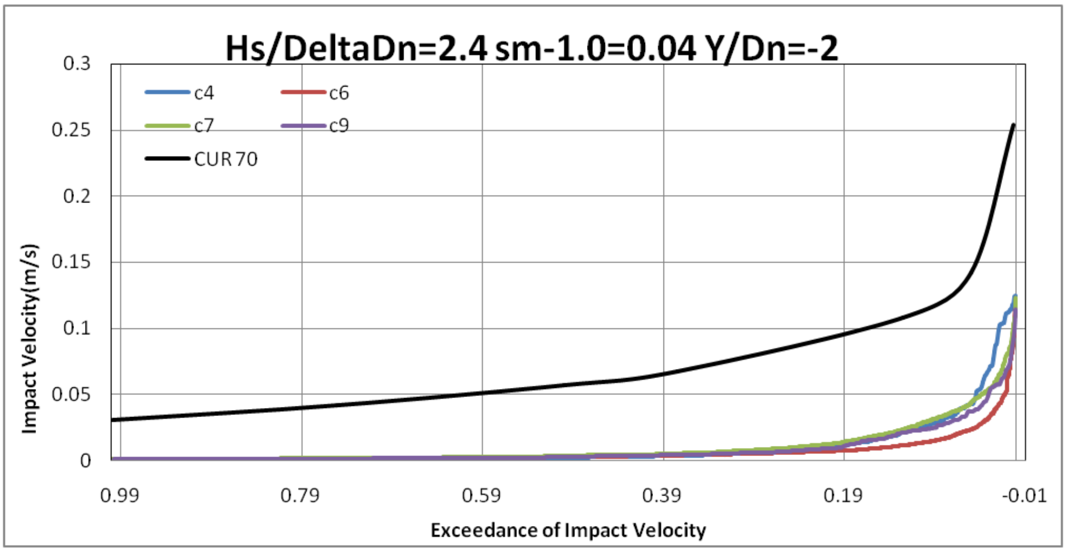

Figure 6.6 Exceedance curve for Y/Dn=-2 and sm-1.0=0.04

6.3.2.2 *Wave height Dependencies*

Figure 6.6 representing the wave height dependencies of the exceedance of impact velocities. In the figures X axis representing the probability of exceedance of impact velocity and Y axis representing the impact velocity. Cube C4 is used as it shows rocking events in all of the wave series. In the figure for three different wave heights for same C4 cube exceedance curve is plotted. The exceedance curve for CUR 70 (1989) is produced using equation 2.5. Other samples are presented in Appendix 5. It can be seen that that the magnitude of impact velocity increases with increasing wave height and this trend is visible in all the slope position. This result also matches with the result of CUR 70 (1989).

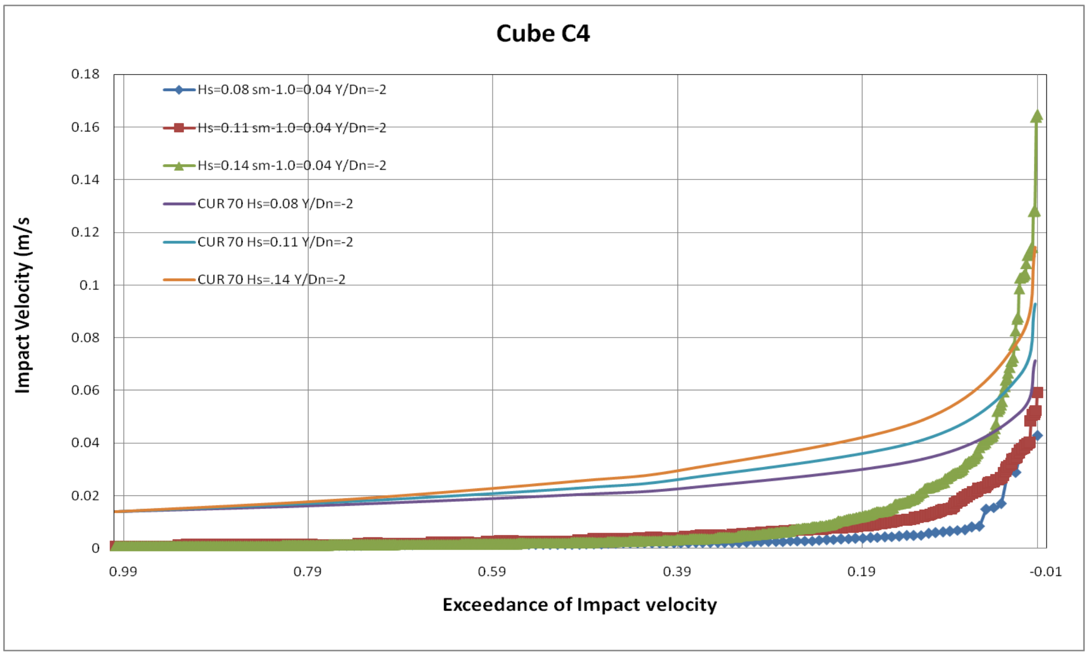

Figure 6.7 Wave Height Dependencies of Cube C4 at Y/Dn=-2 and sm-1.0=0.04

6.3.2.3 Wave Steepness Dependencies

Figure 6.7 representing the dependency of impact velocity over wave steepness of cube C4. Exceedance curves for other instrumented cubes are presented in Appendix 6. In the figures X axis representing the probability of exceedance of impact velocity and Y axis representing the impact velocity. It can be seen from the figures that likewise number of collisions with increasing wave steepness the impact velocity increases and the trend is present over the slope position. CUR 70(1989) research did not include the wave steepness into the equation 2.5 and 2.9. But current research and also Tuan Le's work showing that there is certainly dependency of wave steepness over impact velocity.

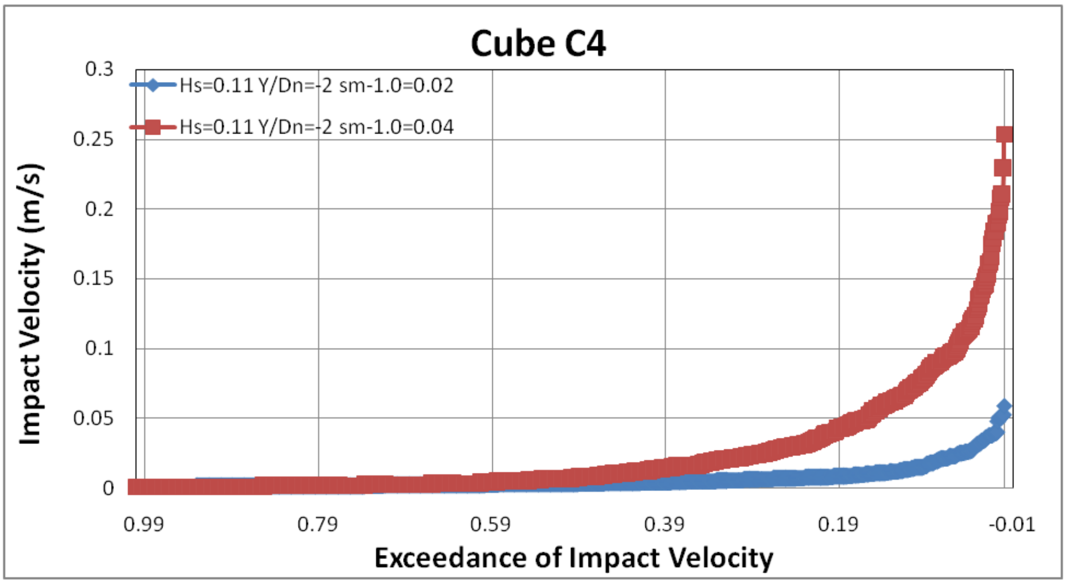

Figure 6.8 Wave Steepness Dependencies of Cube 4, Hs=0.11m & Y/Dn=-2

6.3.3 Spatial Distribution of Impact Velocities

This section is focused for discussion of the spatial distribution of impact velocity in horizontal position for samples and over the slope position.

6.3.3.1 Distribution of impact velocity along horizontal position of cubes

Distribution of impact velocity for the horizontal position of the cubes is produced with the impact velocity ($V_{i2\%}$) with probability of rocking event for each cube. As the instrumented cubes are placed same level along the horizontal axis the distribution of impact velocity is drawn for all the cubes. Figure 6.8 and 6.9 show the exceedance probability of rocking for impact velocity ($V_{i2\%}$) over the horizontal axis. Other figures for different wave height and steepness are presented in Appendix 7. In the figures along X axis exceedance of rocking probability and along Y axis the impact velocity ($V_{i2\%}$) is plotted combining all cube data. From the figures it can be seen that the distribution of impact velocity ($V_{i2\%}$) has the maximum exposure on Y/D_n=-2. This is also represented in table 6.2.

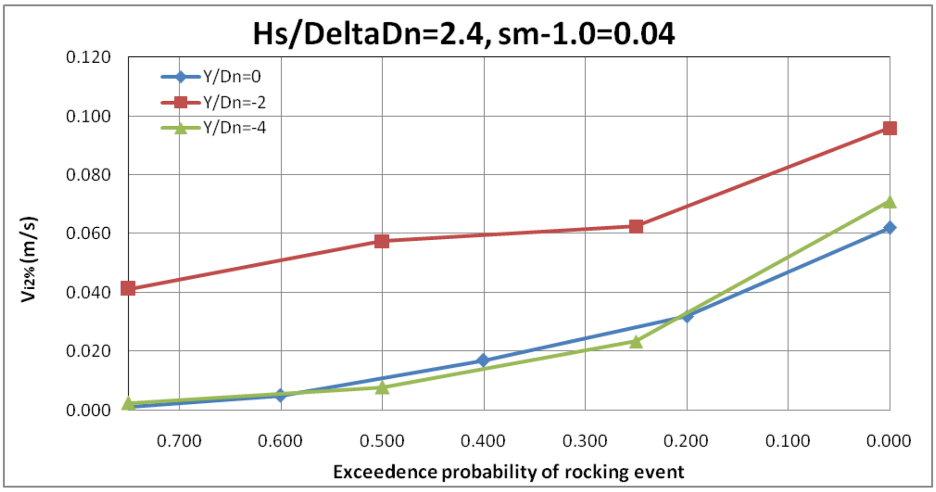

Figure 6.9 Exceedance probability of Rocking event over horizontal axis Hs/ΔDn=2.4, sm-1.0=0.04

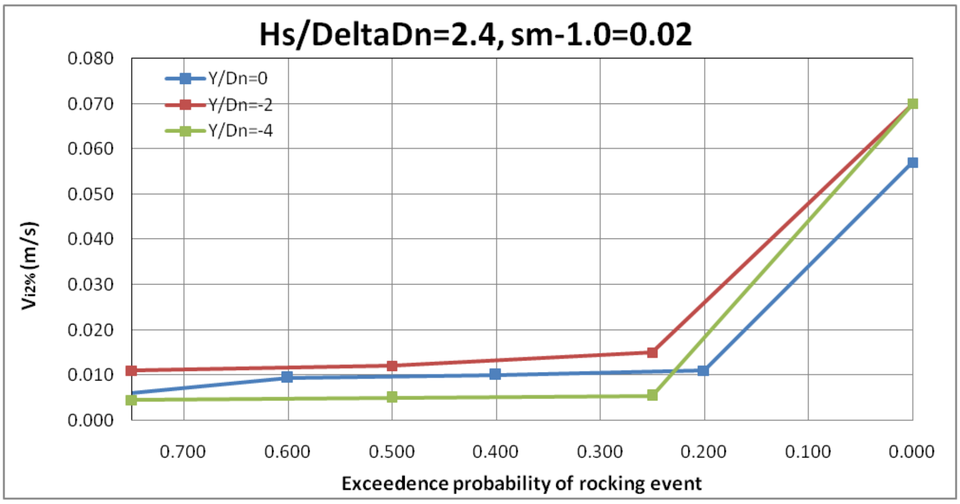

Figure 6.10 Exceedance probability of Rocking event over horizontal axis Hs/ΔDn=2.4, sm-1.0=0.02

6.3.3.2 Distribution over slope position

Figure 6.10 and 6.11 representing the distribution of impact velocity spatially. Other figures are represented in Appendix 8. In the figures along X axis the position of impact velocity over slope and along Y axis the maximum Impact velocity (m/s) is represented. In section 3.5 explain the test situation of position over slope. From the figures it can be seen that the impact velocity is maximum on Y/D_n=-2 and the trend is similar for all the instrumented cubes used. Due to no movement found for Hs=0.08 over Y/D_n=-4 figure 6.37, 6.38 and 6.39 are representing straight line but the trend is similar and maximum impact velocity found on Y/D_n=-2. CUR 70 (1989) research concluded that the maximum impact velocity is found on Y/D_n=0 but in current research as well as the research done by Tuan Le (Section 2.2.4) both are showing that the impact velocity is maximum Y/Dn=-2 which means just below the water line.

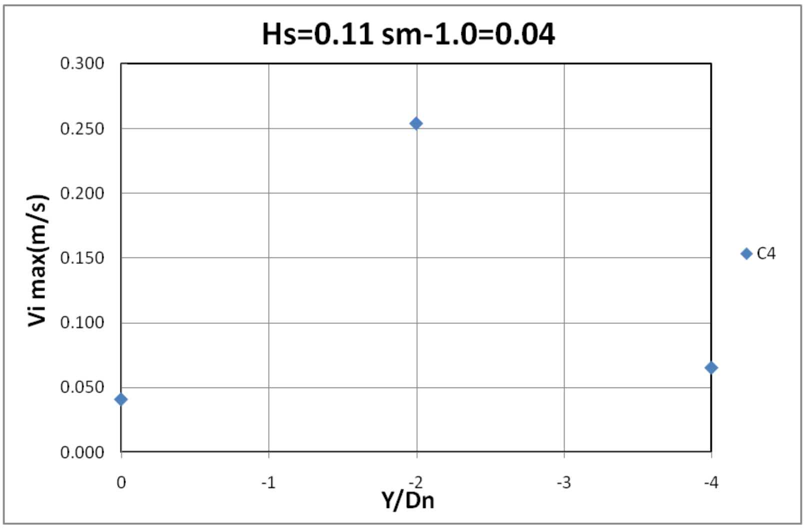

Figure 6.11 Spatial Distribution of Impact Velocity Cube C4 Hs=0.11m and sm-1.0=0.04

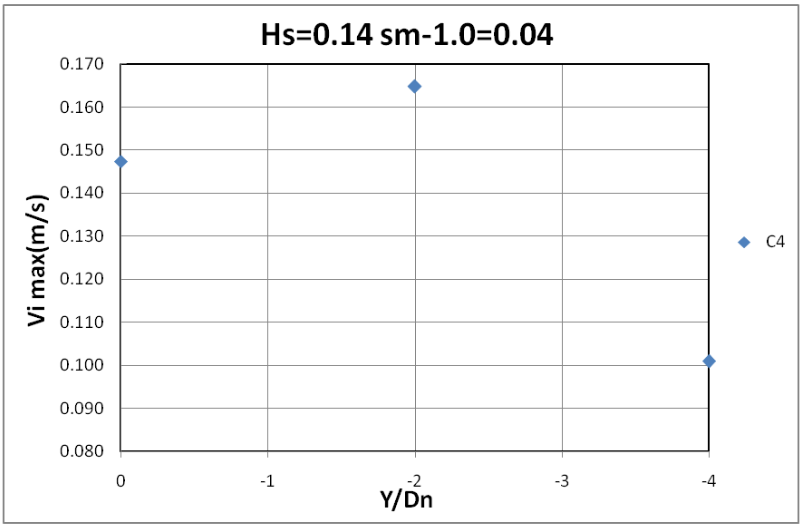

Figure 6.12 Spatial Distribution of Impact Velocity Cube C4 Hs=0.14m and sm-1.0=0.04

7. Conclusions & Recommendations

In this research a breakwater with a randomly placed double layer of cubes is tested to understand rocking of cubes in a double layer and to validate and update previously conducted research CUR70 (1989). A novel measurement approach using stand-alone accelerometers and gyroscopes was applied to this end. Another important aspect of this study is multiple simultaneous measurements of eight instrumented cubes during the experiment. In future research we would like to study single-layer armor systems for which rocking behavior has been studied less.

In this research previously conducted research of CUR70 (1989) and also data from a prototype tetrapod placed in a double layer slope from Deltares was analyzed. After that a model breakwater with randomly placed double layer slope was prepared and eight instrumented cubes were placed to investigate the rocking behavior. Finally, collected data was analyzed and compared with the CUR70 (1989). This chapter gives conclusions and recommendations for future research.

7.1 Angular velocity over Acceleration

Following CUR70, the engineering parameter that should be measured to indicate the potential damage to armor units from rocking is the impact velocity of one unit unto another. Whereas in CUR70 this velocity is obtained from integration of an acceleration measurement during the impact, now the velocity just prior to the impact is measured, following Le (2016).

During the data analysis it’s observed that angular velocity data from the gyroscope provides more distinctive data than acceleration data from the accelerometer. It is found during the analysis that the noise in the acceleration signal is very high and that there is an uncertainty in the threshold value used for the accelerometer data such that it is difficult to detect any movement. On the other hand, the angular velocity signal had a very low noise level, which was distinctive from the actual movement data. Another important aspect is that with angular velocity no integration is required for calculation of impact velocities, while with acceleration integration over the signal before collision is required to obtain the impact velocity. Thus it is concluded based on the performed research that angular velocity data is more reliable than the acceleration data from the accelerometer for identifying rocking behavior.

7.2 Magnitude of Impact Velocities

During this research a comparison with the CUR70 (1989) was made, both for tetrapods and for cubes in a double layer. From the analysis of the data from both tetrapods and cubes it can be concluded that the impact velocity are in the same order of magnitude in both studies. This conclusion also matches with research conducted by Tuan Le on an embedded cube on a similar slope.

7.3 Number of Collisions

During this research the number of collisions is analyzed for varying wave height, wave steepness and position on slope for several cubes in a randomly placed double layer. It was found that the number of collisions over the number of waves for a cube on average is 0.319 and increases with increasing wave steepness and is maximum at $Y/D_n = -2$. There were no data available for Tetrapod for varying wave steepness and slope position so number of collision is analyzed with only varying two different wave heights and also for tetrapod it is found that number of collision increases with increasing wave height. From this analysis for both cubes and tetrapod it may be concluded that the assumption of number of collision in CUR 70(1989) research was inaccurate comparing to this study.

7.4 Influence of wave steepness

The existing empirical equation for the impact velocity (CUR70, 1989) did not include a wave steepness parameter. But in the current research it was found that the magnitude of impact velocity of the cubes is influenced significantly by the wave steepness. In the analysis it is found that $s_{m-1.0}$=0.04 results in a higher probability of exceedance for certain impact velocity comparing with $s_{m-1.0}$=0.02. So it is recommended to include a parameter that incorporates the wave steepness in the equation of impact velocities.

7.5 Distribution of Extreme Impact Velocity over Slope

During this research the influence of a different position (elevation) of the cube on the extreme impact velocities is determined. The analysis shows that the maximum impact velocity is found on Y/D_n=-2. CUR 70 (1989) concluded that the maximum impact velocity lies on Y/D_n=0. Le (2016) also concluded that the impact velocity is maximum at Y/D_n=-2. So both current and Le's research indicate that the results from CUR70 (1989) are not correct for cubes, and the maximum impact velocity lies around Y/D_n=-2 for cubes.

7.6 Spatial Distribution over Extreme Impact Velocity

During this study the spatial distribution of impact velocity is produced for different horizontal position of the cubes. This distribution gives the indication that the position along horizontal plane gives variation in impact velocities. From this it can be concluded that the position of the armor unit along horizontal position has significant effect on the impact velocities.

7.7 Measurement Techniques

This study is analyzed measurement conducted using a novel measurement approach sing stand-alone accelerometers and gyroscopes for tetrapod and real-time data collection approach from accelerometer and gyroscope using multiple sensors (eight) on cubes simultaneously. The standalone method with no wire attached gives the unit full flexibility of movement during experiment. The realtime data collection using multiple sensors provides the statistics for spatial variability of rocking behavior.

The applied sensors provided by Deltares have proved very effective. The sensors show the same order of magnitude as in the previously conducted research CUR70 (1989), where 100 kHz accelerometers were used. During this research it is found that a 50Hz sampling rate is sufficient for capturing the movement of the armor unit. During the sensor checking it is found that the gyroscope has 0.74% error on average with maximum of 1.66 rad/sec and standard deviation of 0.0724 rad/sec for angular velocity.

7.8 Low frequency sensor over High Frequency sensor

During the CUR 70 (1989) research used the high frequency (100 kHz) sensor which was able to detect the acceleration during the impact directly and used integration of this acceleration to calculate the impact velocity whereas Tinyduino sensor is a low frequency (62.5Hz) sensor and therefore the calculation from the data relied on the impact velocity before collision which is really a new concept and during this study the result shows that even with this low frequency sensor can give the impact velocity with same order of magnitude as comparing with previously used high frequency sensor. Even the Tetrapod data using the stand alone mode for 33Hz frequency gives the same order of magnitude with respect to the CUR 70(1989) data. The falling test conducted for the sensor validation which shows less than 1% error also done in the same order of magnitude of angular velocity with respect to the data from the instrumented cubes during the test program. So from the result from this study it can be concluded that it may be possible to calculate the impact velocity even with the low frequency sensor (Tinyduino) which are really cost effective.

7.9 Recommendations

This section presents the recommendations based on the work performed as well as a discussion on future opportunities for further research.

7.9.1 Experiment on Laboratory

3D Printing of Instrumented Armor Unit: During this research work the manufacturing of instrumented cubes took the longest period of time so for this reason 3D printing of armor unit is may be a solution for solving this for future work although this will require the adjustment of density for armor unit.

Data collection: During this research program due to short length of the cable extension cable needed and due to the connection problem after first three test program 50% instrumented cubes malfunctioned due to water penetration through this connection between the extension cable and instrumented cubes cable which is really undesirable. Although the cable used for connecting the instrumented cubes was really good and flexible it is found that it makes the cubes vulnerable to water. Wireless connection for data collection from instrumented unit may also be a good solution. The drawback of wireless connection is longevity of battery which may create difficulties. So for future work watertight wireless connection is recommended.

Different types of Armor unit in a single layer: The present study was initiated to study modern single-layer armor units such as Xbloc, Accropode, Coreloc and Cubes in a single layer.However, first the connection was made to the existing knowledge on double layer units. Due to time limitations it was not possible to test these armor unit types. So for future work it is recommended to use different type of armor unit for analyzing rocking behavior.

Distribution for Tetrapod: As no data was present for tetrapod over different positions on the slope no conclusion can be obtained for tetrapod and it is recommended to check the distribution over slope for Tetrapod in future research.

Applicability of Tinyduino sensors: During this study Tinyduino sensors was found very accurate for data collection and have both accelerometer and gyroscope. So it is recommended to use this sensor for future work.

7.9.2 Impact Velocity Formula

Single Layer Armor Unit: So far the formula regarding the impact velocity is only addressing the double layer armor unit but now a days single layer armor unit is more commonly used and for future research it is recommended to incorporate the formula for single layer armor unit types.

Wave steepness parameter: During this study it is found that the impact velocity formula from the CUR 70(1989) is incomplete without introducing a parameter that incorporate the wave steepness factor as the result shows that there is certainly a relation between the wave steepness and the impact velocity. So for future research it is recommended that this formula is updated using a parameter incorporating wave steepness.

Angular Velocity: As the result from this study shows that newly introduced calculation method of impact velocity using the angular velocity gives same order of magnitude. As the assumption made during this calculation were very simplified to avoid complexity during calculation so it is recommended to validate this new concept and incorporate angular velocity updating the formula used in this study for impact velocity calculation.

Number of Collision: As the result of this study supported by previously conducted study by Le (2016), the number of collision is not limited to 3 times and is continuous after initiation of rocking it is recommended that this should be incorporated in the software application “Rocking”. It is also recommended that the assumption for number of collision for this study is validated for future work.

Position on Slope: In CUR 70(1989) the maximum impact velocity was found on the water line relative to the armor unit but the position was not well defined on the research but during this study it is found that the extreme impact velocity appears on Y/Dn=-2 which is also supported by Le(2016). So for future study it is recommended to update the formula of impact velocity incorporating the position of the slope position Y/Dn=-2.

Spatial Distribution: Spatial distribution of the impact velocity indicates that the horizontal position of armor unit has influence on the impact velocity so it is recommended that for future works to validate and incorporate in the impact velocity formula.

Types of armor unit: During CUR 70(1989) only cubes and Tetrapod in double layer features the formula so for future research it is recommended to extend this formula for different types of armor unit.

References

Battjes. J. A. (1969). Run-Up Distributions of Waves Breaking on Sloping Walls. Delft: Delft University of Technology.

Bosman, G., Meer, J. W., Hoffmans, G., Schüttrumpf, H., & Verhagen, H. J. (2008, September). Individual overtopping events at dikes. In International Conference on Coastal Engineering (ICCE), 2008, Hamburg.World Scientific.

Boyce, W. E., & Di Prima, R. C. (2010). Elementary Differential Equations and Boundary Value Problems. New York:Wiley and Sons.

Burcharth, H. F. (1992). Design of rubble mound breakwaters. Structural Integrity. Aalborg: Aalborg University.

Burcharth, H. F., & Zhou, L. (1995). Rubble mound breakwater failure modes. Aalborg: Aalborg University.

Burcharth, H. F., Liu, Z., & Troch, P. (1999). Scaling of core material in rubble mound breakwater model tests. In FifthInternational Conference on Coastal and Port Engineering in Developing Countries. COPEDEC.

Chella, M. A., Torum, A., &Myrhaug, D. (2012). An overview of wave impact forces on offshore wind turbine substructures. Energy Procedia, 20, 217-226.

CIRIA, CUR & CETMEF (2007). The RockManual. The use of rock in hydraulic engineering (Vol. 683). CIRIA.

Civiel Centrum Uitvoering Research en Regelgeving (1989). Golfbrekers. Sterkte Betonnen Afdekelementen. Integratie van Fasen 1-3. Verslag werkgroep 1. Civiel Centrum Uitvoering Research en Regelgeving.

Civiel Centrum Uitvoering Research en Regelgeving (1990a). Golfbrekers. Sterkte Betonnen Afdekelementen. Samenvatting onderzoek. Verslag werkgroep 1. Civiel Centrum Uitvoering Research en Regelgeving.

Civiel Centrum Uitvoering Research en Regelgeving (1990b). Golfbrekers. Sterkte Betonnen Afdekelementen. Toepassingen. Verslag werkgroep 1. Civiel CentrumUitvoering Research en Regelgeving.

Dai, Y. B., & Kamel, A. M. (1969). Scale Effect Tests for Rubble-mound Breakwaters: Hydraulic Model Investigation. US Army EngineerWaterways Experiment Station.

Frostick, L. E., McLelland, S. J., & Mercer, T. G. (Eds.). (2011). Users guide to physical modelling and experimentation: Experience of the HYDRALAB network. CRC Press.

Gent, M. R. A., & Luís, L. (2013). Application of Cubes in a single layer. In Proc. 6th SCACR conference on applied coastal research, Lisbon.

Gent, M. R. A. (2002). Low-exceedance wave overtopping events, WL Delft project id. DC030202/H3803.

Gijsman, R., de Haan, F. S., de Koning, R. J., Le, T. N., & Steeneken, S. P. (2015). Part 2 - Report Durban Dig Out Port (Multidisciplinary Project Report). Delft: Delft University of Technology.

Goseberg, N., Nistor, I., & Stolle, J. (2015). Tracking of “Smart" debris location based on RFID technique. In Proceedings of Coastal Structures & Solutions to Coastal Disasters Joint Conference, Boston.

Henk Jan Bakkenes (June 2002), Matrix decomposition Method (M.Sc Thesis), Delft: Delft University of Technology, pp 22-24.

J. W. Van der Meer (1990). Handleiding Rocking. “Rocking armor units: Number, Location and Impact Velocity”. Coastal Engineering 15, 1991, Elsevier Science Publishers B.V, Amsterdam

Mier, J. G. M., & Lenos, S. (1991). Experimental analysis of the load-time histories of concrete to concrete impact.Coastal engineering, 15(1-2), 87-106
Pullen, T., Allsop, N. W. H., Bruce, T., Kortenhaus, A., Schüttrumpf, H., & Meer, J. W. (2007). Wave Overtopping Of Sea Defence And Related Structures. Environment Agency, ENW, KFKI.

Schüttrumpf, H., &Oumeraci, H. (2005). Layer thicknesses and velocities of wave overtopping flowat seadikes. Coastal Engineering, 52(6), 473-495.

Sokolewicz, M. J. (1986). Impulsbelastingen voor kubussen en tetrapodes als gevolg van rocking bij golfaanval (MSc Thesis). Delft: Delft University of Technology

Tiny-Circuits (n.d.). Tiny Duino. Retrieved fromhttps://www.tiny-circuits.com/.

T.N. Le (2016). Rocking of a single cube on a breakwater slope (MSc Thesis). Delft: Delft University of Technology

U.S. Army Corps of Engineers. (1984). Shore ProtectionManual.Washington DC: USACE.

Appendices

Appendix 1: Data Processing Matlab Script

```
%% This Program is created for processing the raw data from Tinyduino
Processors.
%for measuring impact velocity for rocking of Breakwater Armor unit
%The measurement are Acceleration in "g" and Angular velocity in "rad/s"

%%Input Variables

data= load(uigetfile({'.txt'},'File Selector')); %loading the Raw data into
the program

t= data(:,1); %Time in ms
ax= data(:,2); %accelaration in X direction
ay= data(:,3); %accelaration in Y direction
az= data(:,4); %accelaration in Z direction
gx= data(:,5); %angular velocity along X direction
gy= data(:,6); %angular velocity along Y direction
gz= data(:,7); %angular velocity along Z direction


%% Finding impact velocity from Accelaration

a= sqrt(ax.^2+ay.^2+az.^2); %Resultant accelaration magnitude (g)
ap=1;        %Peaks of accelaration
tpa=0;       %Time of Peaks for accelaration
cpa=0;       %Count of Accelaration Peaks
Vat=0;        %Impact Velocity from Accelarometer
tvat=0;       %Time impact velocity
g=input('g = ');%Gravitational Accelaration

%plotting resultant Acceleration Magnitude to find Threshold
figure
plot (t,a); hold on;
xlabel('Time     (ms)');ylabel     ('accelaration     (g)');title('plotting
Accelaration Data');

%Threshold Data for removing noise from data and Identifying Peaks T1,T2,T3
disp('Theshold Data for Acceleration for removing noise');
T1=input('Threshold Value T1 = ');%1.05
T2=input('Threshold Value T2 = ');%1.025
T3=input('Threshold Value T3 = ');%1

for i=2:length(a)-1

    if (a(i)>a(i-1) && a(i)>a(i+1) && a(i)>T1)
       ap(i)=a(i);
       tpa(i)=t(i);
       cpa=cpa+1;
       Vat(i)= (abs((1/3)*(t(i)-t(i-1))*(a(i)-T3)))*g/1000;
       tvat(i)=t(i);
    elseif (a(i)>a(i-1) && a(i)<a(i+1) && a(i)>T1)
       ap(i)=a(i);
```

```
        tpa(i)=t(i);

    else
        ap(i)=T3;
        tpa(i)=t(i);

    end
end

Va=transpose(Vat);
tva=transpose(tvat);

%% Finding impact velocity from Angular Velocity

w= sqrt(gx.^2+gy.^2+gz.^2); %Resultant angular velocity magnitude (rad/s)
%wp=0;        %Peaks of Angular Velocity
tpavt=0;      %Time of Peaks for Angular Velocity
cpav=0;      %Count of Angular Velocity Peaks
Vwt=0;        %Impact Velocity from Angular Velocity

figure
%plotting angular velocity Data
plot (t,w,'r-'); hold on;
xlabel('Time  (ms)');ylabel  ('angular  velocity  (rad/s)');title('plotting
Angular Velocity Data');


%Threshold Data for removing noise from data and Identifying Peaks
disp('Theshold Data for Angular Velocity for removing noise');
T4=input('Threshold Value T4 = ');
T5=input('Threshold Value T5 = ');

Dn= input('Nominal Diameter of Armor Unit Dn = '); %Nomimnal Diameter of
the armor Unit

for j=2:length(w)-1
    if(w(j)>w(j-1) && w(j)>w(j+1) && w(j)>T4)
        Vwt(j)=Dn*w(j);
        tpavt(j)=t(j);
        cpav= cpav+1;

    end
end
Vw=transpose(Vwt);
tpav=transpose(tpavt);
```

Appendix 2: Wave Gauge Calibration Parameter & Wave Data

tijdstap in meetbestand				
0.01				
Tp (s),	f-resol/Tp	fmin (Hz),	fmax (Hz),	tresh
1.6,	0.025,	0.02,	-1,	0.005
kolom met tijden (0 voor geen)				
1				
kolomno GHM,	pos (m),	schaalfact naar m		
2,	0.000,	0.025		
3,	0.290,	0.025		
4,	0.671,	0.025		

Wave Gauge Calibration Parameter

Measured Wave Data

Test ID	Gauge 1		Gauge 2		Gauge 3		Avarage	Avarage
	H_{mo} (m)	$T_{m-1.0}$ (s)	H_{mo} (m)	$T_{m-1.0}$ (s)	H_{mo} (m)	$T_{m-1.0}$ (s)	H_{mo} (m)	$T_{m-1.0}$ (s)
0811356	0.0843	1.1036	0.0827	1.2078	0.0798	1.1427	0.0823	1.1514
0811364	0.0874	1.1033	0.0891	1.0667	0.0839	1.1426	0.0868	1.1042
0816056	0.0863	1.6839	0.0892	1.6839	0.0838	1.5606	0.0864	1.6428
0816064	0.0872	1.6841	0.0935	1.6841	0.0861	1.6003	0.0889	1.6562
1113156	0.1187	1.3336	0.1155	1.2801	0.1079	1.3615	0.1140	1.3251
1113164	0.1205	1.3061	0.1223	1.3061	0.1108	1.2074	0.1179	1.2732
1118556	0.1265	1.8291	0.1197	1.8291	0.1068	1.7784	0.1176	1.8122
1118564	0.1275	1.8826	0.1262	1.7775	0.1095	1.7775	0.1211	1.8125
1415047	0.1468	1.5616	0.1461	1.5616	0.1439	1.5244	0.1456	1.5492
1415056	0.1472	1.4222	0.1489	1.5610	0.1465	1.5610	0.1475	1.5147
1415064	0.1462	1.4224	0.1498	1.5605	0.1498	1.4883	0.1486	1.4904
1421247	0.1484	2.0001	0.1444	2.4609	0.1535	2.2076	0.1488	2.2229
1421256	0.1507	2.0000	0.1482	2.2842	0.1507	2.2842	0.1499	2.1895
1421264	0.1493	2.0001	0.1508	2.4613	0.1492	2.2068	0.1497	2.2227

Appendix 3: Number of Collisions

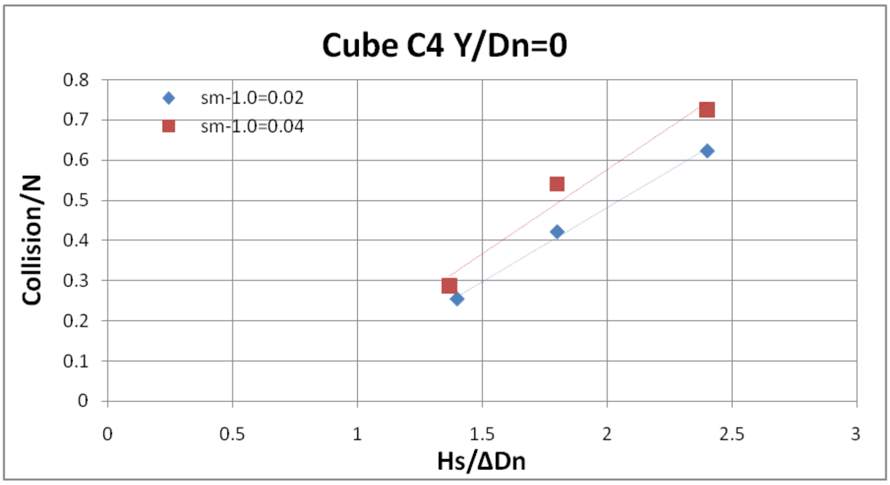

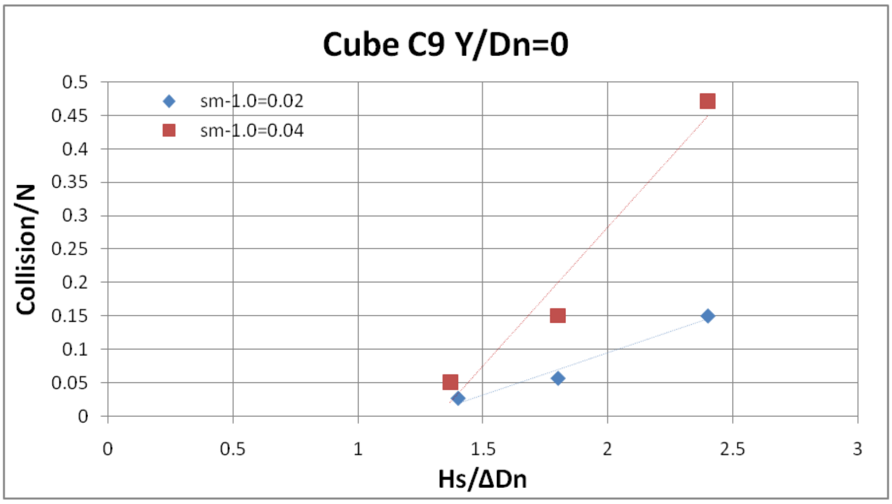

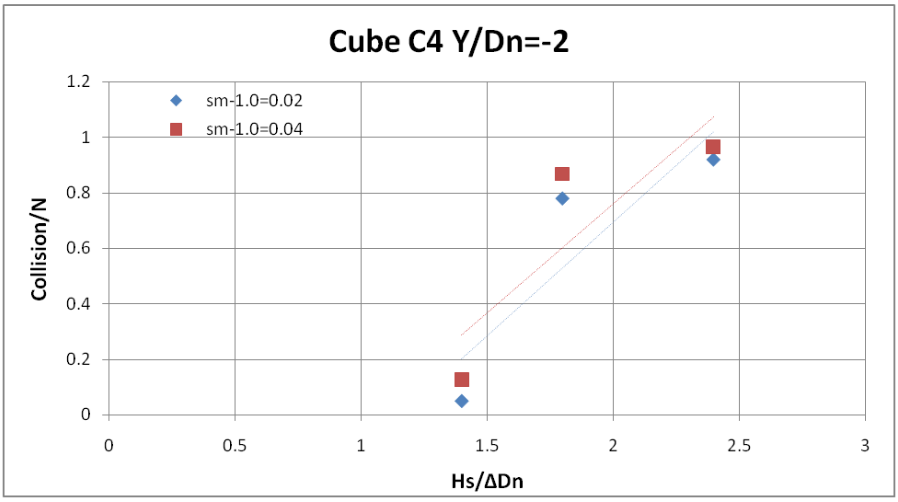

Appendix 3: Number of Collisions

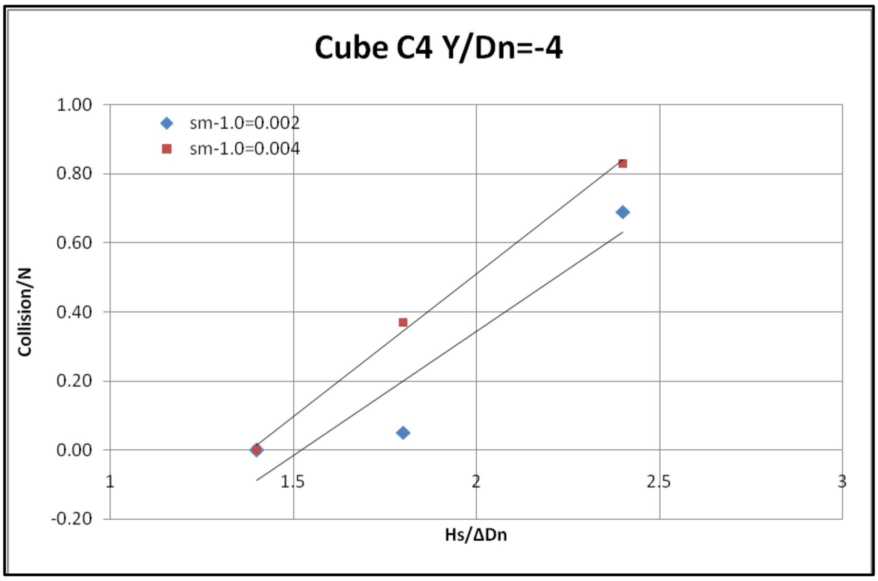

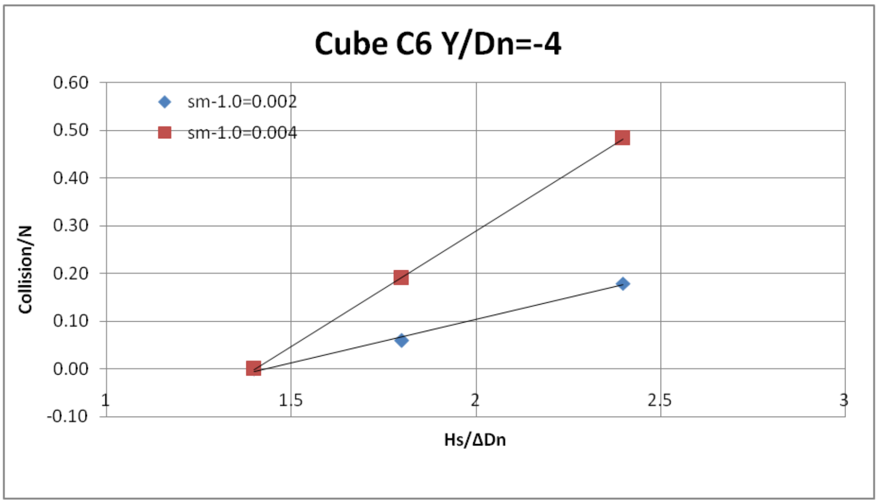

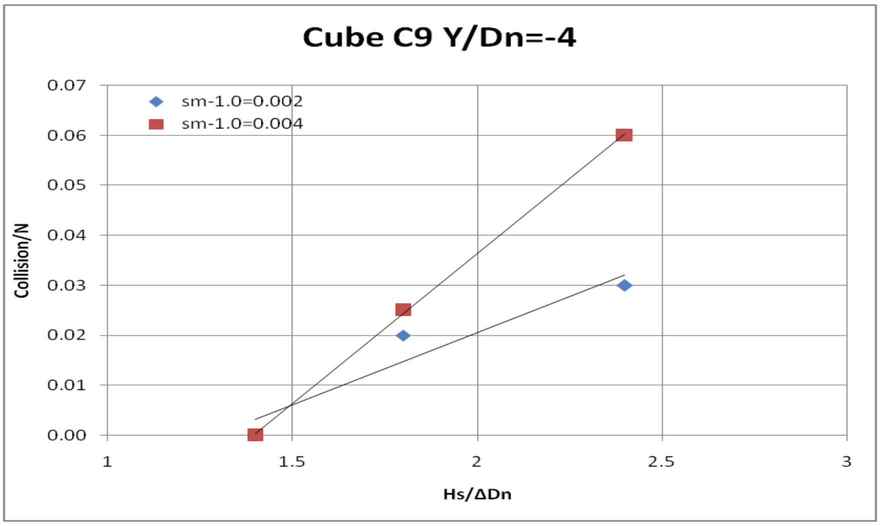

Appendix 4: Exceedance Curves representing order of Magnitude for Impact Velocities

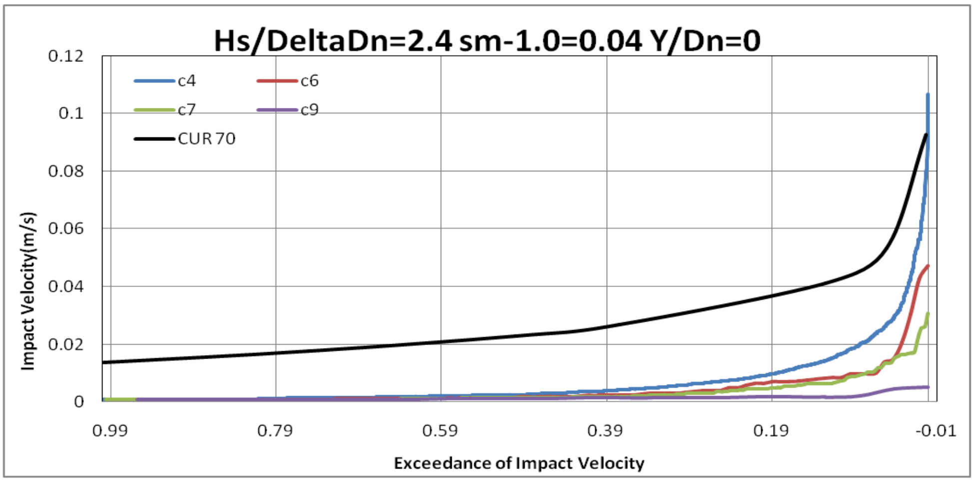

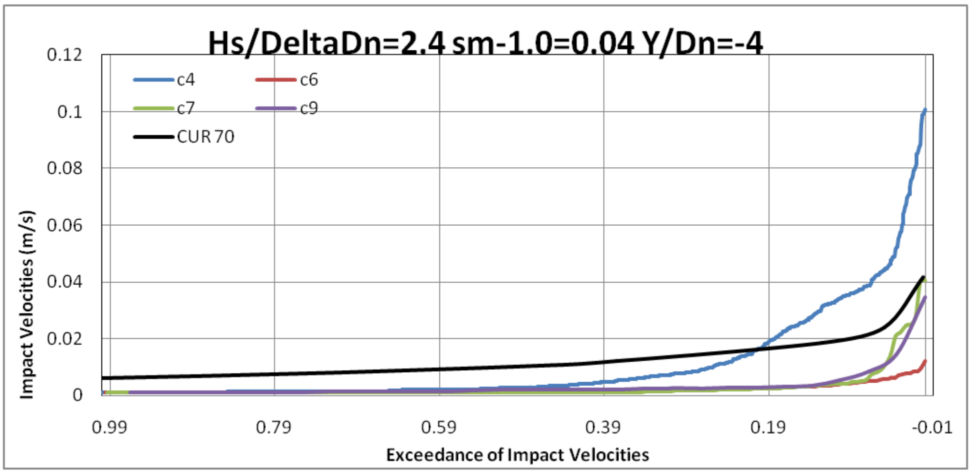

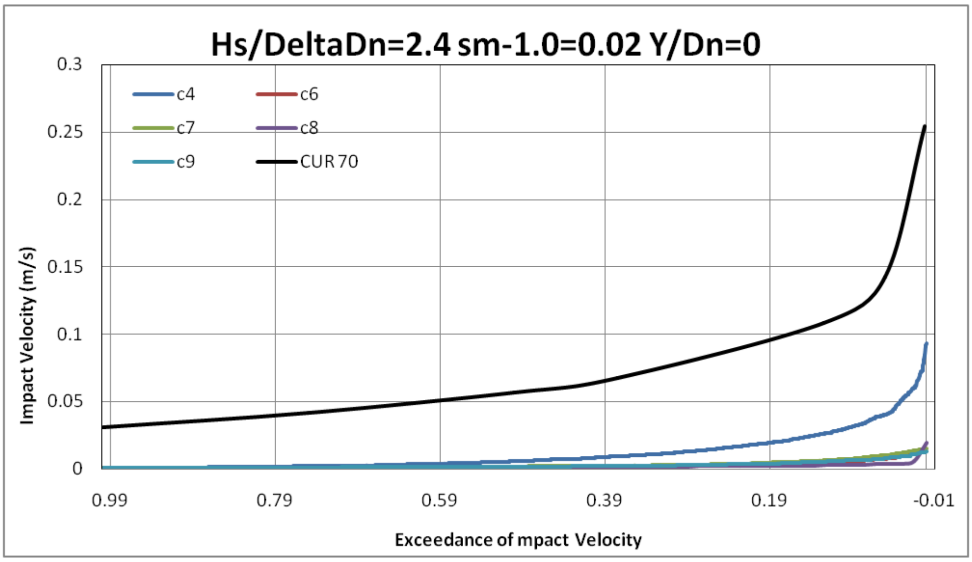

Appendix 4: Exceedance Curves representing order of Magnitude for Impact Velocities

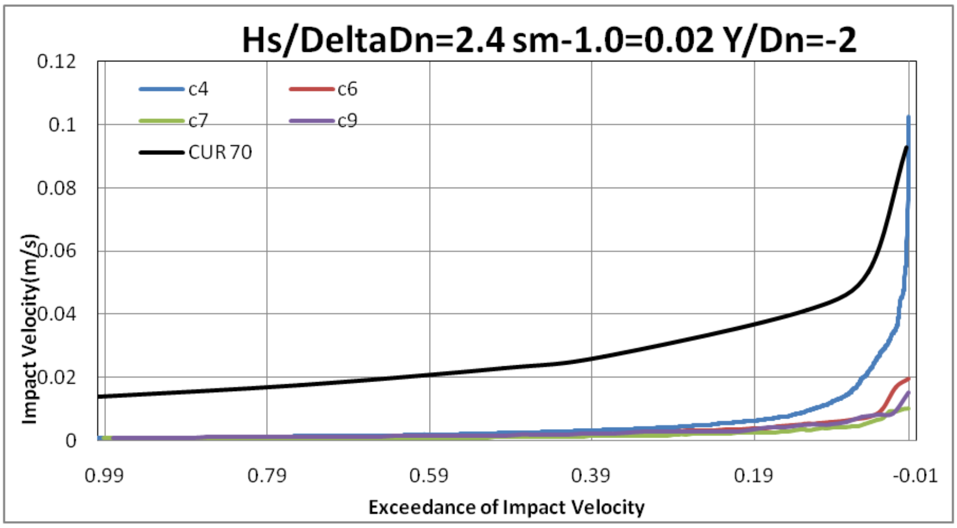

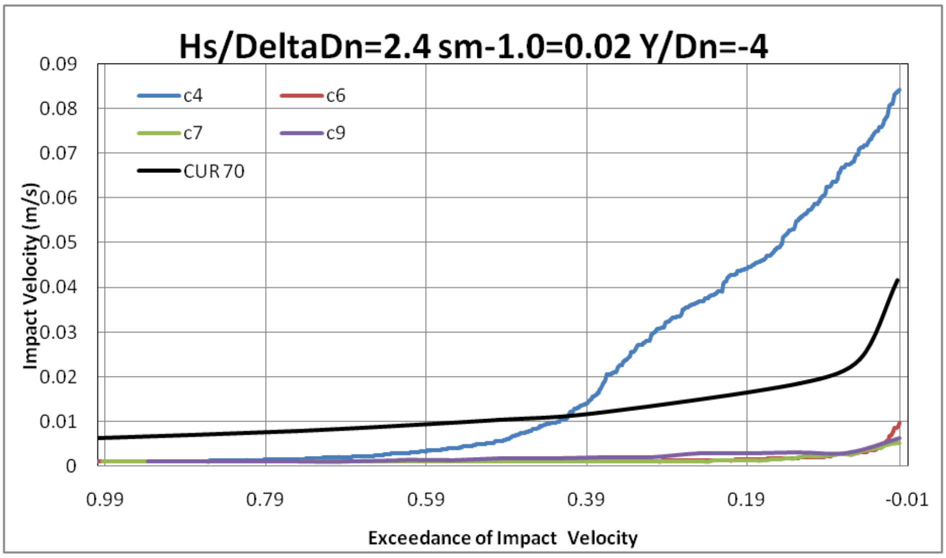

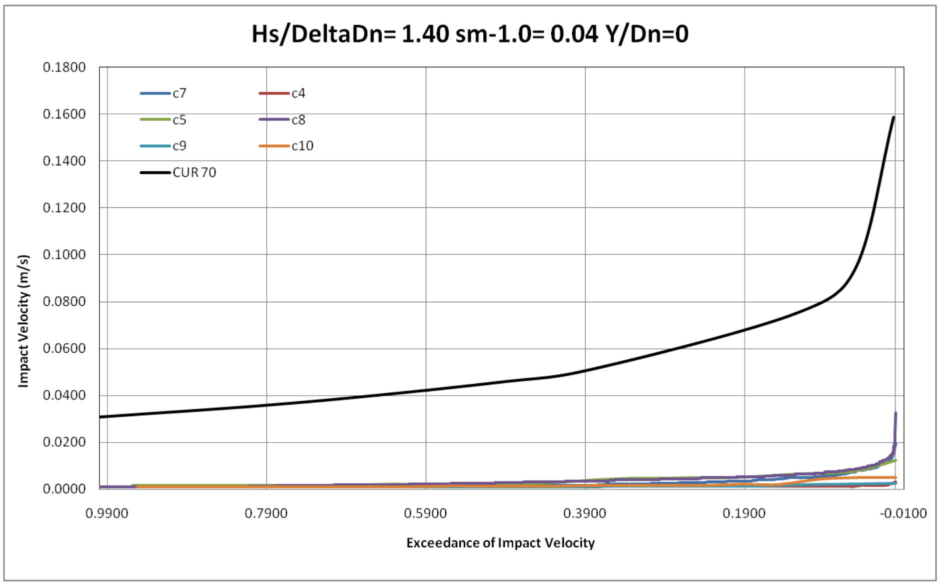

Appendix 4: Exceedance Curves representing order of Magnitude for Impact Velocities

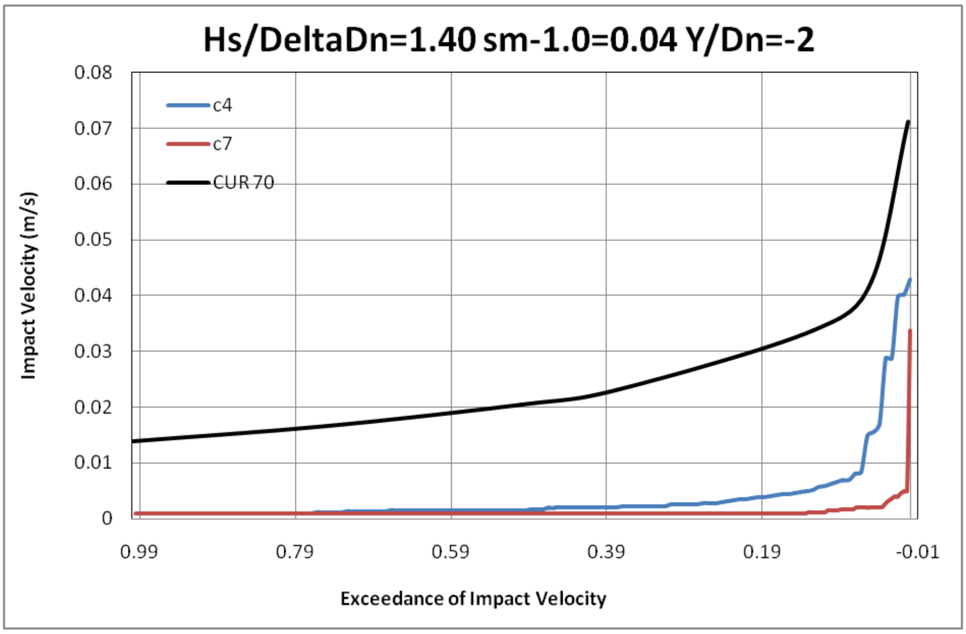

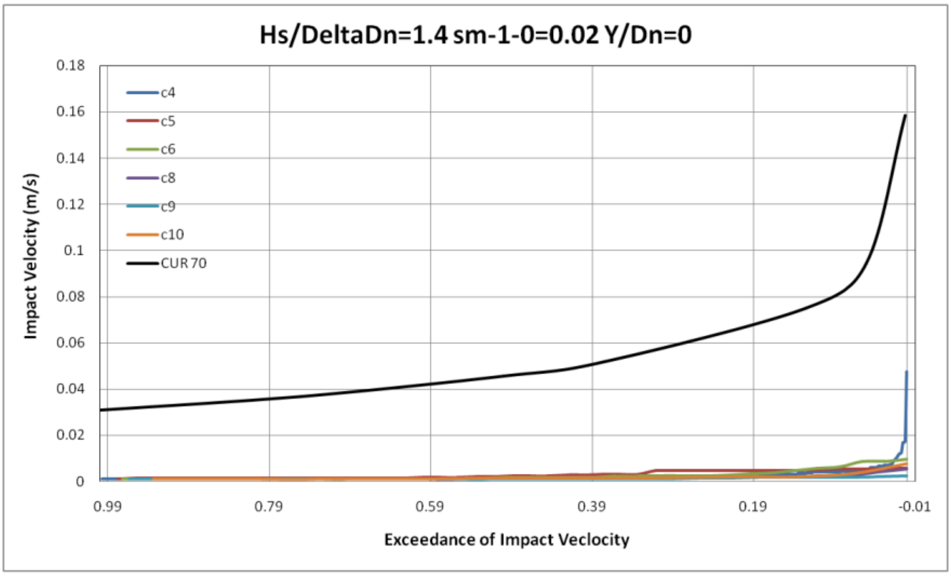

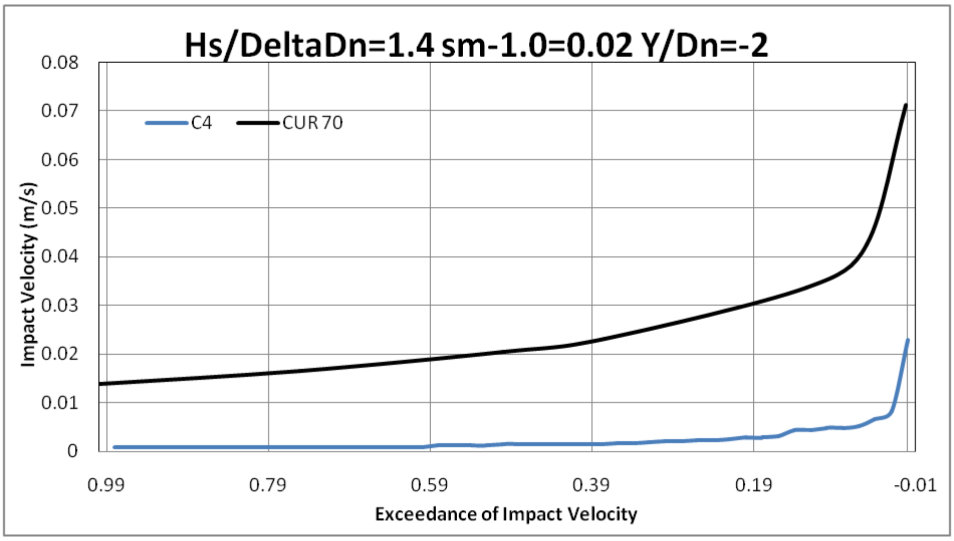

Appendix 4: Exceedance Curves representing order of Magnitude for Impact Velocities

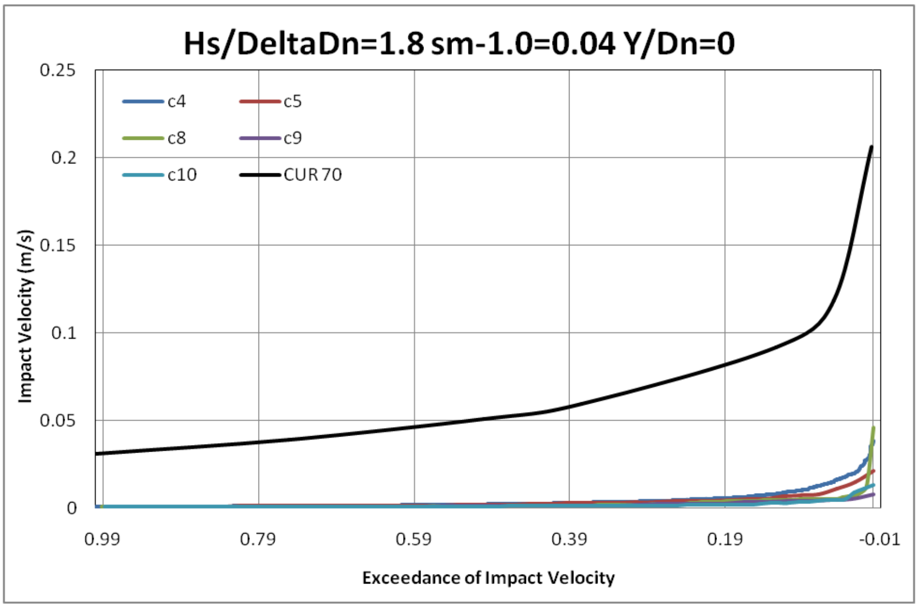

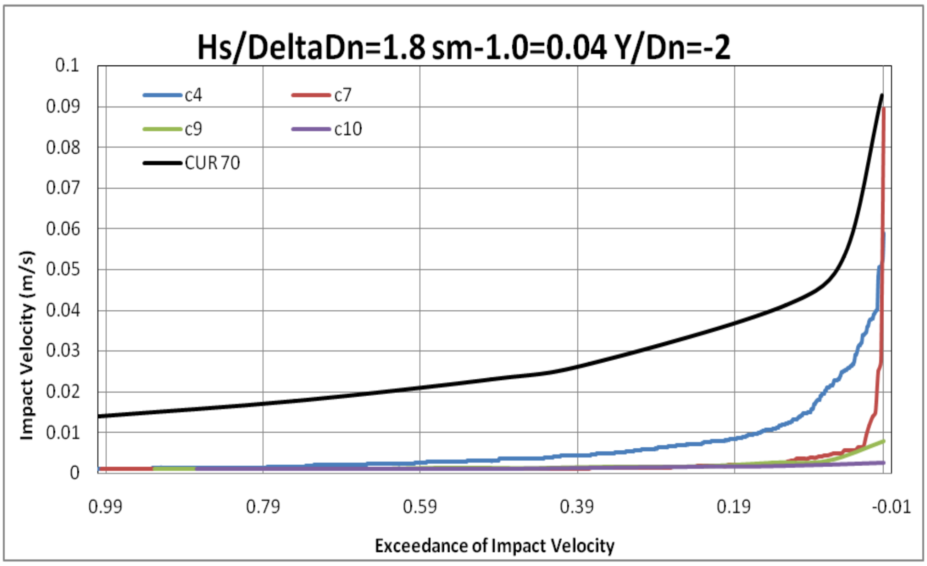

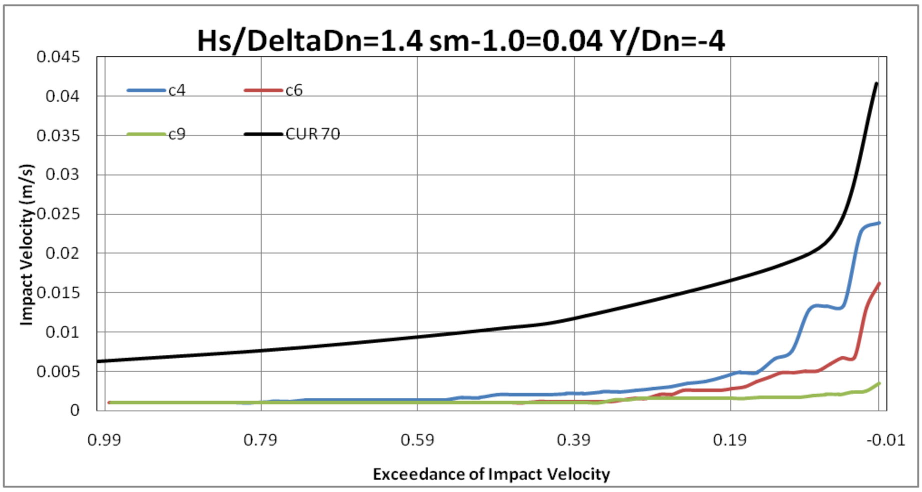

Appendix 4: Exceedance Curves representing order of Magnitude for Impact Velocities

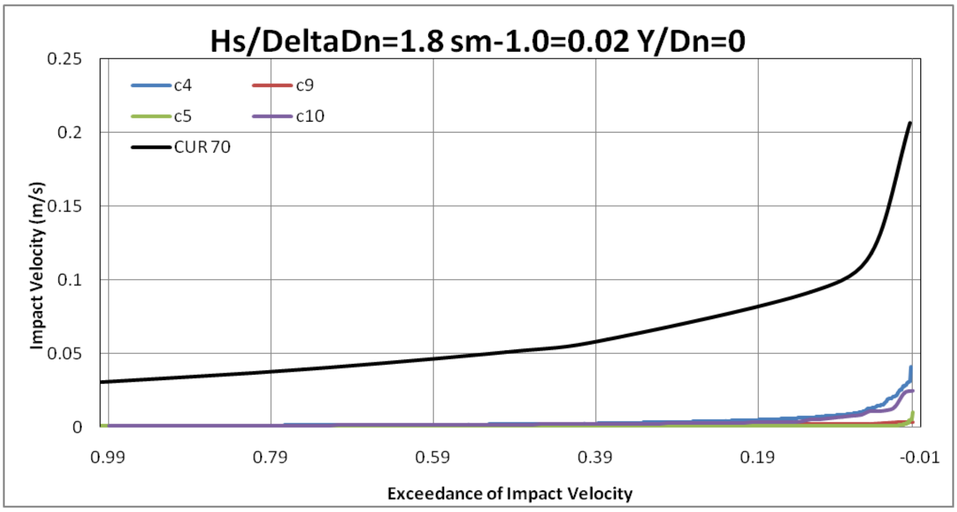

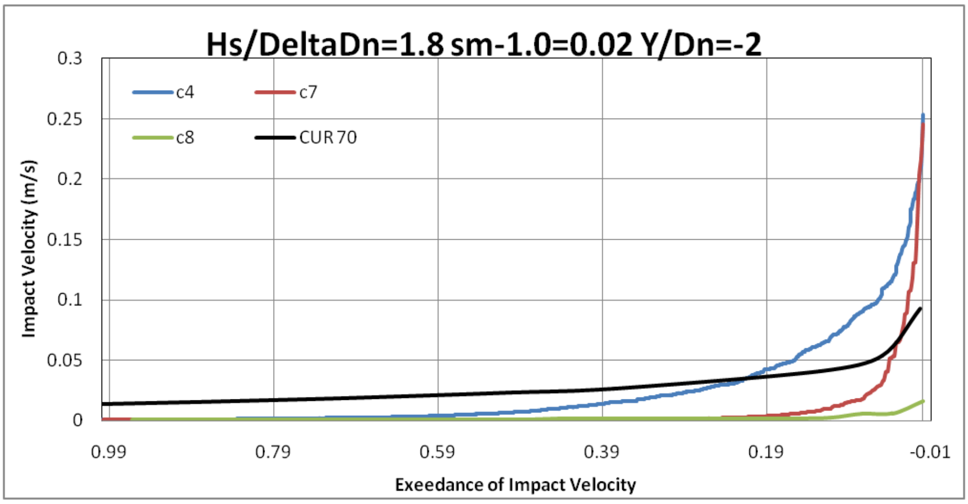

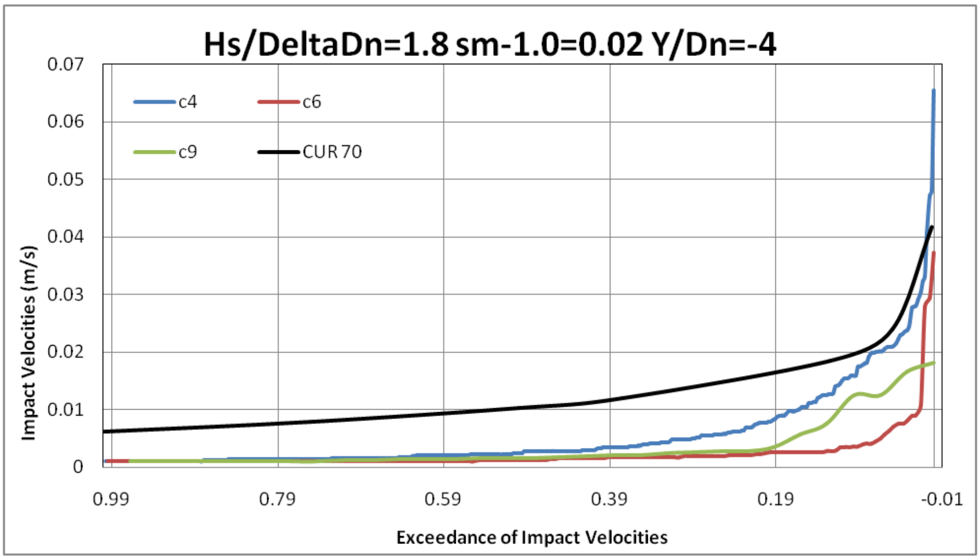

Appendix 5: Exceedance Curve for Wave Height Dependencies

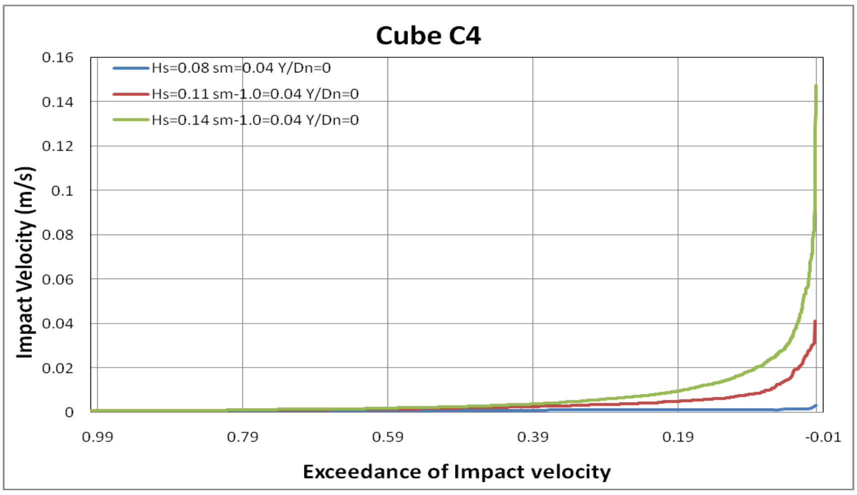

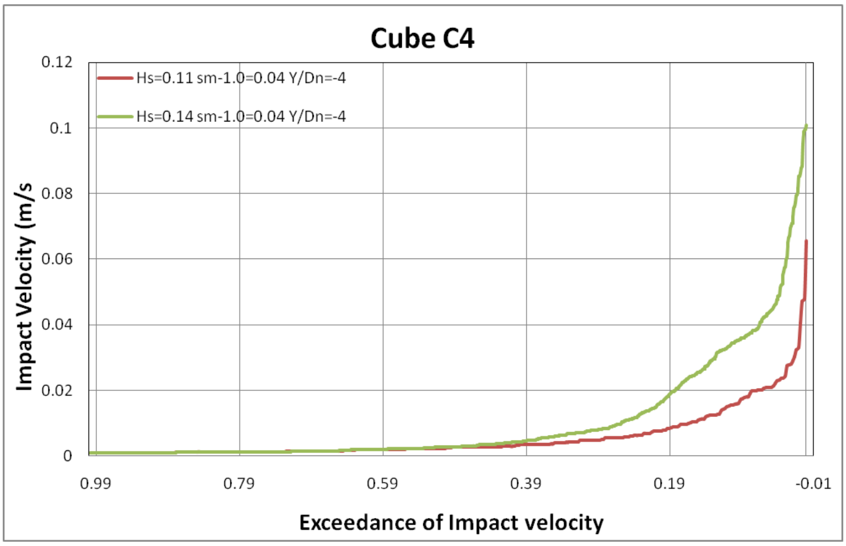

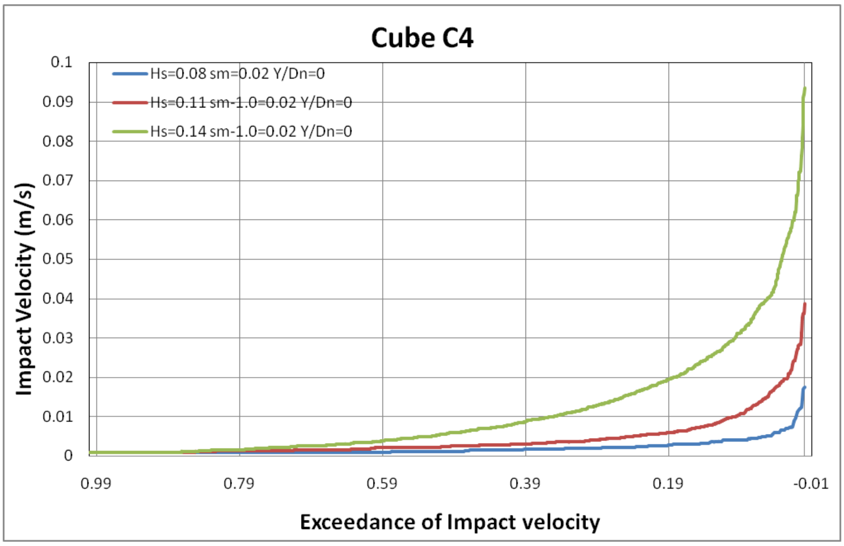

Appendix 5: Exceedance Curve for Wave Height Dependencies

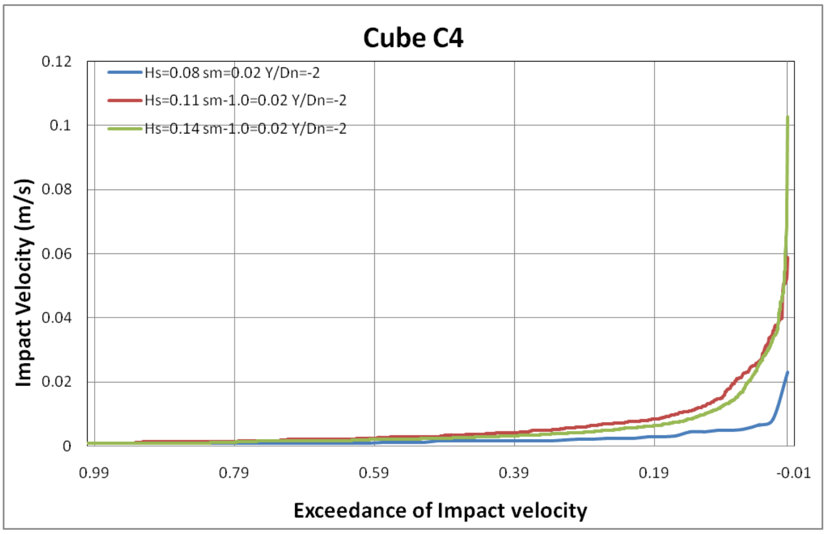

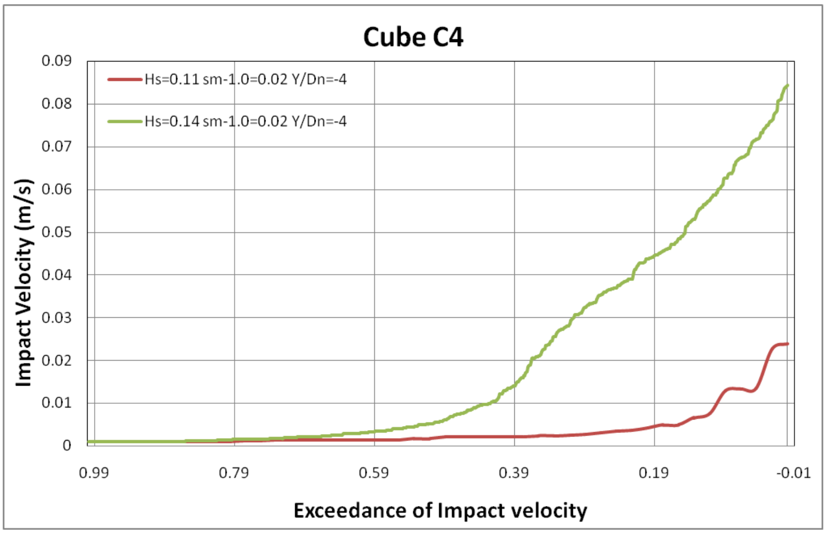

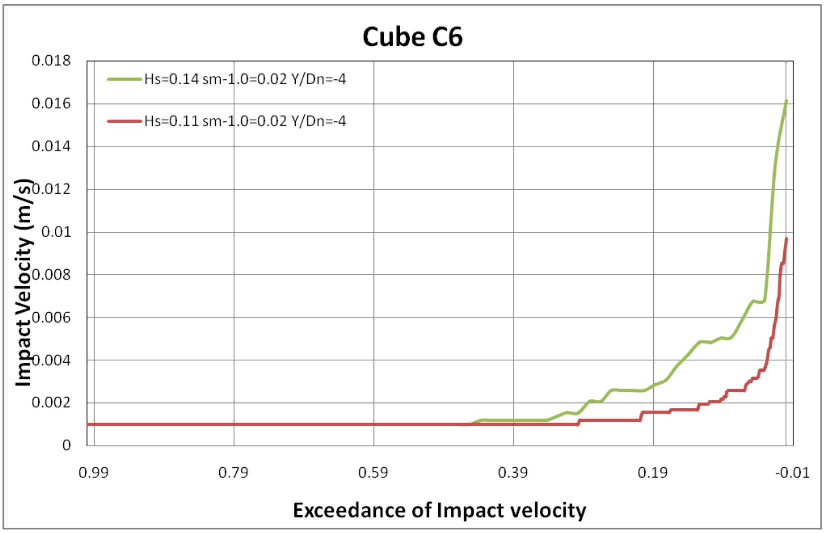

Appendix 5: Exceedance Curve for Wave Height Dependencies

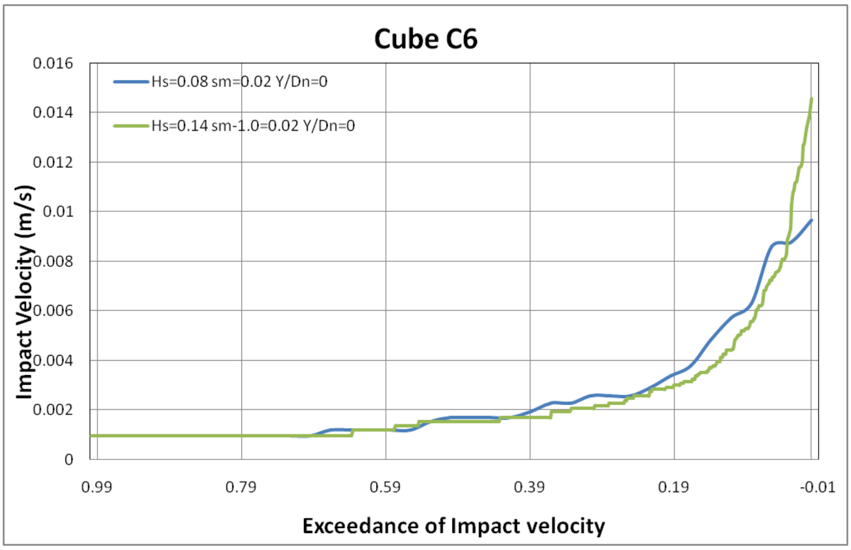

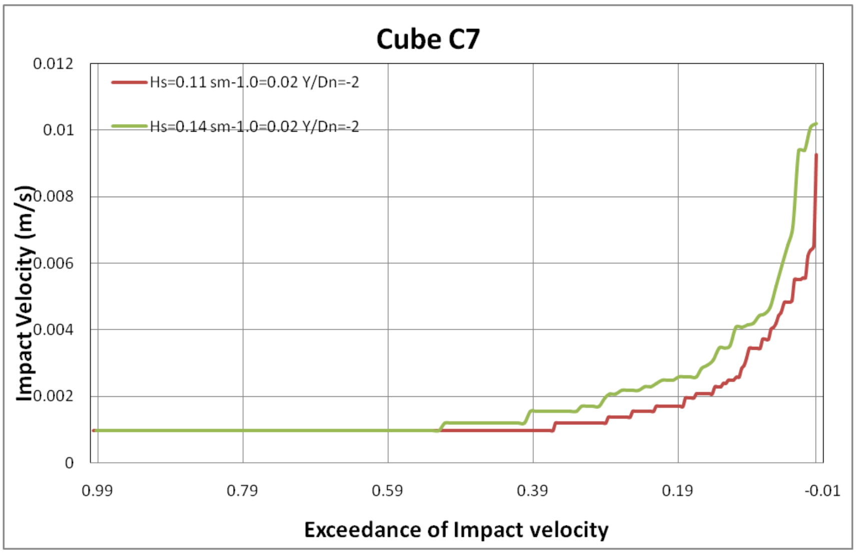

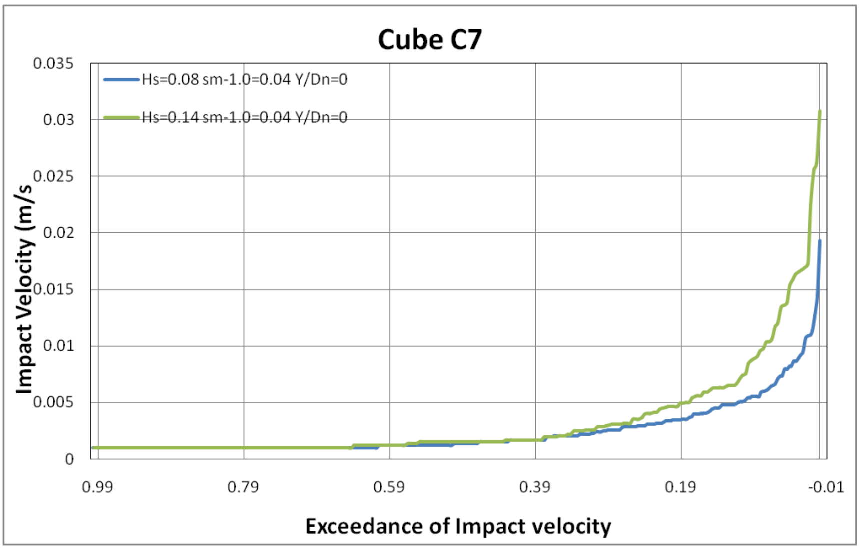

Appendix 5: Exceedance Curve for Wave Height Dependencies

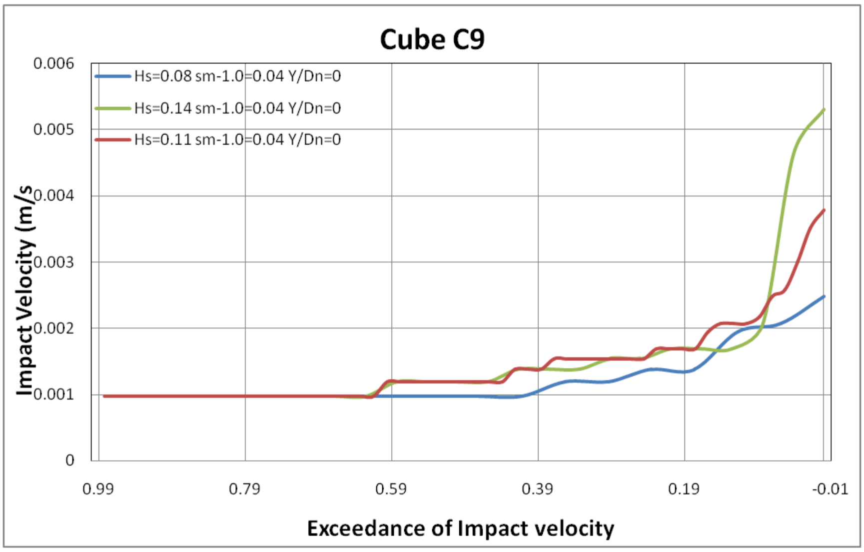

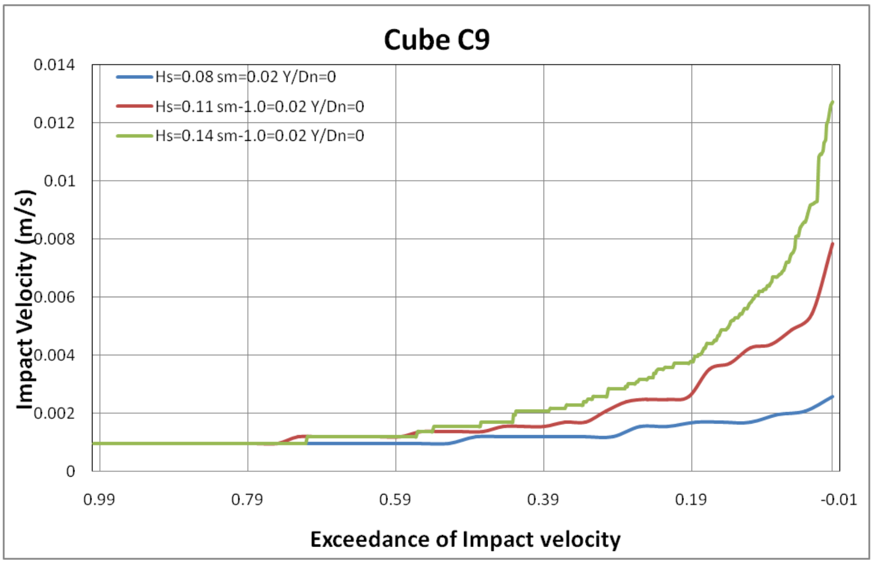

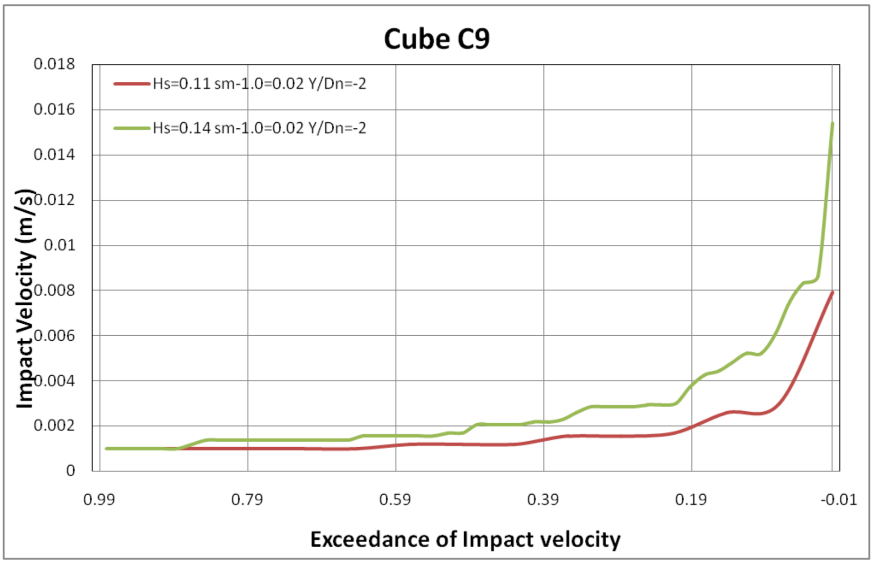

Appendix 5: Exceedance Curve for Wave Height Dependencies

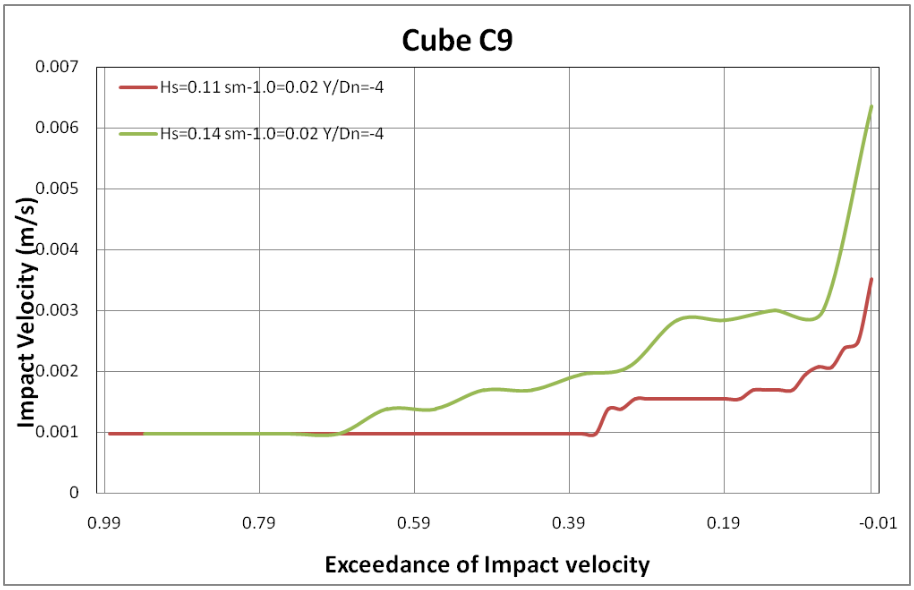

Appendix 6: Exceedance Curve for Wave Steepness Dependencies

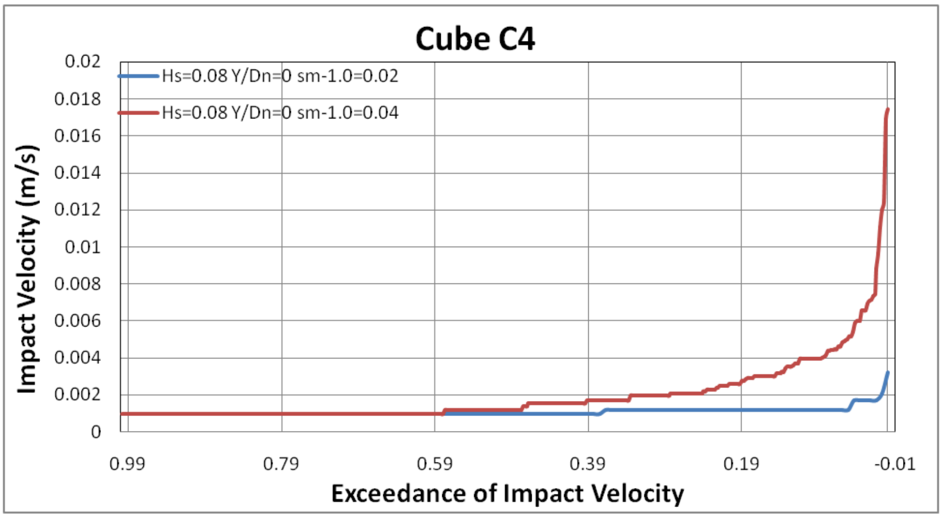

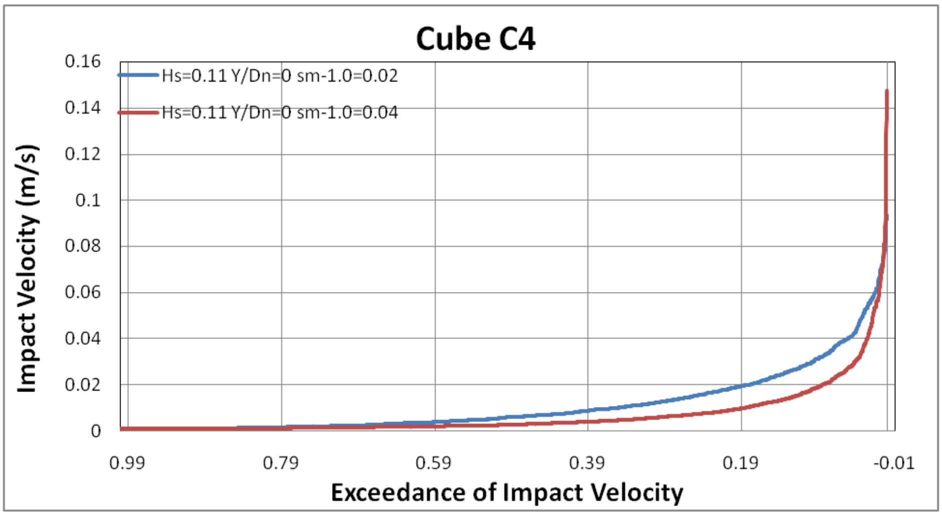

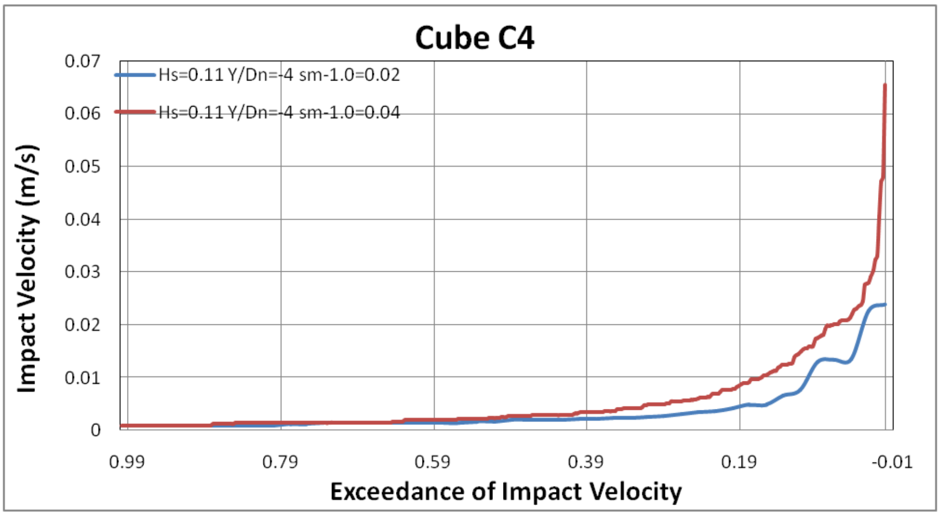

Appendix 6: Exceedance Curve for Wave Steepness Dependencies

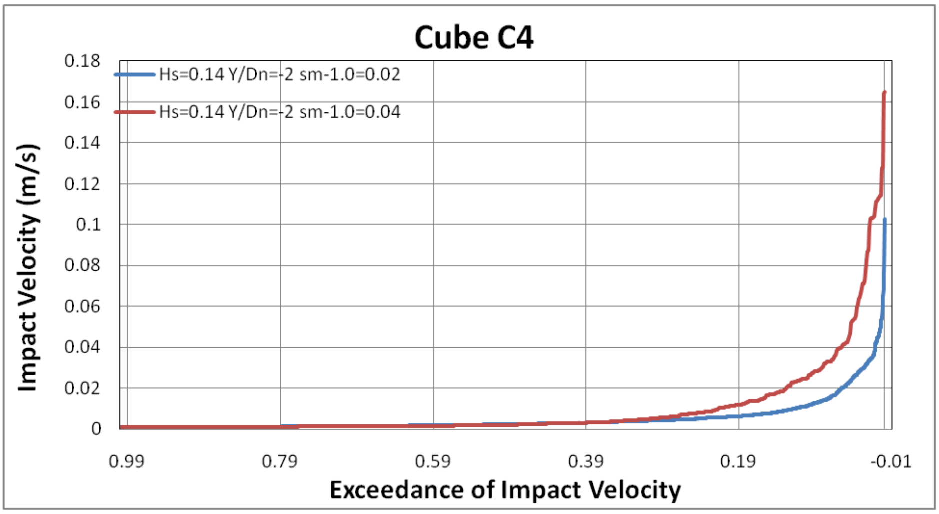

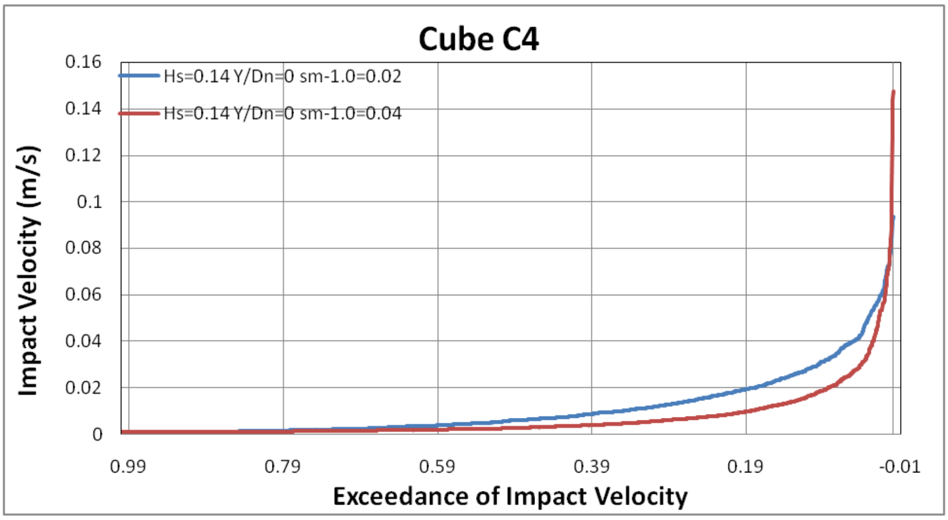

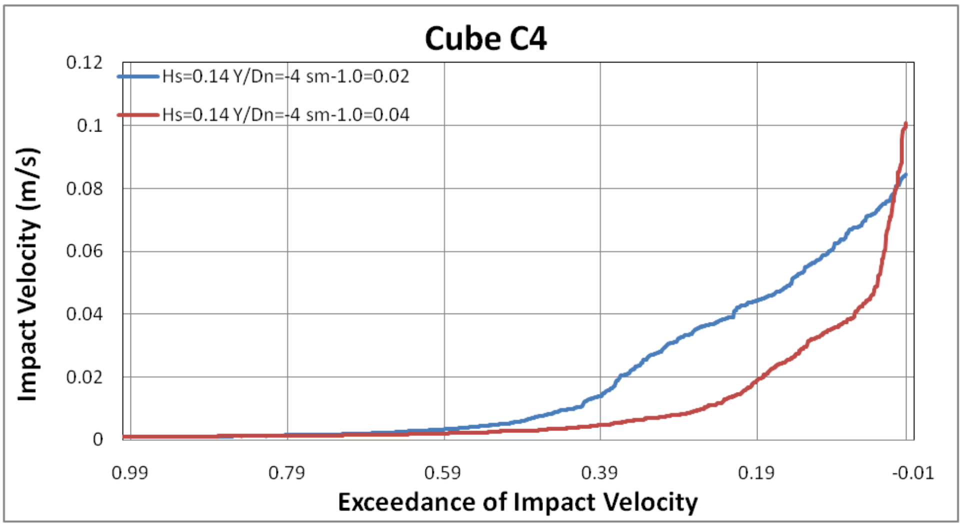

Appendix 6: Exceedance Curve for Wave Steepness Dependencies

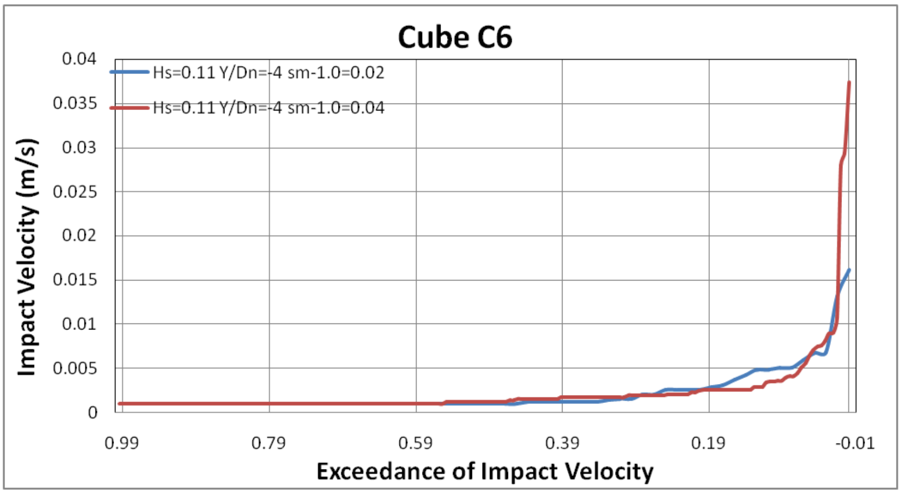

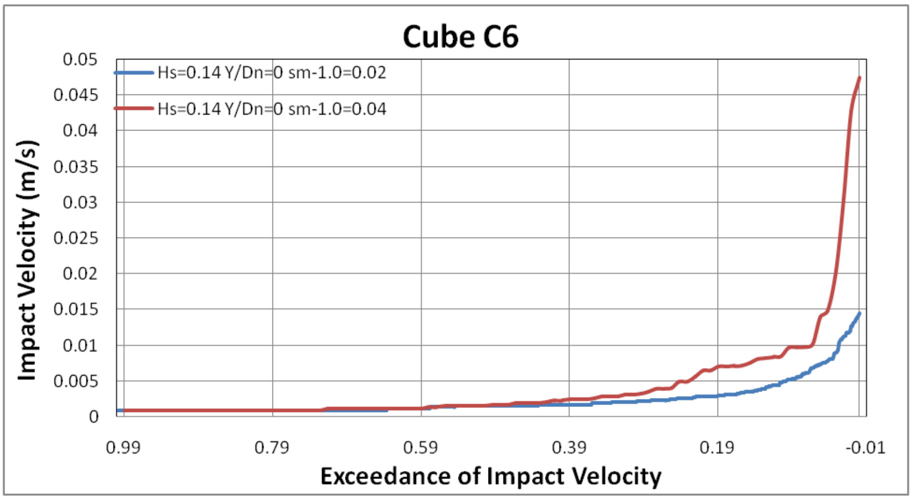

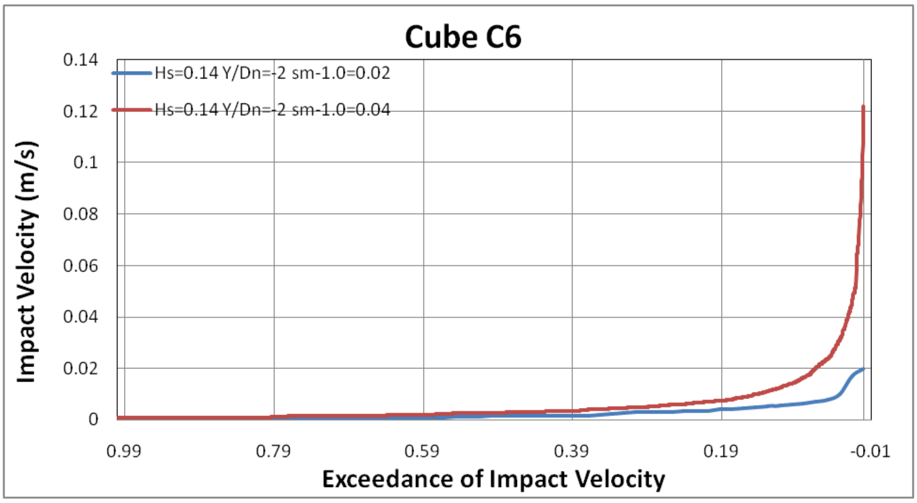

Appendix 6: Exceedance Curve for Wave Steepness Dependencies

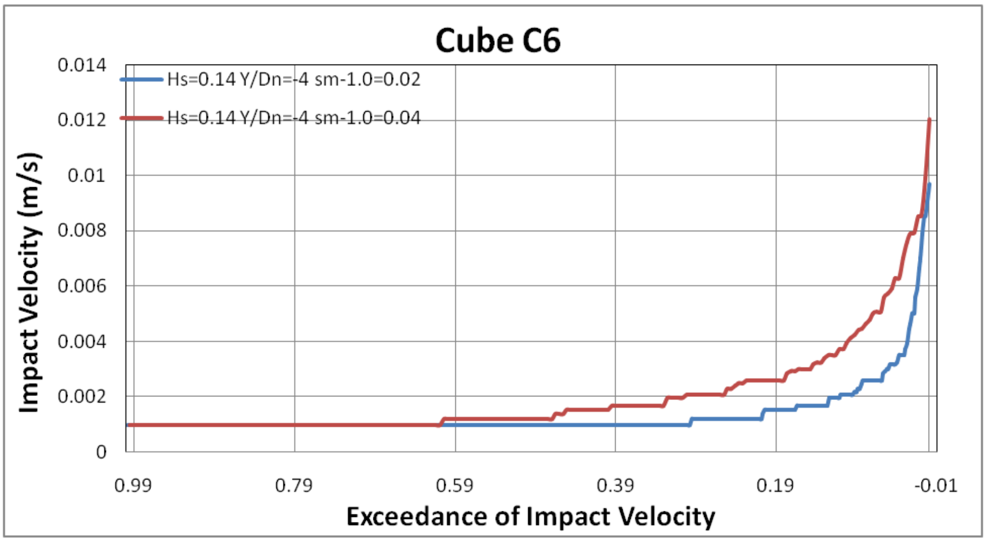

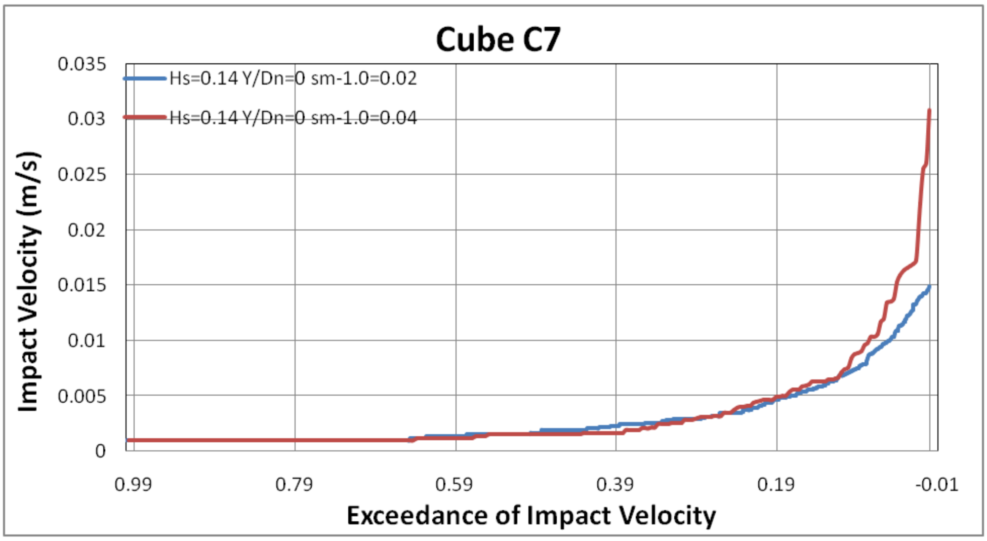

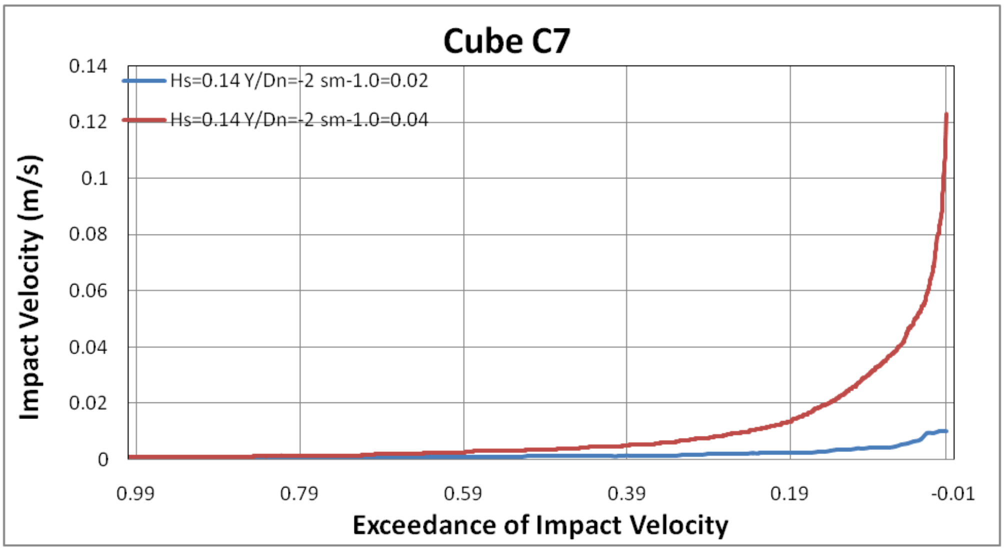

Appendix 6: Exceedance Curve for Wave Steepness Dependencies

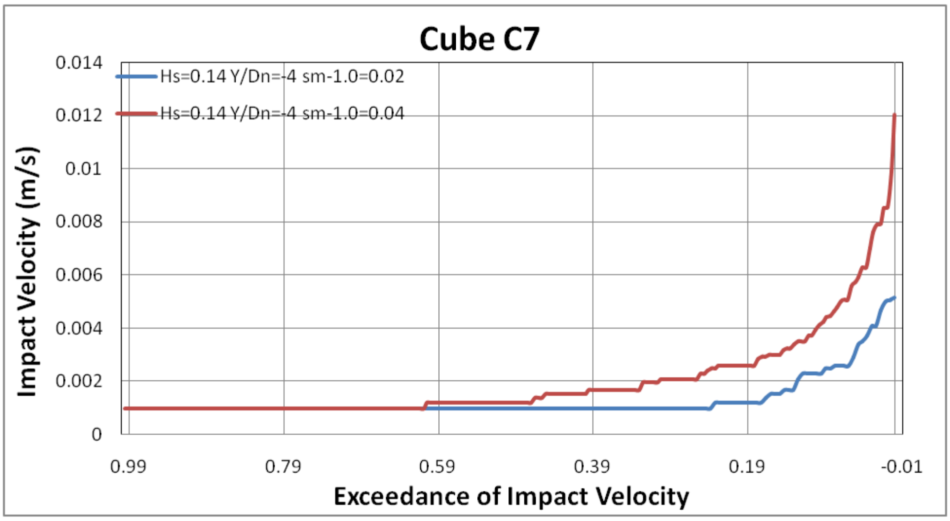

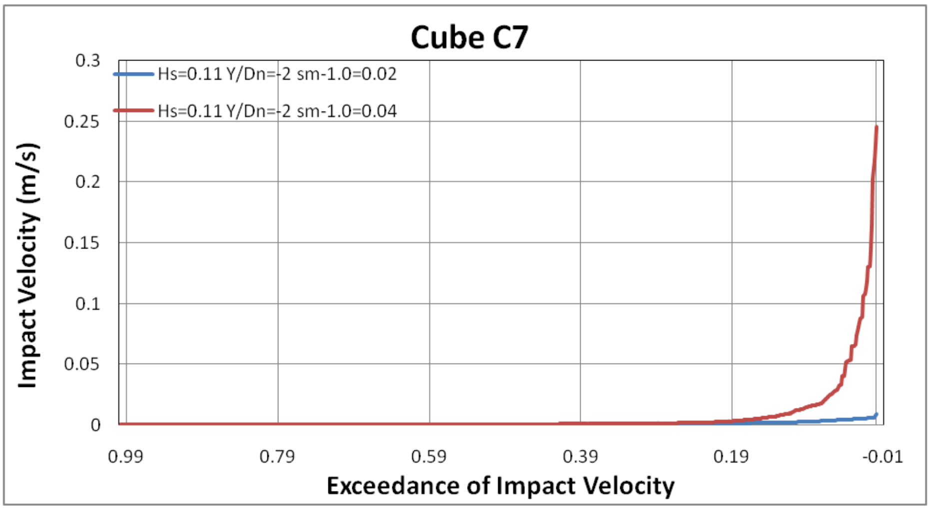

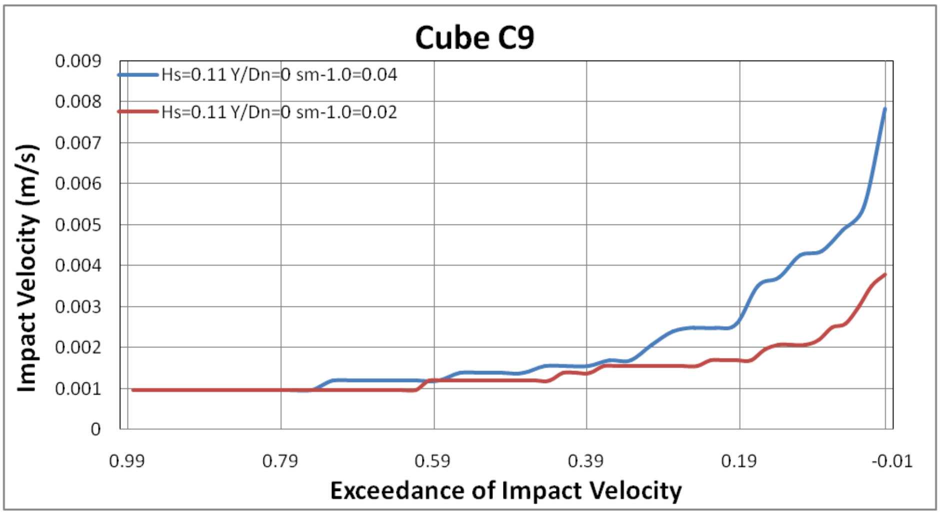

Appendix 6: Exceedance Curve for Wave Steepness Dependencies

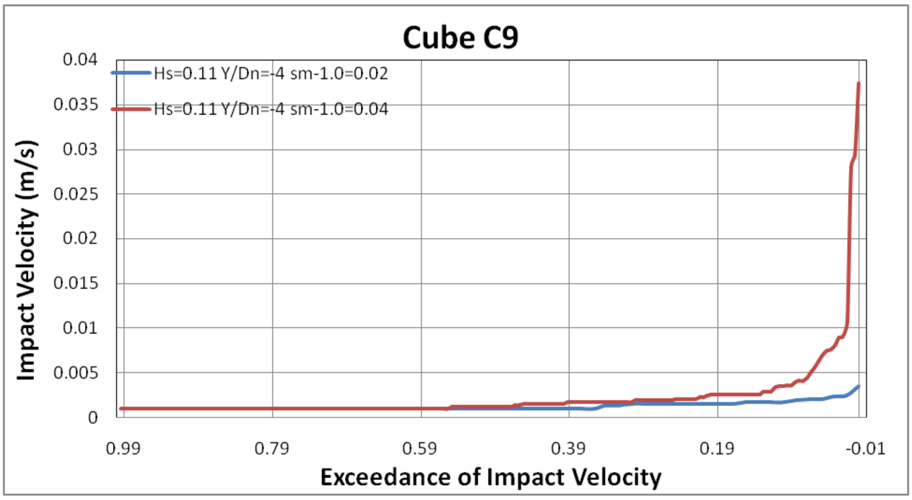

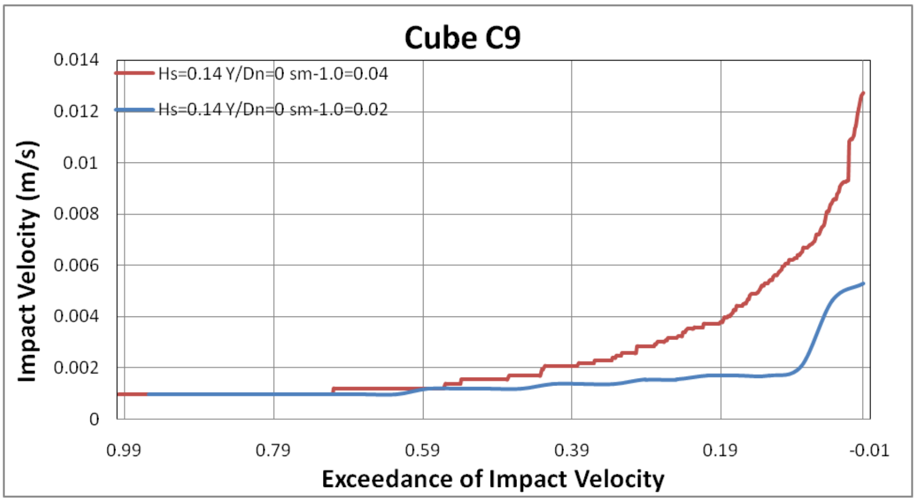

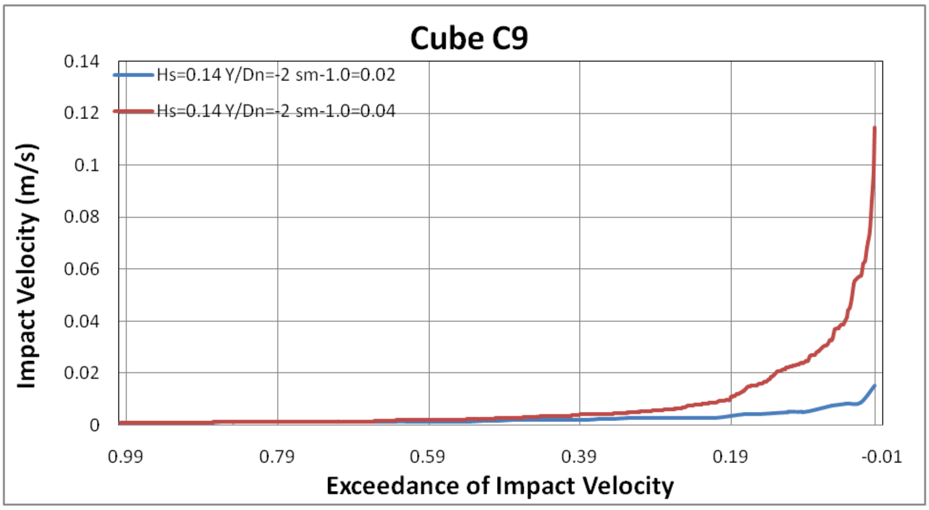

Appendix 6: Exceedance Curve for Wave Steepness Dependencies

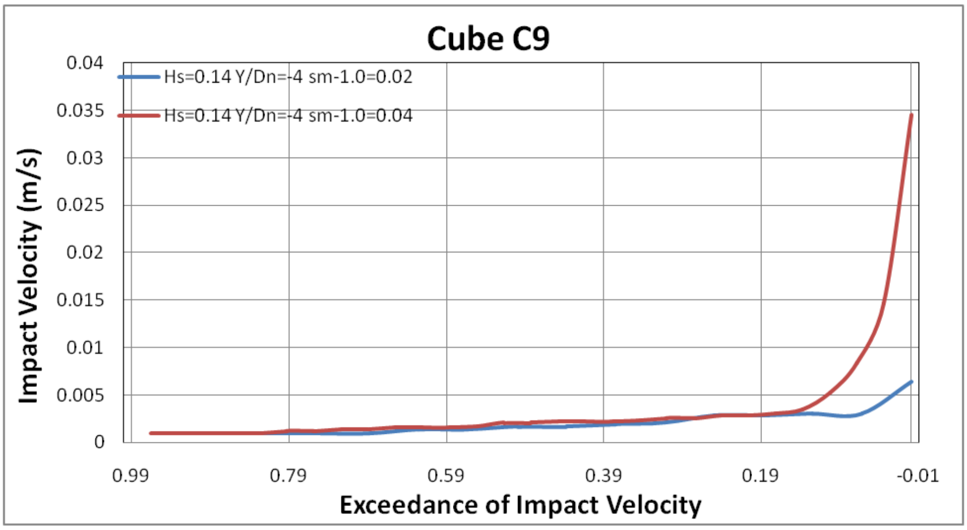

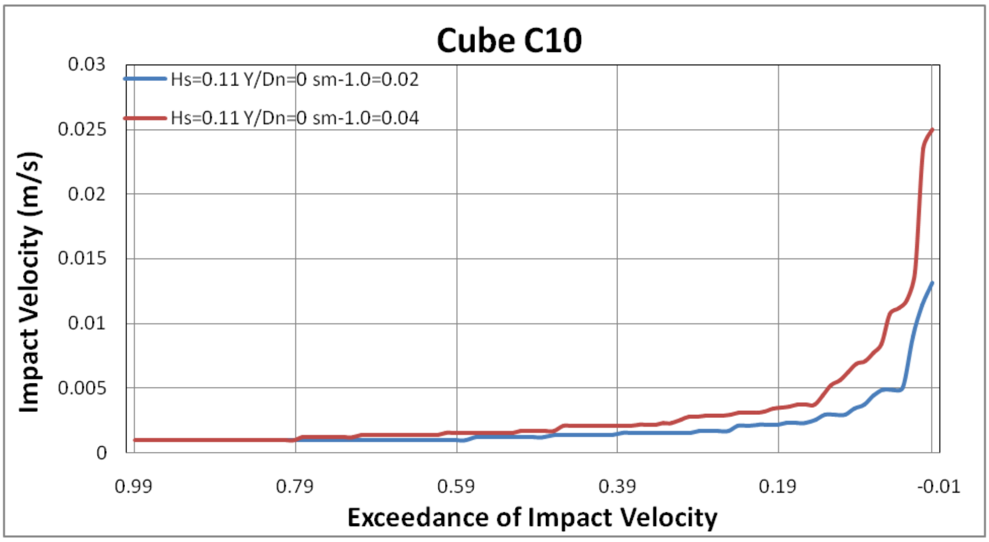

Appendix 7: Spatial Distribution on Horizontal Position of Cubes

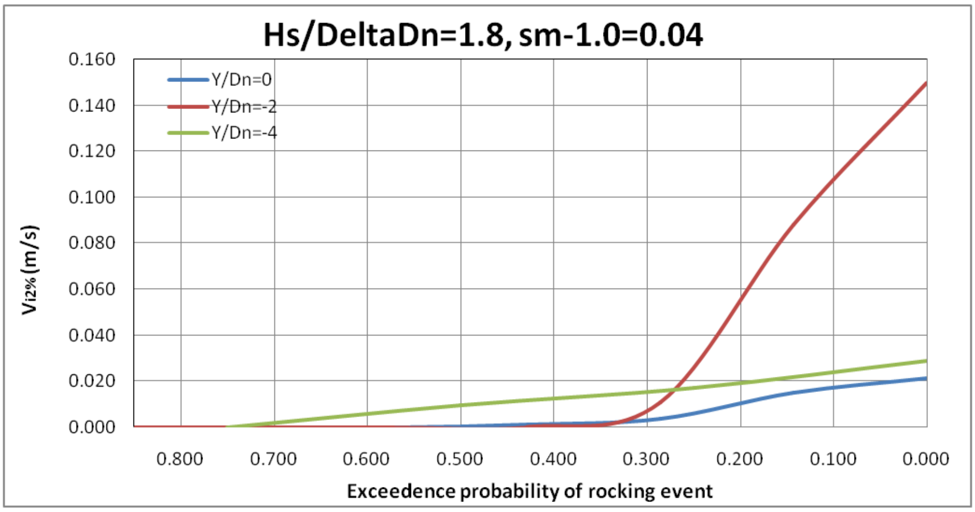

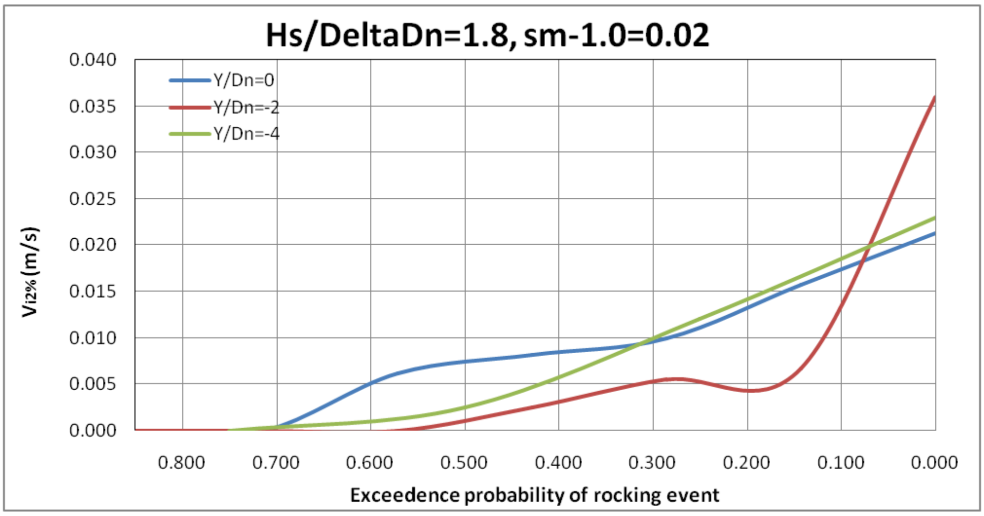

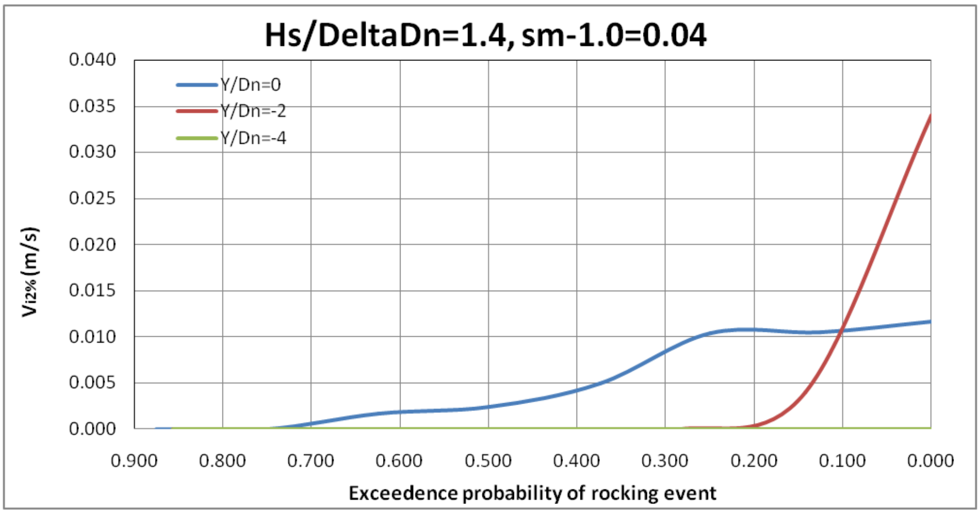

Appendix 7: Spatial Distribution on Horizontal Position of Cubes

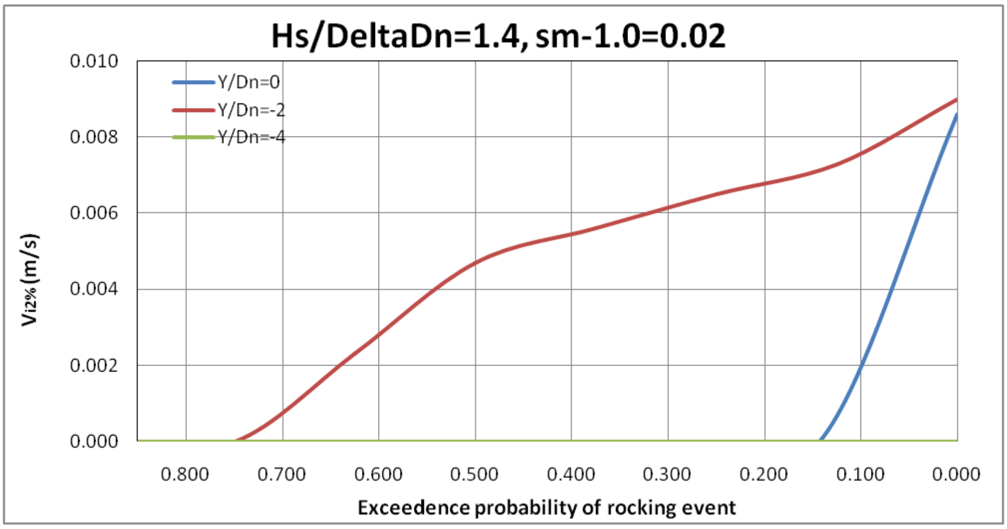

Appendix 8: Distribution over slope position

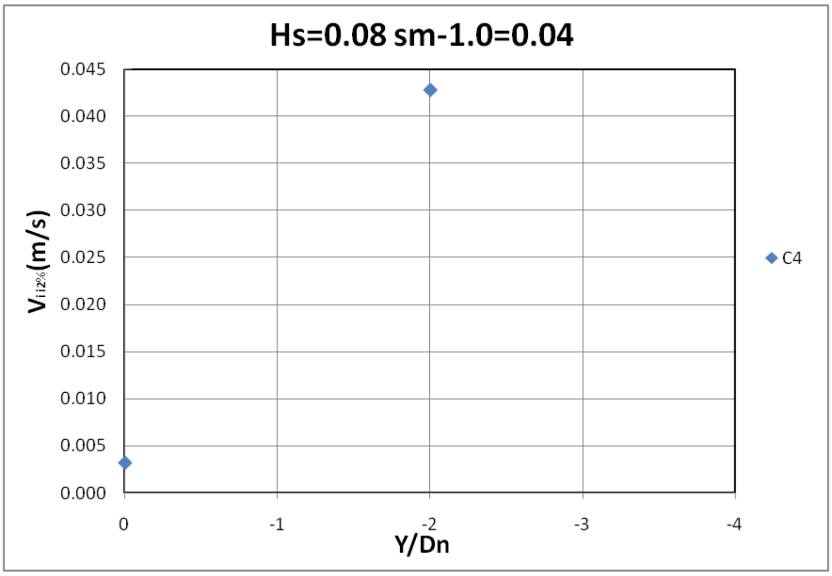

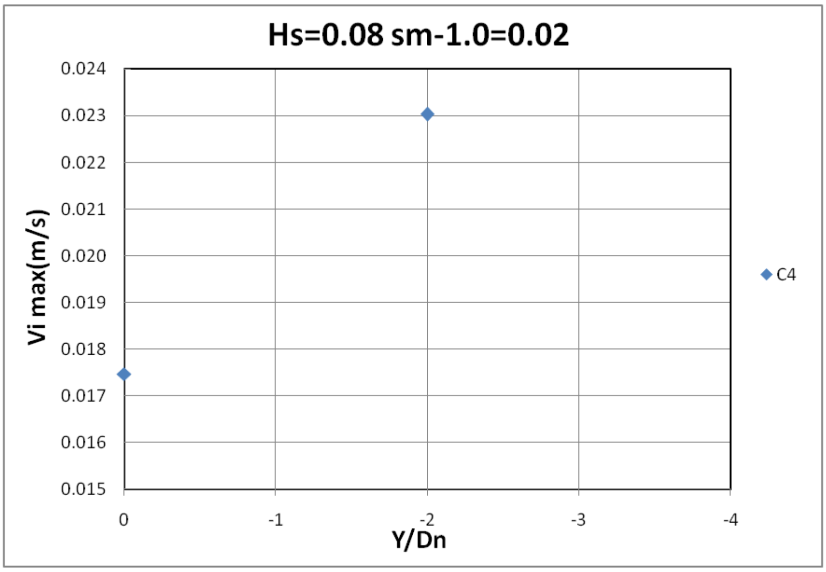

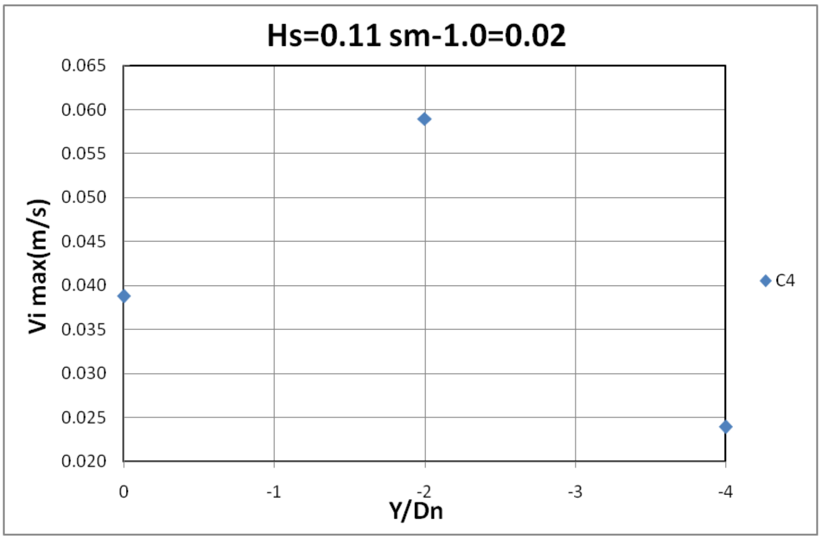

Appendix 8: Distribution over slope position

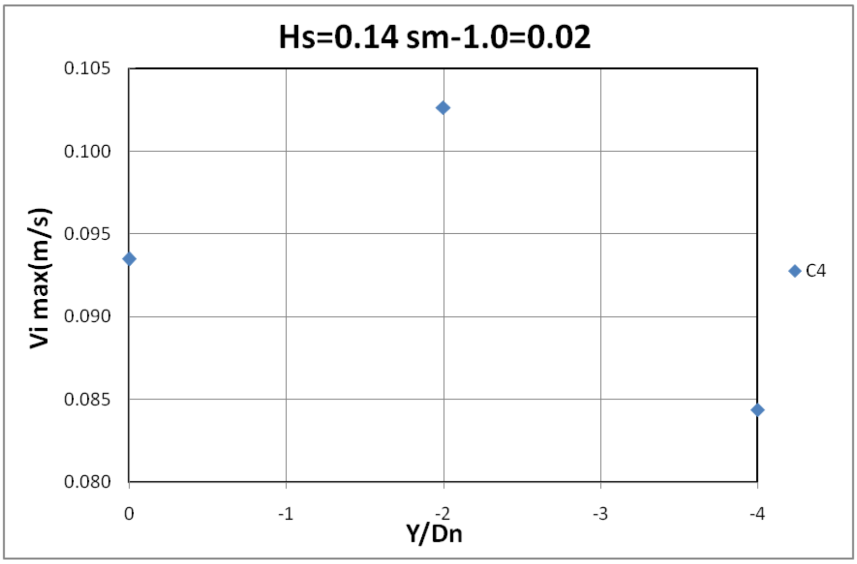

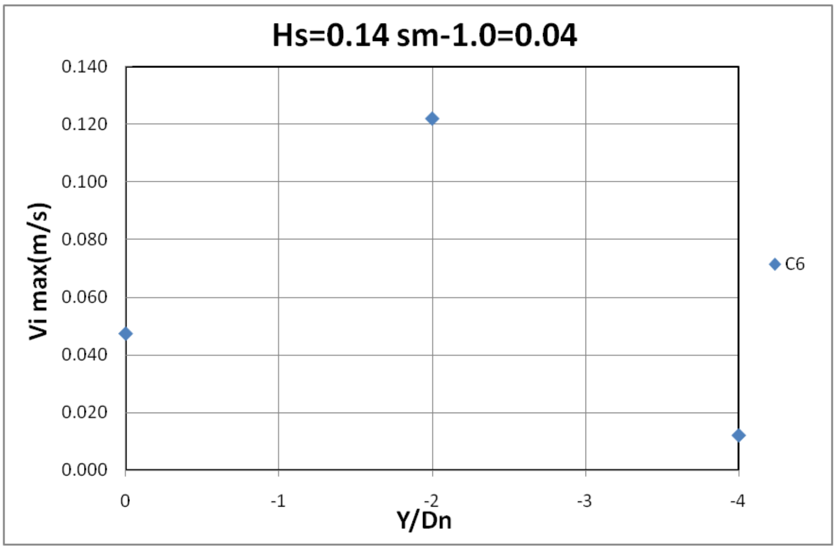

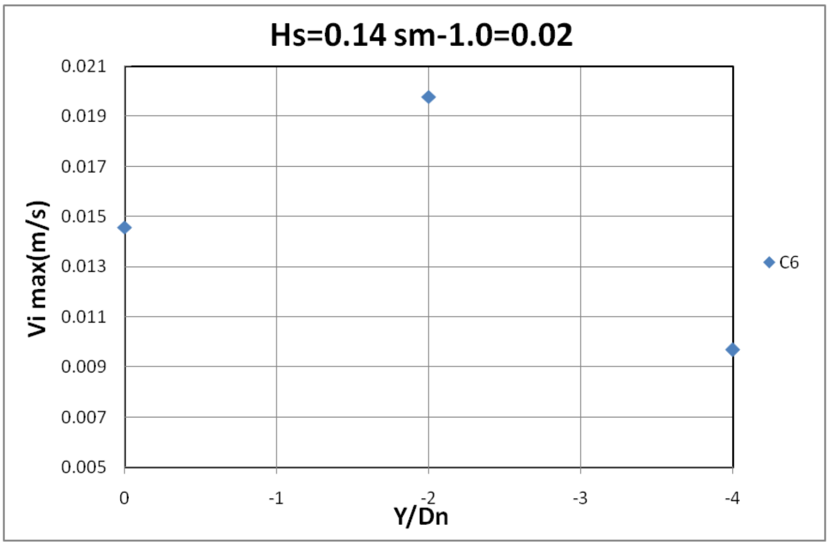

Appendix 8: Distribution over slope position

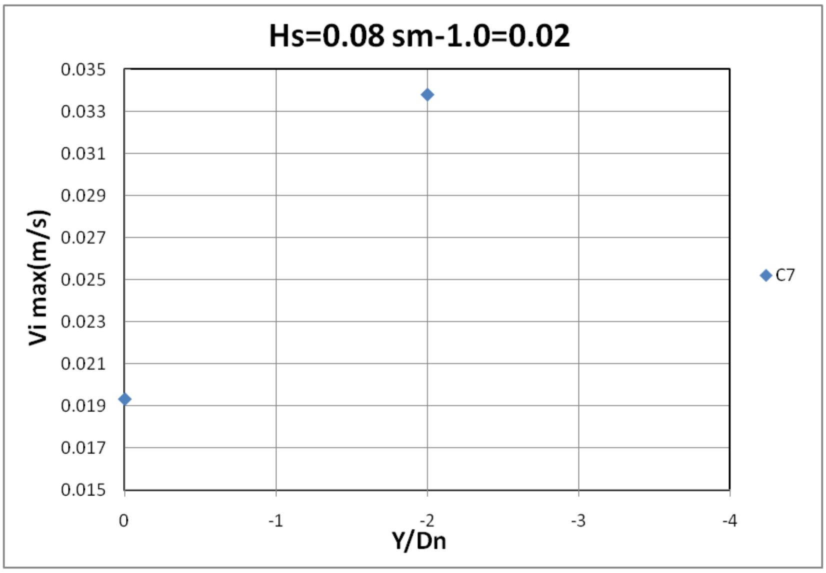

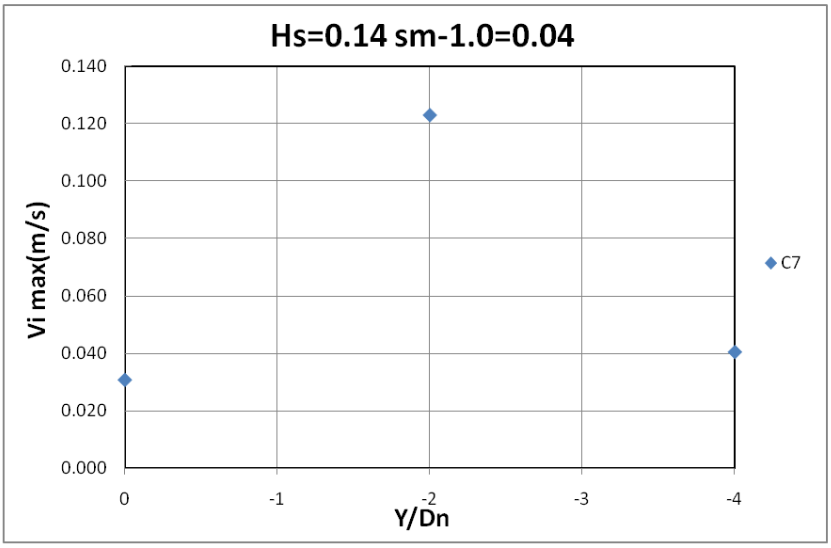

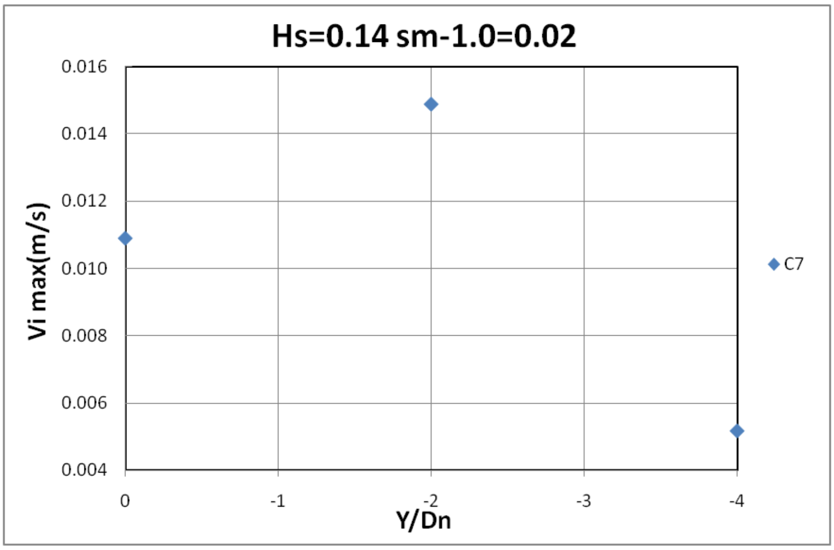

Appendix 8: Distribution over slope position